



Universiteit Utrecht

Master thesis

Impact of contour soil bunds on soil moisture conservation and crop yield in the Bokole watershed, southwestern Ethiopia



Experimental field (1) in the Bokole watershed cultivated with maize at harvest time

Imke W.F. Erven

Supervisors: dr. Rens van Beek and dr. ir. Geert Sterk

Tutor at Hawassa University: Kebede Wolka

Faculty of Geosciences, Department of Physical Geography

Utrecht University, The Netherlands, June 2017



Abstract

In Ethiopia, contour bunds are the main soil and water conservation measure. Their beneficial action can be attributed to a reduction in slope length and slope angle, which reduces the runoff velocity and the consequent soil loss, and an increase in infiltration. In turn, these benefits can positively influence crop yields as attested in earlier studies (Vancampenhout et al., 2006; Nyssen et al., 2007; Teshome et al., 2013; Wolka et al., 2016). However, these studies did not address the effect of soil bunds on the soil moisture content. Therefore, the present study is conducted to quantify the importance of contour soil bunds on soil moisture and yield and to indicate the effect of possible other parameters on yield, like rainfall, temperature, soil depth, slope and soil fertility. The study is conducted in two experimental fields cultivated with maize in the Bokole watershed in southwestern Ethiopia, which contain plots with and without soil bunds.

The FAO AquaCrop model is used to simulate the daily soil water balance, the crop development and the total attainable crop yield. The AquaCrop input data is determined by conducting laboratory and field measurements and using recommended values by the FAO (2012). The model was calibrated for the measured soil moisture content and the total aboveground dried biomass to get accurate simulations for the study area. After calibration, the FAO AquaCrop model simulates the soil moisture and the biomass well with regard to the measured parameters. To determine the effect of the soil bunds, the results of the plots with soil bunds are compared to the results of the plots without soil bunds.

There is no difference in soil moisture content between the plots with soil bunds and the plots without soil bunds. However, the variation of soil moisture within the plots result in small changes in maize yield, but no consistent pattern could be recognized. Furthermore, the biomass and yield are, on average, 11.6% and 13.6% higher in plots with soil bunds in field 1, respectively, but in field 2, the biomass and the yield are, on average, 21.0% and 21.5% lower in plots with soil bunds, respectively. This contradiction in the findings is mostly due to the difference in soil fertility stress, which is 5.1% lower for plots with soil bunds in field 1, but is 7.5% higher for plots with soil bunds in field 2. The soil fertility stress ranges between 25% and 80% between the plots and is the dominant parameters leading to the variation in maize yield between the plots. The maize yield differs from 1.5 ton ha⁻¹ to 5.7 ton ha⁻¹ in field 1 and from 1.3 ton ha⁻¹ to 2.6 ton ha⁻¹ in field 2. When the variation in soil fertility stress is eliminated it can be seen that the maximum green canopy cover, the soil depth and the gap between the soil moisture content at field capacity and at saturation are also important parameters affecting the maize yield. A higher maximum green canopy cover and a deeper soil positively influence the yield, while the gap between the soil moisture content at field capacity and at saturation only significantly influence the yield when it is approximately smaller than 5 %vol, which triggers aeration stress more easily. In addition, when comparing the maize yields produced under different weather conditions, which are based on the weather conditions from 2005 to 2016 in the Bokole watershed, it is clear that the temperature has more influence on the maize yield than rainfall in the Bokole watershed.

On the whole, no significant differences in parameters between plots with and without soil bunds are observed. This is most likely due to the young age of the soil bunds and the sufficient availability of water, which makes the immediate effect of soil bunds with regard to soil conservation unnecessary. Nevertheless, the maize yield varies between the plots, which is observed to be dominantly caused by variation in soil fertility stress, maximum green canopy cover, soil depth and slope between the plots. Moreover, the soil moisture at permanent wilting point, at field capacity and at saturation influence the water and aeration stress and, therefore, variation in these soil properties cause small differences in the maize yield.

Keywords: Soil contour bunds; FAO AquaCrop; Soil moisture content; Maize yield; Ethiopia; Crop modelling

Table of contents

1. Introduction	1
2. Study area and experimental setup	5
2.1 Study area	5
2.2 Experimental setup	6
3. Materials and methods	7
3.1 FAO AquaCrop	7
3.1.1 Soil water balance	7
3.1.2 Crop development	9
3.1.3 Soil evaporation and crop transpiration	13
3.1.4 Aboveground biomass	14
3.1.5 Yield formation	14
3.1.6 Management practices	15
3.2 AquaCrop simulations	15
3.3 Data	17
3.3.1 Climate data	17
3.3.2 Crop data	18
3.3.3 Soil data	20
3.3.4 Management aspects	25
4. Results	27
4.1 Measured data	27
4.1.1 Weather conditions	27
4.1.2 Soil properties	27
4.1.3 Soil moisture measurements	28
4.1.4 Crop and yield measurements	32
4.2 AquaCrop simulations: effect of soil bunds	33
4.2.1 Effect of treatment: bunds versus no bunds	33
4.2.2 Effect of location within the plot	35
4.3 AquaCrop simulations: effect of soil moisture	37
4.3.1 The effect of soil moisture on biomass between the plots	37
4.3.2 The effect of soil moisture on biomass within the plots	37
4.4 AquaCrop simulations: effect of soil fertility	38
4.4.1 Variable soil fertility stress	39
4.4.2 Average soil fertility stress	42
4.5 AquaCrop simulations: effect of inter-annual variability	46

4.5.1 Effect of temperature and rainfall on soil moisture and biomass	46
4.5.2 Effect of temperature and rainfall on stress conditions and biomass	49
5. Discussion.....	51
5.1 Evaluation of methods	51
5.2 Evaluation of the FAO AquaCrop model	51
5.3 Maize yield	53
5.4 Effect of soil bunds on soil moisture and maize yield	53
5.5 Effect of soil fertility, canopy cover, soil depth and slope on maize yield	55
5.6 Effect of weather conditions on maize yield	57
6. Conclusion.....	59
7. Recommendations.....	63
Acknowledgements	64
References.....	65
Appendices.....	72
Appendix 1 – Makkink equation to estimate the reference evapotranspiration	72
Appendix 2 – Crop and water stress parameters.....	73
Appendix 3 – Walkley and Black method.....	75
Appendix 4 – Hydrometer method	76
Appendix 5 – Pedotransfer function developed by Saxton and Rawls (2006).....	77
Appendix 6 – Measured soil moisture content for field 1.....	78
Appendix 7 – Measured soil moisture content for field 2.....	79
Appendix 8 – Statistically significant difference in soil moisture within plots.....	80
Appendix 9 – Overview of measured parameters.....	83
Appendix 10 – Overview of the results of the default AquaCrop simulation	85

List of figures and tables

List of figures

Figure 1. Contour soil and stone bund (Wolka et al., 2016).....	2
Figure 2. Location of the Bokole watershed and the study area.	5
Figure 3. Schematic top view of the experimental setting.....	6
Figure 4. Calculation scheme of AquaCrop (Raes et al., 2011)	7
Figure 5. Variation of green canopy cover during the crop cycle (Raes et al., 2011).....	9
Figure 6. The green canopy cover (Raes et al., 2011)	9
Figure 7. Water stress curves (Steduto et al., 2012).	10
Figure 8. Adjustment of a Ks curve for ET_0	12
Figure 9. CC measured with the GreenCropTracker Tool and Photoshop CC 2017.	19
Figure 10. The soil moisture kit and the method of the FDR.	23
Figure 11. Total amount of rainfall and growing degree days (GDDs).	27
Figure 12. The average measured soil moisture content for plots with soil bunds.....	30
Figure 13. The average measured soil moisture content for plots without bunds.....	30
Figure 14. The average measured soil moisture content for plot 1 of field 1.....	31
Figure 15. The average measured soil moisture content for plot 2 of field 2.....	31
Figure 16. Measured soil moisture content over time.....	31
Figure 17. Simulated average soil moisture content for plots with and without bunds.	34
Figure 18. Simulated average biomass for plots with and without bunds.....	34
Figure 19. Simulated average water balance for plots with and without bunds.....	34
Figure 20. Boxplots of the simulated average soil moisture content and the biomass for all locations with significant different soil moisture contents	38
Figure 21. The amount of stress and total biomass and yield between the subplots for field 1.....	39
Figure 22. The amount of stress and total biomass and yield between the subplots for field 2.....	39
Figure 23. The soil moisture content at field capacity and at saturation and the average soil moisture content	40
Figure 24. The total available water plotted with stress.....	41
Figure 25. The gap between the soil moisture content at field capacity and at saturation plotted with the stress	41
Figure 26. The biomass simulated with the variable soil fertility stress and with the average soil fertility stress plotted together for each plot	42
Figure 27. The simulated average soil moisture content and the simulated biomass for 2006, 2007, 2008 and 2014.....	47
Figure 28. The averaged actual soil moisture content and the total biomass for all measurement locations plotted for each year between 2005 and 2016	48
Figure 29. The amount of stress, biomass and yield for each year between 2005 - 2016 for field 1... ..	49
Figure 30. The amount of stress, biomass and yield for each year between 2005 - 2016 for field 2... ..	49

List of tables

Table 1. Different AquaCrop simulations performed in this study	16
Table 2. Makkink coefficient adjusted for the Bokole watershed (Ogolo, 2014).....	18
Table 3. Observed crop parameters and important dates and periods of the growing period.....	18
Table 4. Calculated and measured soil properties	28
Table 5. Statistically significant difference in soil moisture between fields	29
Table 6. Statistically significant difference in soil moisture content between plots.....	29
Table 7. Calculated and measured crop and yield parameters.....	32
Table 8. Input and output parameters for the locations of the within pot simulation.....	36
Table 9. Input and output parameters of the average fertility simulation for the center of the plots orderd from highest biomass to lowest biomass.....	45
Table 10. Adjusted sowing dates for field 2 for each year.....	46

1. Introduction

At a global scale, soil erosion is the most prevailing cause of land degradation, accounting for 70% to 90% of the total land degradation (Teshahunegn et al., 2014). This can also be seen in Ethiopia, where reports indicate a soil loss of about 42 ton ha⁻¹ year⁻¹ (Wagayehu and Drake, 2003), which is more than four times as much as the acceptable rate of 10 ton ha⁻¹ year⁻¹ (Young, 1997). The main type of land degradation in Ethiopia is water erosion (Bewket, 2006), which is a selective process that removes organic matter and lighter particles such as clay and silt from the soil (van der Zanden, 2011). The nonproductive coarse material remains behind, reducing the resilience of the soil and making the soil more prone to additional erosion (Wolka et al., 2016). Besides, the removal of organic matter reduces the nutrient availability of the soil, which is needed for plant growth and, therefore, erosion negatively affects crop production (Wolka et al., 2011). Stoorvogel and Smaling (1990) report that the removal of nitrogen, phosphorus and potassium due to erosion was 60 kg ha⁻¹ year⁻¹, while crops only take 20 kg ha⁻¹ year⁻¹ out of the soil (Kidane and Alemu, 2015). Furthermore, soil erosion stimulates runoff and discourages infiltration and groundwater recharge, which results in water stress and inevitably crop failure (Teshahunegn et al., 2014; Kidane and Alemu, 2015). The above mentioned consequences are all in-situ effects of soil erosion, but soil erosion also has off-site effects like the sedimentation of reservoirs, lakes and rivers downstream (Amare et al., 2014).

Ethiopia is a poor country that relies on agriculture, of which almost 97% is rain-fed and, therefore, depends on the patterns of seasonal rain (Biazin and Stroosnijder, 2012). Ethiopia has a high spatial and temporal rainfall variability, with approximately 70% of the rain falling between May and August (Gebreegziabher et al., 2009). As a result of climate change, the variability in rainfall will increase and rainfall will become more intense (Wolka et al., 2016). It is expected that this will increase the risk of surface runoff, water erosion, droughts and eventually also negatively influence crop yields (Wolka et al., 2016).

Another cause for the enormous amount of land degradation in Ethiopia is the increasing demand for food together with poor management practices (Kidane and Alemu, 2015). The increasing demand for food is a direct result of the enormous increase in population, which has grown with 63% over the last 20 years (Wallace, 2000; Kidane and Alemu, 2015). The increasing demand forces farmers to either increase the production per unit area or cultivate more land (Wolka et al., 2013). On the one hand, cultivating more land is forcing farmers to move onto hillslopes with a gradient of more than 30 degrees, which is far above the advised maximum slope angle of 20 degrees and will enhance land degradation (Kidane and Alemu, 2015). On the other hand, cultivating the same area more exhaustingly without appropriate and sufficient management will probably also lead to land degradation (Wolka et al., 2013). In addition, the conversion of forest to agricultural land and excessive grazing by livestock have also accelerated land degradation in Ethiopia (Girmay et al., 2008).

The government of Ethiopia recognized the consequences of land degradation after the great droughts of 1973 and 1974 and took measurements to quantify the amount of soil loss (Wolka et al., 2013; Abate et al., 2015). The severity of the problem forced them to implement soil and water conservation (SWC) measures and plant trees to strengthen the soil (Gebremichael et al., 2005). The idea was to construct physical SWC measures along the contour lines that function as a barrier for surface runoff and thereby reduce slope length and gradient, retain soil moisture and sediment and reduce erosion (Bewket, 2006; Wolka et al., 2016).

The most widely used SWC measures in Ethiopia are contour soil bunds and stone bunds (figure 1) (Wolka et al., 2016). One of the main reasons why contour bunds are used is because it is not a very difficult technique and can be constructed and maintained by farmers without external assistance



Figure 1. Typical contour soil bund (a) and contour stone bund (b) in the Bokole watershed. (Wolka et al., 2016)

(Bewket, 2006). Contour bunds function as a physical barrier which slow down runoff water and trap eroded sediments and organic matter transported downstream (Alemu and Kidane, 2014). Reducing runoff velocity is favorable because more water can infiltrate and less erosion occurs, which leads to more available nutrients, increasing soil moisture contents and increasing crop production (Waelti and Spuhler, 2013). The material transported downstream is deposited at the upslope sides of the bunds, reducing soil loss and gradually change the slope angle of the fields developing terraces, which makes the fields more suitable for cultivation (Nyssen et al., 2000; Gebremichael et al., 2005). The steeper the slopes, the more effect contour bunds have on the slope angle (Gebremichael et al., 2005). Besides, the interval between the bunds depends on the slope of the soil, so the steeper the slope the closer the bunds need to be to each other (Waelti and Spuhler, 2013).

Contour bunds are constructed along a contour at regular intervals in order to slow down the water most efficiently, and can be made from stones or soil (Hengshijk et al., 2005). Soil bunds are made by digging a channel and placing the soil at the downslope side of the channel, forming a small bund (figure 1a). The empty channel traps runoff and sediment and needs to be maintained regularly (Wolka et al., 2016). Stone bunds are made by making a little trench and placing larger stones at the downslope side of it and smaller stones are used to build the rest of the bunds. Afterwards, the soil from the trench is piled up in front of the bund (figure 1b) (Nyssen et al., 2007). Grass or other plants are often planted on the bunds to get more stability (Critchley and Graham, 1991).

On the whole, the benefits of contour bunds are the reduction in slope length and slope angle, which reduces the runoff velocity and the soil loss and increases infiltration. However, contour bunds also have disadvantages. The accumulation of sediments and, hence, nutrients behind the bunds can create soil fertility gradients in the topsoil (Wolka et al., 2016). Furthermore, arable land is lost to the construction of contour bunds and farmers are concerned that bunds will be attractive nesting places for rats (Nyssen et al., 2007). Moreover, if the contour bunds are not properly aligned the runoff can be concentrated to one spot increasing the volume and erosive power of the flow (Alemu and Kidane, 2014). Nevertheless, multiple studies found the few disadvantages to be insignificant to the many benefits of contour bunds (Gebremichael et al., 2005; Nyssen et al., 2007; Alemu and Kidane, 2014).

Previous studies indicate that soil bunds can reduce soil erosion with 48% to 84% (Tesfaye, 2008; Teshome et al., 2012) and stone bunds can reduce soil erosion with 64% to 73% in different parts of Ethiopia (Vancampenhout et al., 2006; Meshesha et al., 2015). Furthermore, a study conducted in Ethiopia on farmers' perceptions about the contour bunds showed that approximately 94% of the farmers believed the potential of bunds to improve cropland productivity (Bewket, 2006). A similar study was conducted in the Bokole watershed by Wolka et al. (2016), where soil bunds were first introduced in 2000, while stone bunds were already practiced in the area for many years. The majority of the farmers observed an improvement in crop yield in less than two years after the construction of

the bunds (Wolka et al., 2016). However, the effect of stone bunds on crop yield takes more time than for soil bunds, which is probably because a newly built stone bund is porous, which is less effective in trapping runoff, but eventually the pore spaces clog and runoff is effectively slowed down and sediment is trapped behind the stone bunds (Wolka et al., 2013). Even though Wolka et al. (2016) observed a substantial rise in crop yield due to contour bunds, they did not find significant differences in soil properties between fields with and without contour bunds. Wolka et al. (2016) stated that the performance of crops is not only a function of soil fertility but can also be due to an increase in soil moisture, but this was never studied.

To understand the effect of contour soil bunds on crop yield, it is important to quantify the soil moisture changes and related crop yields. Using a model, such as the FAO AquaCrop model, it is possible to simulate soil moisture and crop yield for various field management situations (Abedinpour et al., 2012). AquaCrop was developed by the Food and Agriculture Organisation (FAO) of the United Nations and tries to balance simplicity, accuracy and robustness (Steduto et al., 2009). Only a small number of parameters and input data is required to simulate the crop yield response to water, which makes it a non-expensive tool to evaluate the effects of contour bunds (Biazin and Stroosnijder, 2012). Furthermore, the effect of soil contour bunds on runoff and erosion has been assessed in a separate, but related MSc research, carried out by Mrs Shannon de Roos.

AquaCrop has been used by researchers worldwide to simulate crop yields for different crops and all have found positive results (Hsiao et al., 2009; Heng et al., 2009; Andarzian et al., 2011; Mkhabela and Bullock, 2012). In addition, Todorovic et al. (2009) reports that, except in extreme water stress conditions, AquaCrop performs as well as other models, such as CropSyst and WOFOST, while it needs less input information. AquaCrop has also been used in the Northern Highlands of Ethiopia by Araya et al. (2010) and Tsegay et al. (2012). Araya et al. (2010) reports that AquaCrop can be used to evaluate water use efficiency and assess crop yields for scenarios with alternative water management strategies in teff and Tsegay et al. (2012) reports that AquaCrop could help improve the water productivity of teff. Moreover, Biazin and Stroosnijder (2012) used AquaCrop to simulate the effect of tied-ridges in the Rift Valley Drylands of southern Ethiopia. They reported that AquaCrop is able to simulate root zone soil water, canopy cover and crop yields pretty well.

The main objective of this study is to quantify the influence contour soil bunds have on soil moisture conservation and how it affects maize yield on a hillslope scale in the Bokole watershed. To better establish the main objective it is divided into the following sub-objectives:

1. To quantify the amount of increased soil moisture content, aboveground dried biomass and maize yield due to contour soil bunds;
2. To simulate the soil moisture content and crop production with FAOs AquaCrop for plots with and without contour soil bunds;
3. To determine which locations within a plot benefit most from contour soil bunds;
4. To determine which parameters have the largest influence on the aboveground biomass production, which is related to the maize yield;
 - a. *How does the variation in soil moisture content within plots impact the aboveground biomass by stressing growth conditions?*
 - b. *How does the variation in soil fertility between plots influence the aboveground biomass?*
 - c. *How does the variability in rainfall and temperature impact the aboveground biomass by stressing growth conditions?*

The study is conducted on two fields, which are located close together in the Bokole watershed in southwestern Ethiopia. Both fields consist of several plots with and without soil bunds. The second

chapter gives a more detailed explanation of the study area and the experimental setup of the study. The main objective of the study is determined by achieving the sub-objectives. The first sub-objective is achieved by conducting fieldwork and measuring the soil moisture every other day for 3 weeks in August and the total yield is determined at the end of the growing period. The second sub-objective is achieved by simulating the conditions for each subplot separately in FAOs AquaCrop. The third sub-objective is determined by conducting simulations for multiple locations within a plot. The soil moisture content is measured at different locations within the plots and the other input parameters are assumed constant over the entire plot. Therefore, the simulations per location within a plot only differ in soil moisture. These simulations make it possible to see the effect of location within the plot (e.g. close to bund, in the middle of the plot, etc.) on the soil moisture content, the aboveground biomass and the yield. The fourth sub-objective is determined by conducting multiple simulations in AquaCrop. Sub-objective 4a is determined by comparing the results of the simulations used to determine sub-objective 3 for soil moisture with the results for aboveground biomass. Sub-objective 4b is determined by comparing the aboveground biomass of the simulations with variable soil fertility stress for each subplot and the simulations with an average soil fertility stress for the whole field. Changes between the simulations with and without average soil fertility stress indicate the effect of soil fertility stress on the aboveground biomass. Sub-objective 4c is determined by conducting simulations with average soil fertility stress for different weather conditions of previous years over the period 2005 – 2016. All simulations are conducted with the FAO AquaCrop model, which is described in the first part of the third chapter as well as an overview of which AquaCrop simulations are performed for this study. The second part of the third chapter describes the method and the data acquisition. The model and fieldwork results are shown in chapter 4 and discussed in chapter 5. The objectives are answered and an overall conclusion is given in chapter 6 and lastly, final recommendations are given in chapter 7. In addition, the appendices show more detailed explanations of certain methods and tables with more detailed data and results.

2. Study area and experimental setup

2.1 Study area

The study area is located in the Bokole watershed, which is 500 km southwest of the Ethiopian capital Addis Ababa (figure 2). The watershed drains into the reservoir of the Gibe III hydro-electric power plant on the Omo River. It covers about 54 km² and has 11,798 inhabitants (Wolka et al., 2013). The topography varies between 1160 and 2400 meters above sea level (Wolka et al., 2016). The mean annual rainfall is approximately 1750 mm in the upper part of the watershed (Wolka et al., 2016) and ranges between 1400 and 1600 mm in the lower part of the watershed (SNNPRC-BoFED, 2004). The average minimum and maximum temperature are, respectively, 12.2 °C and 22.0 °C for the upper part of the watershed and 22.6 °C and 25.0 °C for the lower part of the watershed (SNNPRC-BoFED, 2004). The climate in the Bokole watershed is classified as a tropical savannah climate (Aw) using the Köppen classification (climate-data.org [date of search: 19-05-2016]). The soil type in the Bokole watershed is mainly classified as orthic Acrisol, but dystric Nitosol also cover a small part of the watershed (Wolka et al., 2016). More specifically, the study area is located between 6°58'40" - 6°59'02"N latitude and 37°17'47" - 37°17'57"E longitude (figure 2c.), which is in the upper part of the Bokole watershed. It is located close to a small city called Gessa. The altitude of the study area is approximately 1735 meters above sea level. Furthermore, the average annual rainfall in the study area is 1950 mm, which is higher than the average mentioned above.

The crops which are cultivated in the entire Bokole watershed are maize (*Zea mays L.*), sorghum (*Sorghum bicolor*), teff (*Eragrostis tef*), and haricot bean (*Phaseolus vulgaris*). In addition, Barley (*Hordeum vulgare*), wheat (*Triticum aestivum*), pea (*Pisum sativum*), Enset (*Ensete ventricosum*) and bean (*Vicia faba*) are also grown in the upper part of the watershed and sweet potato (*Ipomoea batatas*) and cassava (*Manihot esculenta*) are commonly cultivated in the lower watershed (Wolka et al., 2016). However, only maize is cultivated on the experimental fields.

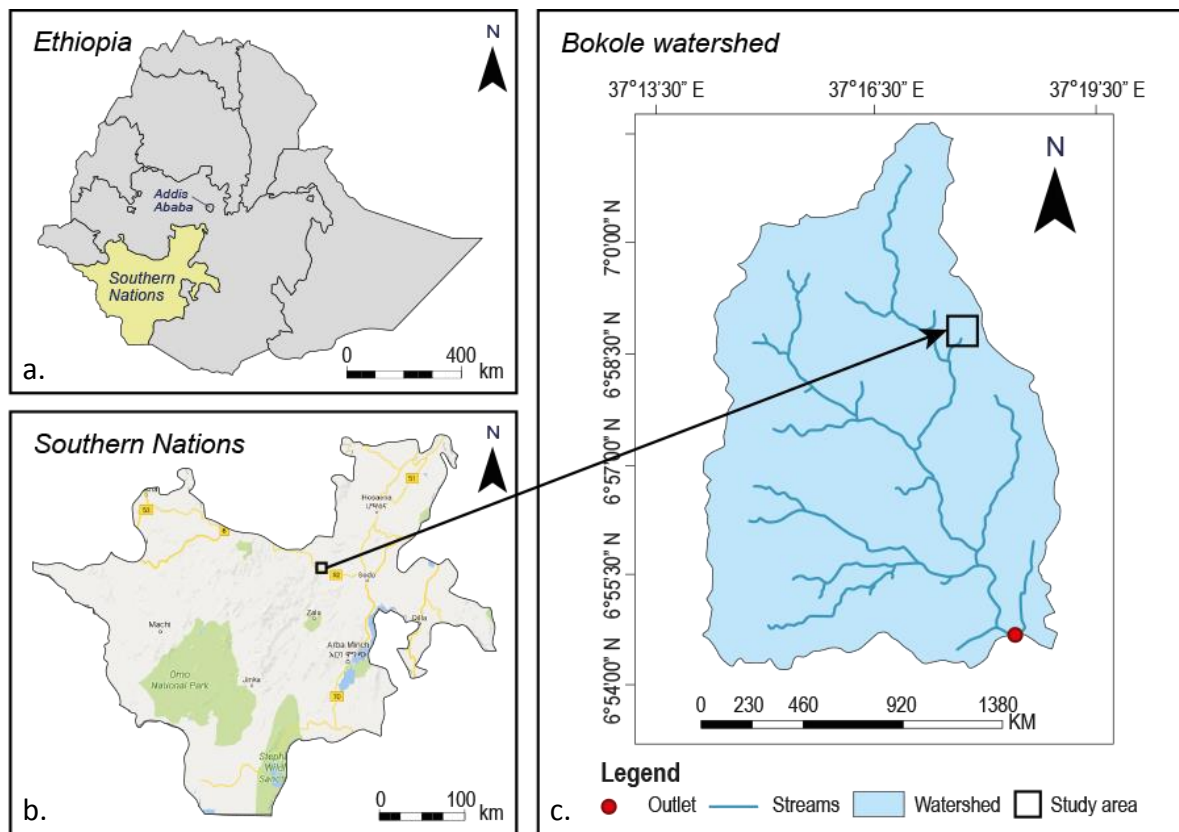


Figure 2. Location of the Bokole watershed and the study area. a. Location of the study area within Ethiopia. b. Location of the study area in the Southern Nations regional state. c. Location of the study area in the Bokole watershed.

Contour bunds are widely used as a SWC measures in the Bokole watershed, where contour soil bunds are mostly found in the upper part and contour stone bunds in the lower part due to the availability of stones (Wolka et al., 2016). Since the study area is located in the upper part of the Bokole watershed, it only uses contour soil bunds.

2.2 Experimental setup

For this study, 2 experimental fields with each 6 plots cultivated with maize will be used to determine the effect contour soil bunds have on the soil moisture content and the maize yield. Figure 3 gives a schematic view of the experimental fields. The two experimental fields are located close together and are both situated in the upper part of the Bokole watershed and contain only contour soil bunds. The soil bunds were constructed 8 years ago, but due to lack of maintenance they more or less disappeared. In the beginning of 2016, the soil bunds were reconstructed for this study, except for the control plots. However, the presence of old soil bunds was still visible on the control plots shown by a bump in the middle of the control plots. On each field there are two control plots which do not contain any contour bunds. The control plots are plot 2 and 5 for field 1 and plot 3 and 5 for field 2 (figure 3). The other plots each contain 3 contour soil bunds, in the beginning, in the middle and in the end of the plot. Each plot is divided in an upper plot (a) and a lower plot (b). For the plots containing bunds, subplot a is located between the upper and middle bund and subplot b is located between the middle and the lower bund. The middle bunds are often not located in the middle of the plot. But, in general, the upper part is smaller than the lower part of the plot. For the control plots, the boundary between plot a and b is the middle of the plot. All measurements are conducted for each subplot. The length and width of the plots differ from each other, but in average the plots of field 1 are 18m by 7m and the plots of field 2 are 16m by 9m. For additional support, the bunds are grown with grass and weeds. In addition, seeds of *Sesbania sesban* were directly sown on plot 1 and 3 of field 1 and on plot 1 and 6 of field 2 in May 2016. During the fieldwork conducted for the study, the *Sesbania sesban* had a maximum height of approximately 50 cm. Therefore, they did not interfere much with processes imported for this study. In the future, the *Sesbania sesban* is expected to increase the soil fertility because it is a N₂-fixing legume (Phiri et al., 1999).

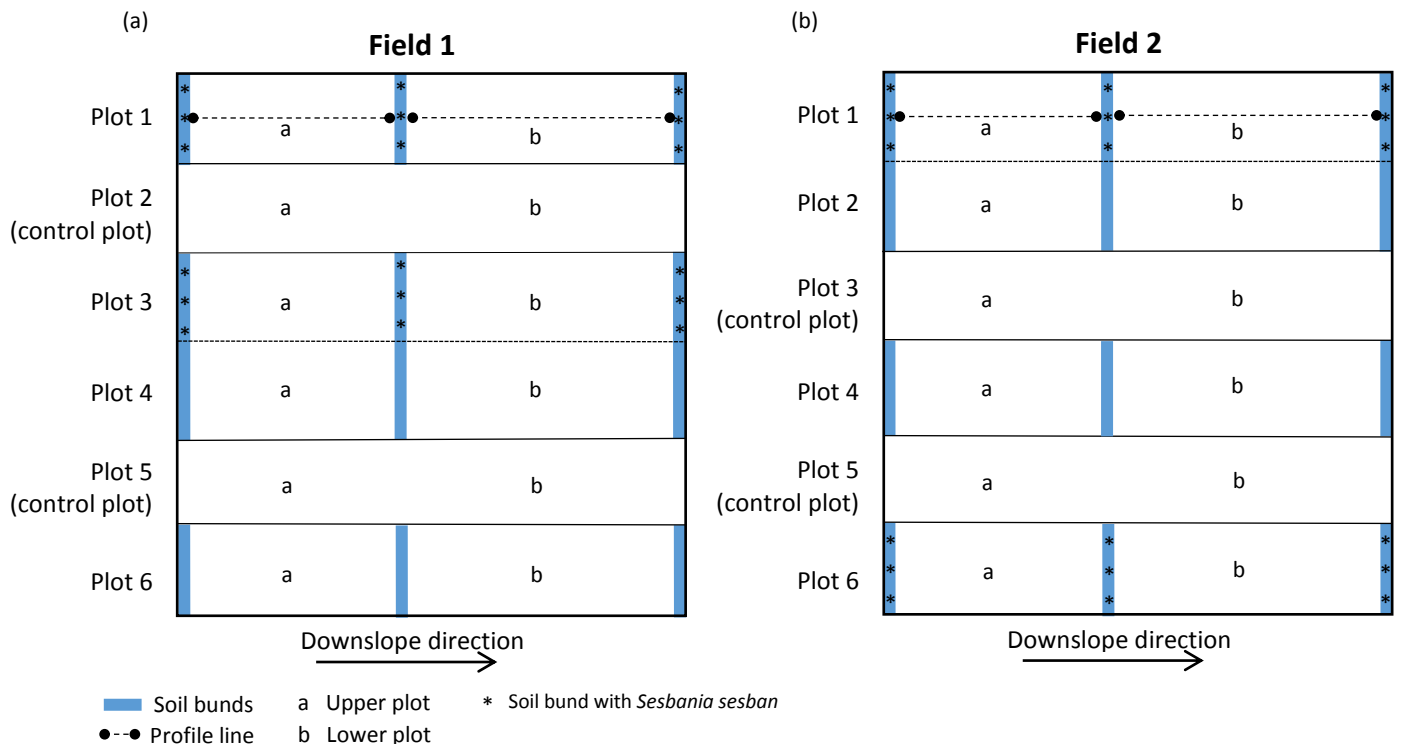


Figure 3. Schematic top view of the experimental setting in (a) field 1 and (b) field 2. The blue lines indicate contour soil bunds and the dashed line represents the profile line along which measurements are conducted.

3. Materials and methods

3.1 FAO AquaCrop

In this study, the FAO AquaCrop model is used to simulate crop yield response to soil moisture availability. AquaCrop evolves from the approach used by Doorenbos and Kassam (1979). In this approach the relative evapotranspiration is crucial in estimating the crop yield, but AquaCrop only uses the transpiration and a normalized water productivity to estimate the crop yield (Biazin and Stroosnijder, 2012). AquaCrop separates the evapotranspiration (ET; mm) into soil evaporation (E; mm) and crop transpiration (Tr; mm) and the final yield (Y; g m⁻²) into biomass (B; g m⁻²) and harvest index (HI; %) (Steduto et al., 2009). These separations avoid the confusing effect of the non-productive consumptive use of water and allows the partitioning of functional relations as response to environmental conditions (Steduto et al., 2009). Furthermore, the AquaCrop model also distinguishes itself from other models because it uses green canopy cover (CC; %) instead of leaf area index (LAI) and it normalizes the water productivity values (WP; g m⁻² mm⁻¹) for atmospheric evaporative demand and CO₂ concentration (Raes et al., 2011). Besides estimating the crop yield, AquaCrop can also simulate the soil water content, using basic soil and weather data by means of a daily soil water balance of the root zone (Raes et al., 2011).

AquaCrop uses a calculation scheme, which simulates the following processes with a daily time step: soil water balance, crop development, soil evaporation and crop transpiration, aboveground biomass and the partitioning of biomass into yield (figure 3) (Raes et al., 2011). Furthermore, management practices need to be indicated in AquaCrop, since they affect the soil water balance, the crop development and the crop yield (Raes et al., 2011). In the next paragraphs, these processes will be discussed step-by-step.

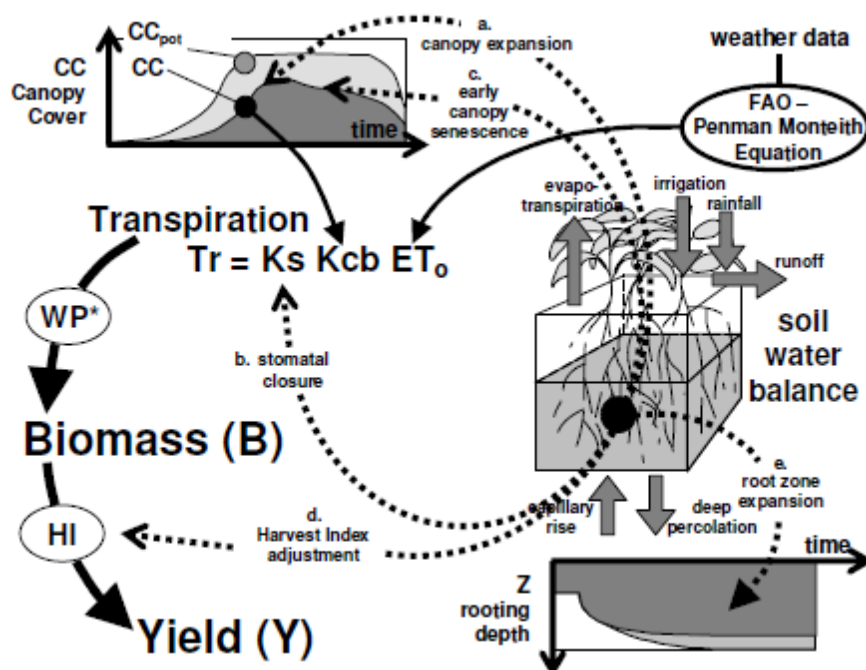


Figure 4. Calculation scheme of AquaCrop with indication (dotted arrows) of the processes affected by water stress. CC is the simulated canopy cover, CC_{pot} is the potential canopy cover, K_s is the water stress coefficient, K_{cb} the crop coefficient, ET₀ the reference evapotranspiration, WP* the normalized crop water productivity and HI is the Harvest Index. (Raes et al., 2011)

3.1.1 Soil water balance

The root zone can mathematically be described as a reservoir (Lievens, 2014). The amount of water retained in the root zone can be determined by keeping track of the incoming (precipitation, irrigation,

capillary rise) and outgoing (deep percolation, evapotranspiration) fluxes at the boundaries of the root zone (Raes et al., 2011). The amount of water stored in the root zone can be described as an equivalent depth (eq. 1) or as a shortage (eq. 2) (Raes et al., 2010).

$$Wr = 1000 \theta Z \quad (eq. 1)$$

$$Dr = Wr_{FC} - Wr = 1000(\theta_{FC} - \theta)Z \quad (eq. 2)$$

Where Wr is the soil water content of the root zone expressed as a depth (mm), θ is the actual soil moisture content in the root zone ($m^3 m^{-3}$), Z is the effective rooting depth (m), Dr is the root zone depletion (mm) and FC stands for field capacity. The root zone depletion is the amount of water that is required to bring the water amount in the root zone back to field capacity, which is the maximum amount of water that can be held in the root zone against gravitational forces (Raes et al., 2010). It is useful to express the water content as a shortage when water stresses need to be assessed and irrigational schemes need to be made and as a depth when the soil water balance of the root zone is calculated (Raes et al., 2010).

To simulate the amount of deep percolation (DP; mm), a drainage function is used which simulates the drainage out of a soil profile, the redistribution of water into a soil layer and the infiltration of rainfall by describing the amount of water lost by free drainage over time between saturation and field capacity (eq. 3) (Raes, 1982; Raes et al., 2010).

$$\frac{\Delta\theta}{\Delta t} = \tau(\theta_{SAT} - \theta_{FC}) \frac{e^{\theta - \theta_{FC}} - 1}{e^{\theta_{SAT} - \theta_{FC}} - 1} \quad (eq. 3)$$

Where $\frac{\Delta\theta}{\Delta t}$ is the drainage ability ($m^3 m^{-3} day^{-1}$), θ_{SAT} is the soil moisture content at saturation ($m^3 m^{-3}$), θ_{FC} the soil moisture content at field capacity ($m^3 m^{-3}$), θ the actual soil moisture content ($m^3 m^{-3}$) and τ is the drainage characteristic. The drainage characteristic describes the decrease in soil water content of a soil layer at the first day of free drainage (eq.4) (Raes et al., 2010).

$$\tau = 0.0866 K_{sat}^{0.35} \quad (eq. 4)$$

Where K_{sat} is the saturated hydraulic conductivity ($mm day^{-1}$). Then, the amount of water which percolates out of the bottom of the soil profile at the end of each day can be determined with eq. 5 (Raes et al., 2010).

$$DP = 1000 \frac{\Delta\theta}{\Delta t} \Delta z \Delta t \quad (eq. 5)$$

Where Δz is the thickness of the draining soil profile (m) and Δt is the time step, which is 1 day.

AquaCrop determines the amount of water lost by surface runoff with the runoff curve number method developed by the US Soil Conservation Service (USDA, 1964). The runoff process is described by eq. 6, which uses the amount of rainfall and the potential maximum storage, which can be determined with eq. 7 (Raes et al., 2010).

$$R = \frac{(P - 0.2S)^2}{P + S - 0.2S} \quad (eq. 6)$$

$$S = 254 \left(\frac{100}{CN} - 1 \right) \quad (eq. 7)$$

Where R is the amount of water lost by surface runoff (mm), P is the amount of rainfall, $0.2 S$ is the initial abstraction (mm), S is the potential maximum storage (mm) and CN is the Curve Number. During rainfall, water infiltrates the soil until the topsoil becomes saturated, which happens when the amount of rainfall equals the initial abstraction. Afterwards, additional rainfall becomes surface runoff (Raes et al., 2010). The value of CN depends on the land use or land cover (e.g. fallow, row crops, forest,

etc.), the treatment or practice (e.g. contoured, terraced, etc.) and the hydrologic soil group (Dingman, 2015). The Natural Resources Conservation Services (NRCS) defines four hydrological soil groups which are largely based on the minimum infiltration capacity. A lower minimum infiltration capacity results in a higher CN (Dingman, 2015). Furthermore, the value of S is adjusted to reflect the antecedent moisture conditions (AMC). AMC can be divided into three soil wetness conditions: AMC I (dry but above wilting point), AMC II (average) and AMC III (near saturation) (Dingman, 2015). In AquaCrop, the required input CN refers to the value for AMC II (Raes et al., 2012). But, when the soil wetness conditions are near wilting point or saturation, CN will be adjusted in AquaCrop due to adjustments in S for AMC I (eq. 8) and AMC III (eq. 9), respectively (Michel et al., 2005).

$$S_I = \frac{S_{II}}{0.42} \quad (eq. 8)$$

$$S_{III} = \frac{S_{II}}{2.3} \quad (eq. 9)$$

Where S_I is the potential maximum storage for AMC I (mm), S_{II} is the potential maximum storage for AMC II (mm) and S_{III} is the potential maximum storage for AMC III (mm).

The minimum infiltration capacity is approximately the same as K_{sat} (Dingman, 2015). Therefore, the default value for CN in AquaCrop is based on K_{sat} (Raes et al., 2012). However, CN can also be specified by the user. Furthermore, field practices, like soil bunds, can limit or even prevent surface runoff. When soil bunds are present on the field runoff is prevented and water that cannot infiltrate due to excessive rain is stored between the bunds (Raes et al., 2010). But, water that overtops the soil bunds is lost to surface runoff (Raes et al., 2010).

3.1.2 Crop development

AquaCrop uses the green canopy cover (CC; %) to describe crop development. The expansion, conductance, ageing and senescence of the canopy cover determines the amount of water that is transpired (T_r ; mm) (Raes et al., 2011). The green canopy cover is the soil surface covered by the green canopy divided by the unit ground surface area and ranges from 0%, when the soil is bare, to 100%, when there is full canopy cover (figure 6). The crop parameters needed to describe the canopy cover are depicted in figure 5, where CC_0 is the initial canopy cover at 90% emergence (%), CC_x the maximum canopy cover (%), CGC the canopy growth coefficient (% day⁻¹) and CDC is the canopy decline coefficient (% day⁻¹) (Raes et al., 2011). The CC_x is the highest CC which is reached and is normally reached around the time of fully flowering, after which the canopy cover is constant until it starts to decline. CGC describes the canopy expansion between crop emergence and full development and CDC describes the declining phase as the crop reaches maturity (Raes et al., 2011).

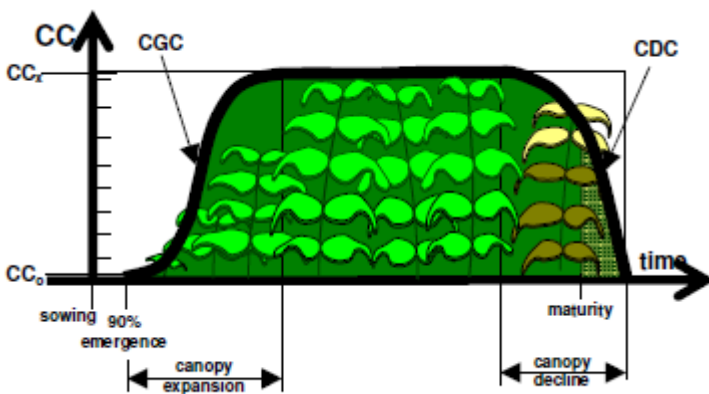


Figure 5. Variation of green canopy cover (CC) during the crop cycle without any stress conditions. (Raes et al., 2011)

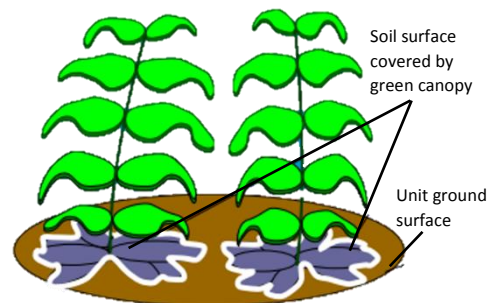


Figure 6. The green canopy cover (Raes et al., 2011)

The canopy cover is simulated with three equations. Eq. 10 describes the exponential growth and is applicable when $CC \leq 0.5CC_x$. But, when the canopy grows further and covers more soil, the radiation capture and the photosynthesis begin to increase less than is assumed in eq. 10 due to mutual shading among the plants (Steduto et al., 2012). Therefore, CC is described with eq. 11 when $CC > 0.5CC_x$ (Raes et al., 2010).

$$CC = CC_0 e^{t*CGC} \quad (eq. 10)$$

$$CC = CC_x - 0.25 \frac{(CC_x)^2}{CC_0} e^{-t*CGC} \quad (eq. 11)$$

Where t is time in days. As the crop approaches maturity, CC starts to decline due to canopy senescence. Canopy senescence starts due to biological aging of the crops and is indicated by the yellowing of the leaves. When canopy senescence starts, the transpiration and the photosynthesis decline and the biomass production is slowed down (Steduto et al., 2012). When senescence starts, the decline in green canopy cover is described by eq. 12 (Raes et al., 2012).

$$CC = CC_x \left[1 - 0.005 \left(e^{\frac{CDC}{CC_x} t} - 1 \right) \right] \quad (eq. 12)$$

Furthermore, stress coefficients (Ks) are used to model the effect of stress on crop development (Lievens, 2014). Ks is an indicator of the relative intensity of the effect on a specific growth process and growth stage and varies from one, when there is no stress, to zero, when there is full stress (Steduto et al., 2012). As long as the upper threshold of a stress indicator is not passed, there is no stress and Ks is 1. But, when the lower threshold is passed the stress is at its maximum and Ks is 0. The value of Ks between 0 and 1 depends on the shape factor, which determines the shape of the Ks curve. The thresholds and the shape factor are crop specific parameters (Steduto et al., 2012). In general, AquaCrop distinguishes four types of stresses: water stress, aeration stress, soil fertility stress and temperature stress. Water stress leads to canopy expansion stress and when it is severe enough it triggers early senescence (Steduto et al., 2009). Aeration stress leads to stomatal closure. The soil fertility stress decreases the growing capacity of the crops. And, temperature stress impedes the biomass production. Furthermore, figure 7 shows the Ks curve of the water and aeration stress.

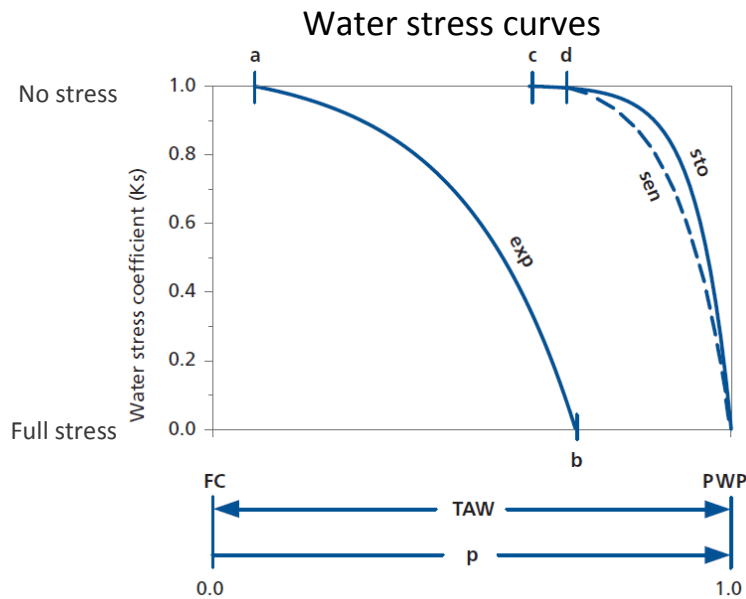


Figure 7. The Ks curves of the canopy expansion stress (exp), the senescence (sen) and the stomatal closure (sto), where a and b are the upper and the lower threshold for expansion stress, respectively, c and d are the upper threshold for stomatal closure and senescence, respectively, and the lower threshold for stomatal closure and senescence is at permanent wilting point. (Steduto et al., 2012)

When the soil moisture content drops below the upper threshold for canopy expansion, canopy expansion stress will start to occur. When the soil moisture content drops below the lower threshold for canopy expansion, it is completely halted (Raes et al., 2010). This is determined with eq. 13 and eq. 14, respectively. If the root zone depletion exceeds $Dr_{exp,upper}$ or $Dr_{exp,lower}$, canopy expansion stress will occur or leaf growth will be halted, respectively. $Dr_{exp,upper}$ and $Dr_{exp,lower}$ are determined with the total available water (TAW; mm), which is determined with eq. 15 (Raes et al., 2010).

$$Dr_{exp,upper} = p_{exp,upper} TAW \quad (eq. 13)$$

$$Dr_{exp,lower} = p_{exp,lower} TAW \quad (eq. 14)$$

$$TAW = 1000(\theta_{FC} - \theta_{PWP}) Z = Wr_{FC} - Wr_{PWP} \quad (eq. 15)$$

Where $Dr_{exp,upper}$ is the upper threshold expressed as a root zone depletion (mm), $p_{exp,upper}$ is the fraction of TAW that can be depleted from the root zone before canopy expansion starts to be limited, $Dr_{exp,lower}$ is the lower threshold expressed as a root zone depletion (mm) and $p_{exp,lower}$ is the depletion fraction of TAW at which there is no longer any canopy expansion growth and Wr_{PWP} is the soil water content of the root zone at permanent wilting point (mm) (Raes et al., 2010). To simulate the effect of canopy expansion stress, CGC needs to be adjusted by multiplying it with the water stress coefficient for canopy expansion growth ($Ks_{exp,w}$) (eq. 16), which is 1 when there is no stress and decreases gradually to 0 when stress increases.

$$CGC_{adj} = Ks_{exp,w} CGC \quad (eq. 16)$$

Due to canopy expansion stress, the CC_x and the maximum rooting depth might not be reached or much later in the season (Raes et al., 2010).

Similar to the canopy expansion stress, early canopy senescence is triggered when the root zone depletion exceeds the upper threshold for early senescence. To simulate early senescence, CDC needs to be adjusted to the degree of water stress with the water stress coefficient for senescence (Ks_{sen}) (Raes et al., 2010). Ks_{sen} is 1 if the soil water depletion in the root zone is below the fraction of TAW that can be depleted from the root zone before canopy senescence is triggered (p_{sen}) and Ks_{sen} is 0 when the root zone depletion exceeds the root zone depletion at permanent wilting point. To simulate a fast enough decline at high root zone depletions, the 8th power of Ks_{sen} is used to determine the adjusted CDC (eq. 17).

$$CDC_{adj} = (1 - Ks_{sen}^8) CDC \quad (eq. 17)$$

When the soil water content is sufficient again, the early canopy senescence is deactivated and gradually goes back to previous conditions (Raes et al., 2010).

On the contrary, when the soil water content exceeds the soil moisture content at anaerobic point, water logging occurs and the root zone becomes deficiently aerated (Raes et al., 2010). Aeration stress imposes stomatal closure and affects the transpiration rate. Due to the positive feedback mechanism of transpiration on canopy development, canopy development will be halted as a result of prolonged water logging, resulting in no canopy growth (Raes et al., 2010).

When the soil fertility is limited, the growing capacity of the crops is decreased (Raes et al., 2010). Consequently, CGC will decrease and the CC_x might not be reached or be reached later, so they need to be adjusted for soil fertility stress (eq. 18 and eq. 19, respectively).

$$CGC_{adj} = Ks_{exp,f} CGC \quad (eq. 18)$$

$$CC_{x,adj} = Ks_{CC_x} CC_x \quad (eq. 19)$$

Where $K_{s_{exp,f}}$ and $K_{s_{CC_x}}$ are soil fertility stress coefficients. For non-limiting soil fertility $K_{s_{exp,f}}$ and $K_{s_{CC_x}}$ will be 1, but if there is complete soil fertility stress they will be 0 and crop growth is no longer possible (Raes et al., 2010). Furthermore, due to limited soil fertility, the canopy cover will gradually decline when the CC_x is reached. Therefore, the CC after CC_x is reached will be simulated with eq. 20 (Raes et al., 2010).

$$CC_{adj} = CC_{x,adj} - f_{CD_{decline}} \left(\frac{(t - t_{full\ canopy})^2}{t_{sen} - t_{full\ canopy}} \right) \quad (eq. 20)$$

Where $f_{CD_{decline}}$ is the average daily decline of the canopy cover (fraction per day), t is the time after full canopy cover is reached (days), $t_{full\ canopy}$ is the time when full canopy cover is reached (days) and t_{sen} is the time when canopy senescence is started (days). Furthermore, soil fertility stress also decreases the biomass normalized water productivity (WP^* ; $g\ m^{-2}\ mm^{-1}$).

Lastly, the temperature stress depends on the amount of growing degree days (GDD; $^{\circ}C^{-1}\ day$). GDDs are determined by subtracting a base temperature, which is crop specific, from the average air temperature (Raes et al., 2011). When the average air temperature of a day is lower than the base temperature, there are no GDDs produced that day. GDDs are used to describe crop development in AquaCrop and determine the amount of temperature stress. A high amount of GDDs result in less temperature stress and vice versa.

In AquaCrop, the upper and lower thresholds for water stress are adjusted to the evaporating power of the atmosphere (ET_0). The default stress response curves are for an ET_0 of $5\ mm\ day^{-1}$. For the days when the actual ET_0 is lower or higher than $5\ mm\ day^{-1}$, the response curves need to be adjusted (figure 8) (Raes et al., 2010). A log term is included to make the adjustment greater when the soil is wet then when it is dry, because there is less impact of evaporative demand when the soil is dry (Raes et al., 2010).

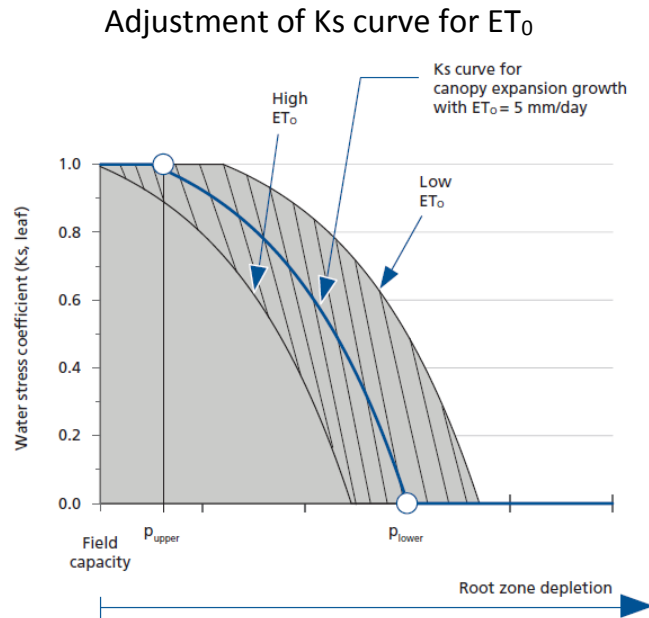


Figure 8. Adjustment for a K_s curve for canopy expansion when the ET_0 is higher or lower than $5\ mm\ day^{-1}$. The hatched area spans the range of adjustment as dictated by ET_0 . (Steduto et al., 2012)

3.1.3 Soil evaporation and crop transpiration

AquaCrop uses the dual crop coefficient approach to determine the evapotranspiration (ET; mm) (Raes et al., 2010). The crop transpiration (Tr ; mm) and the soil evaporation (E ; mm) are determined by multiplying the reference evapotranspiration (ET_0 ; mm) with the crop transpiration coefficient (K_{cb}) and the soil water evaporation coefficient (K_e), respectively. These coefficients distinguish the crop from the reference grass, which is used to determine ET_0 (Raes et al., 2010). The crop transpiration coefficient is proportional to the green canopy cover, while the soil water evaporation is proportional to the part of the soil surface not shaded by green canopy cover. However, after senescence starts the green canopy cover reduces quickly, but the dying canopy cover still reduces soil evaporation. Therefore, AquaCrop adjusts soil evaporation for the sheltering effect of withered canopy cover when the green canopy cover declines by using a coefficient which expresses the sheltering effect of the dead canopy cover (Raes et al., 2010).

Soil evaporation occurs in two stages. When the soil surface is wetted, water is first evaporated from a thin surface layer. This water is called the readily evaporable water (REW). Once REW is removed, water flows from the soil layer below to the surface layer to get evaporated and the amount of soil evaporation will depend on energy availability and hydraulic properties of the soil (Raes et al., 2010). As long as REW is not removed completely, the soil evaporation is at its maximum (eq. 21).

$$E_x = K_e ET_0 = ((1 - CC^*)K_{e_x})ET_0 \quad (eq. 21)$$

Where $(1 - CC^*)$ is the adjusted fraction of the non-covered soil surface, K_{e_x} is the soil evaporation coefficient for a fully wet and non-shaded surface and CC^* is the actual canopy cover adjusted for micro-advection (%), which can be determined with (Raes et al., 2010):

$$CC^* = 1.72CC - CC^2 + 0.30CC^3 \quad (eq. 22)$$

When all REW is removed, the maximum soil evaporation is multiplied by an evaporation reduction coefficient (K_r) to get the actual soil evaporation (eq. 23). K_r depends on the time of the year, weather conditions, transpiration, the relative water content of the soil layer and the hydraulic properties of the soil (Raes et al., 2010).

$$E = K_r E_x \quad (eq. 23)$$

Transpiration is at its maximum if the root zone is well watered and can be determined with eq. 24 (Raes et al., 2010).

$$Tr_x = K_{cb} ET_0 = (CC^* K_{cb_x})ET_0 \quad (eq. 24)$$

Where K_{cb_x} is the coefficient for maximum crop transpiration. After CC_x is reached but before senescence starts the canopy ages slowly which results in a small reduction in transpiration. To simulate ageing effects of the canopy, an adjusted K_{cb_x} is used after CC_x is reached. Furthermore, once senescence starts, transpiration reduces quickly in time. This is simulated by multiplying the adjusted K_{cb_x} with another adjustment factor f_{sen} , which declines from 1 at the start of senescence to 0, when no green canopy cover remains (Raes et al., 2010).

Crop transpiration can be reduced by either a shortage or an excess of water in the root zone. This is simulated by adding a water stress coefficient (K_s) (eq. 25), which is composed of the stress coefficients for water logging, stomatal closure and salinity stress (Allen et al., 1998). The water stress coefficients range between 1, when water stress does not exist and 0, when water stress is at its maximum and Tr is completely stopped (Raes et al., 2011).

$$Tr = ET_0 (K_s * CC^* * K_{cb_x}) = K_s Tr_x \quad (eq. 25)$$

Transpiration consists of water extracted out of the root zone. The amount of water that is extracted by the roots is determined by the root zone extraction term. In addition, the root distribution and total

root volume are also important in determining the amount of transpiration. Therefore, it is possible to implement a water extraction pattern in AquaCrop, dividing the effective root zone in 4 layers with each their own maximum root extraction (Raes et al., 2010). Since the soils in the Bokole watershed are shallow, the differences between the layer are not large.

3.1.4 Aboveground biomass

The aboveground biomass is computed with the crop water productivity (WP; g m⁻² mm⁻¹) and the simulated amount of water transpired (Tr; mm day⁻¹) (Lievens, 2014). The crop water productivity is the aboveground dry matter produced per unit land area per unit of water transpired. The relationship between the produced biomass (B; g m⁻²) and Tr is highly linear (Raes et al., 2011):

$$B = WP \sum Tr \quad (eq. 26)$$

However, AquaCrop uses the normalized water productivity (WP*; g m⁻²) for the simulation of aboveground biomass to correct for the effect of atmospheric CO₂ concentration and evaporative demand of the atmosphere (Lievens, 2014). The use of WP* makes the simulation of biomass applicable to more locations and seasons (Raes et al., 2011). In addition, WP* needs to be adjusted for atmospheric CO₂ when the concentration differs from the reference value, for soils with limiting soil fertility because the reservoir of nutrients gradually depletes when the crop develops. Furthermore, WP* needs to be adjusted for the type of products synthesized during the yield formation because more energy per unit dry weight is required for the synthesis of products rich in lipids and proteins than for the synthesis of carbohydrates (Azam-Ali and Squire, 2002). Before the aboveground biomass is determined, it is first adjusted for air temperature with a temperature stress coefficient (K_{S_b}), which varies between 0, when it is too cold to generate growing degrees that day and 1, when the biomass production is not restricted by the air temperature of that day. The improved equation to compute the aboveground biomass becomes (Raes et al., 2011):

$$B = K_{S_b} WP_{adj}^* \sum \frac{Tr_i}{ET_{0_i}} \quad (eq. 27)$$

Where Tr_i is the amount of transpiration on day i (mm day⁻¹) and ET_{0_i} is the potential evapotranspiration on day i (mm day⁻¹). Furthermore, by normalizing WP, a relationship between B and Tr was formed and crops could be divided in C3 or C4 crops based on their WP*. If WP* is between 15 and 20 g m⁻² the crop is a C3 crop and if WP* is between 30 and 35 g m⁻² the crop is a C4 crop (Raes et al., 2010).

3.1.5 Yield formation

Eventually, crop yield (Y; g m⁻²) is estimated with the simulated aboveground biomass and the harvest index (HI; %) (eq. 28) (Lievens, 2014). HI is the ratio of the yield mass to the total aboveground biomass that will be reached at maturity (Raes et al., 2010).

$$Y = B * HI \quad (eq. 28)$$

Due to water and temperature stresses, HI is continuously altered during the yield formation (Raes et al., 2011). To determine HI, the reference harvest index (HI₀), which is the harvest index for non-stressed conditions, and a multiplier which considers the stresses altering HI (f_{HI}) are used (Raes et al., 2011).

$$Y = f_{HI} HI_0 B \quad (eq. 29)$$

HI₀ is crop specific and f_{HI} depends on the timing and extent of stress during the crop cycle. Together, they adjust for failures and stresses during flowering and before- and during yield formation. During flowering, HI₀ needs to be adjusted for the risk of failure of pollination when water or temperature (heat or cold stress) stress occurs. On the contrary, when the conditions are favorable, the crop will

produce more flowers than necessary and HI_0 needs to be adjusted for excessive young fruits, which are aborted as older fruits grow. Before yield formation, a crop can spend less energy in its vegetative growth resulting in a HI which might be larger than HI_0 . Therefore, HI_0 needs to be adjusted. AquaCrop uses the relative biomass (ratio actual biomass to the potential (non-stressed) biomass) to determine the magnitude of adjustment. During yield formation, vegetative growth can still be possible and if water stress affects leaf expansion it results in an increase of HI_0 . But, if water stress affects crop transpiration during the yield formation there is a negative effect on HI_0 (Raes et al., 2010). At the end of the yield formation, the remaining CC can be below a minimum value, which results in inadequate photosynthesis, which leads to a reduction of HI (Raes et al., 2010). On the whole, the effect of water stress on HI (f_{HI}) can be positive, when there is water stress before yield formation or negative, when there is water stress during yield formation or during flowering (Raes et al., 2011). The computation of f_{HI} is one of the more complex computation procedures of AquaCrop. A more detailed explanation can be found in Raes et al. (2011).

3.1.6 Management practices

In AquaCrop, management practices are divided into field and irrigation management practices (Raes et al., 2011). Field management practices consider the soil fertility level and field-surface practices such as mulches to reduce soil evaporation or the application of soil bunds to control runoff and infiltration (Steduto et al., 2009). The level of soil fertility in AquaCrop ranges from non-limiting to very poor and affect the water productivity, the rate of canopy growth, the maximum canopy cover and the canopy senescence (Raes et al., 2011).

Furthermore, the irrigation management component in AquaCrop divides the crops in rain-fed or irrigated crops (Raes et al., 2011). If the crops are irrigated, the application methods and fraction of surface wetted need to be specified (Raes et al., 2011). It is also possible to specify the water quality of the irrigation water, the timing and amount of applied irrigation of each irrigation event (Raes et al., 2011).

3.2 AquaCrop simulations

AquaCrop simulates the daily green canopy cover, the daily soil moisture, the daily temperature stress, canopy expansion stress, stomatal closure and soil fertility stress, the daily biomass and yield production, the daily runoff, infiltration and drainage and the daily soil evaporation, transpiration and evapotranspiration for each location, which makes it possible to evaluate the differences in soil moisture content and yield. AquaCrop uses a set of four sub-model components that define the environment in which the crops develop: the climate, crop, soil and management component (Raes et al., 2011). For the soil component, initial soil moisture conditions are required for the beginning of the simulations. All simulations begin at 1 January and end at 31 December, but most results are only reviewed and discussed during the growing period. For this study, six different simulations for all subplots on both fields are conducted. Table 1 gives an overview of the different simulations.

First, the default simulation is the original simulation for 2016 with data from the center of the subplots. In this simulation, the measured and calculated data and the data from the literature are used as input. In addition, the measured soil moisture content and the total biomass are used to calibrate AquaCrop to get accurate simulations for the study area. AquaCrop is calibrated for the soil moisture content by changing the soil moisture content at field capacity and at saturation and the REW. These parameters are chosen based on the best fit between the simulated and the measured actual soil moisture content for the specific plot or location. The dried aboveground biomass is calibrated in AquaCrop by changing the soil fertility stress. Therefore, all subplots have their own calibrated soil fertility stress, which is variable between the plots. The default simulation is used to determine the differences between the plots with soil bunds and the plots without soil bunds. In addition, it is used to determine which parameters have the largest influence on the maize yield. Besides, the default simulation is used as the base for the other simulations.

Table 1. The different AquaCrop simulations performed in this study.

Name of simulation	Description
Default simulation	Original simulation, calibrated for 2016, variable soil fertility stress
Within plot simulation	Simulation of different locations within certain plots, calibrated for 2016, variable soil fertility stress
Average fertility simulation	Original simulation of 2016, with average soil fertility stress for each field
Average fertility within plot simulation	Simulation of different locations within certain plots of 2016, with average soil fertility stress for each field
All year simulation	Average fertility simulation for 2005 – 2016
All year within plot simulation	Average fertility within plot simulation for 2005 – 2016

Second, to assess which areas of the plots benefit most from the presence of contour soil bunds, the within plot simulation is performed for different locations within a subplot. Almost all parameters are assumed to be constant within the subplot, except for the soil moisture content, which is measured on different locations within the plot. For each location, AquaCrop is calibrated for the measured soil moisture content. Therefore, the AquaCrop input at different locations only differ in soil moisture content at field capacity and at saturation. The REW remains equal to the calibrated value in the default simulation. A number of plots for each field and a few locations within these plots are selected based on which plots have the largest difference in soil moisture content between locations within the plot, which is determined with IBM SPSS Statistics 20. Where possible, one location at the top, the middle and the bottom of the plot were chosen. The simulated biomass and yield within a subplot indicate a range of biomass and yield which can be produced on a plot and it gives an indication of the effect that changes in soil moisture have on the produced biomass and yield.

Third, the default and the within plot simulations are repeated with an average soil fertility stress, which are referred to as average fertility simulation and average fertility within plot simulation, respectively. For each field, the variable soil fertility stress of all plots is averaged and the simulations are run again to see the effect of soil fertility stress on the biomass and maize yield. Moreover, the variation in soil fertility stress is eliminated, which makes it easier to detect other parameters which significantly influence the maize yield.

Last, the average fertility simulation and the average fertility within plot simulation are used to conduct simulations for each year over the period from 2005 to 2016, which are referred to as the all year simulation and the all year within simulation, respectively. It has to be noted that for the all year and all year within plot simulations, the average soil fertility stress is used. However, there is no data available of the crop development in the fields for previous years. Therefore, all the input parameters remain the same to the situation in 2016, except for the climate data. So, basically the crop development, soil characteristics and management practices of 2016 are simulated for different weather conditions, which are based on the weather conditions in the Bokole watershed for the previous 11 years. The difference in climate data between years influences the soil moisture content, the amount of stress and, hence, also crop development and biomass and yield production. In AquaCrop, the tool 'Project' is used to simulate multiple runs of the same simulation for a number of successive years (Raes et al., 2012). The all year and the all year within plot simulations make it possible to determine the effect of temperature and rainfall on biomass and yield production. It gives an indication of the variation in stress levels and the biomass and yield production for drier and wetter years in the study area.

3.3 Data

3.3.1 Climate data

The weather input variables which are required to run AquaCrop are the daily maximum and minimum temperature, the daily rainfall, the daily reference evaporation and the mean annual CO₂ concentration in the bulk atmosphere. The rainfall and potential evaporation influence the water balance of the root zone, the temperature affects the crop development and the CO₂ concentration affects the crop water productivity (Raes et al., 2011).

Rainfall and temperature

The rainfall and temperature data are obtained by a NMS weather station in a nearby town called Gessa, which is located 5 km northwest of the fields and is 400 to 450 m higher in altitude (Wolka et al., 2016). This weather station has daily records of rainfall and temperature for each year between 2005 and 2016. These records can be used to simulate yield response to water for different weather conditions from the past. However, not all months were accounted for in this record. The years with the most data gaps are 2012, 2013 and 2016, with 2016 only missing data outside the crop growing period. Less importantly, 2011 and 2015 both miss one month outside the crop growing period. Therefore, a data filling procedure for the temperature and for the rainfall was necessary. The average of all available temperature data for every day was taken. These averages were then used to fill the months with missing data. For example, the average of all available temperatures of 1 January of all years is calculated and all years who miss temperature data on 1 January will be given this average to fill the data gap. However, accounting for the missing precipitation data is more difficult. Therefore, the average of each month of each year is calculated and compared with the average of each month for all years. The month with the most similar average to the all year average is used to fill the months with missing data. For example, when January of 2008 is the most similar to the all year average of January, this month will be copied to all the other years who miss data in January. This will be conducted for all months separately, so different years contribute to filling the data gaps.

Atmospheric CO₂

The historical time series of mean annual atmospheric CO₂ concentrations measured at Mauna Loa Observatory Hawaii are used. This data is used to normalize the water productivity to the CO₂ concentration in the atmosphere (Steduto et al., 2009).

Reference evapotranspiration

The reference evapotranspiration is calculated with the Makkink equation, which uses a radiation based approach (Kraalingen and Stol, 1997). Bruin and Lablans (1998) report that the results of the Makkink equation correspond with the results of the Penmann equation. The Makkink equation (eq. 30) only uses the air temperature (T ; °C), the incoming shortwave radiation at the earth's surface (S_t ; MJ m⁻² day⁻¹) and the gradient of the saturation vapour pressure curve (Δ ; kPa °C⁻¹) to estimate the reference evapotranspiration (ET_{MK} ; mm day⁻¹).

$$ET_{MK} = C_{MK} \frac{1000}{\rho\lambda} \frac{\Delta}{\Delta + \gamma} S_t \quad (eq. 30)$$

Where ρ is the water density (1000 kg m⁻³), λ is the latent heat of vaporization (2.45 MJ kg⁻¹), γ is the psychrometric constant (0.067 kPa °C⁻¹) and C_{MK} is the Makkink coefficient (Hendriks, 2010). The Makkink coefficient depends on the climate. Ogolo (2014) determined monthly Makkink coefficients in the Sub Sahelian Region in Nigeria, of which the Guinea Savannah region is the most similar to the study area in Ethiopia, in terms of latitude and climate. However, Ethiopia has a less dry period at the beginning of the year and a drier period at the end of the year. Therefore, the Makkink coefficient found in the Guinea Savannah region in Nigeria is slightly adjusted for those changes in climate. Table 2 shows the Makkink coefficient measured in Nigeria and the adjusted Makkink coefficient used to determine the reference evapotranspiration for Ethiopia. Furthermore, in order to calculate S_t , the

number of bright sunshine hours and the day length are required, which are available for Addis Ababa as monthly averages on Climatemps.com [*date of search: 9-12-2016*] and the sun's shortwave radiation incident at the top of the earth's atmosphere (S_0 ; MJ m⁻² day⁻¹) is needed, which can be determined with the latitude and the day of the year (Hendriks, 2010). An overview of the calculation procedure of the Makkink equation is given in Appendix 1.

Table 2. Makkink coefficient for Guinea Savannah in the Sub Sahelian region in Nigeria and the adjusted Makkink coefficient for the Bokole watershed in Ethiopia (Ogolo, 2014)

	Jan	Feb	Mar	Apr	May	Jun	Jul	Aug	Sep	Oct	Nov	Dec
Nigeria	0.90	0.88	0.81	0.75	0.69	0.65	0.66	0.67	0.66	0.64	0.68	0.78
Ethiopia	0.85	0.85	0.80	0.75	0.69	0.66	0.66	0.66	0.68	0.68	0.73	0.78

3.3.2 Crop data

In AquaCrop the crop component has five major components: phenology, aerial canopy, rooting depth, biomass production and harvestable yield (Steduto et al., 2009). Crops grow and develop during their growing cycle by expanding their canopy and deepening their rooting system, which can be inhibited by stress (Steduto et al., 2009). The majority of the crop and stress parameters for maize can be found in the Reference Manual, Annex III of the FAO (2012), which is given in Appendix 2. The Reference Manual is only used for parameters which could not be measured in the field. Other crop parameters, like the crop type, the planting method and important dates and periods of the growing period (e.g. sowing date, flowering, maturity, etc.) can be estimated on-site by observations (table 3). Only the duration of flowering was not observed in the field. Therefore, the indication given by the FAO was used to define the duration of the flowering stage of maize in the fields (FAO, 2012). AquaCrop uses the date of biological maturity, e.g. when grains are dried out and the maize is ready for harvest, as the end of the growing period, which can differ from the actual harvest date (Raes et al., 2012). The date of biological maturity is set on the day that the farmers wanted to harvest, but due to logistic matters they harvested later. Furthermore, the maize density is measured by counting the plants on 4 m² for each subplot and convert it to plants per hectare.

Table 3. Observed crop parameters in the field and important dates and periods of the growing period for field 1 and field 2. DAP means days after planting.

Observed crop parameters in the field		
Crop type	Grain producing crop	
Planting method	Sowing	
Growing period	Field 1	Field 2
- Date of sowing	19 April 2016	25 March 2016
- Day of emergence	7 DAP	7 DAP
- Start of flowering	65 DAP	68 DAP
- Fully flowering (CC _x is reached)	84 DAP	90 DAP
- Duration of flowering	20 days*	23 days*
- Physiological maturity reached	120 DAP	129 DAP
- Start of senescence	121 DAP	130 DAP
- Biological maturity reached	157 DAP	170 DAP
- Harvest	167 DAP	191 DAP

* Duration of flowering was not observed. Indication given by the FAO was used (FAO, 2012)

Green canopy cover

To determine the green canopy cover digital camera pictures were taken vertically towards the ground surface. For every subplot several pictures were taken at random locations. The images can be analyzed with the GreenCropTracker tool, which calculates a vegetation and gap fraction with the

algorithms discussed in Liu and Pattey (2010), to determine the green canopy cover (CC) (figure 9a). However, the GreenCropTracker tool can only be used when there are little weeds, grass and other green plants between the maize. When there is too much interference from other plants, CC was determined with Photoshop CC 2017. Everything that is not green canopy cover is removed from the picture by giving it a black color (figure 9b). Photoshop CC 2017 determines the percentage black in the picture and CC can be determined by subtracting the percentage of black from 100%.

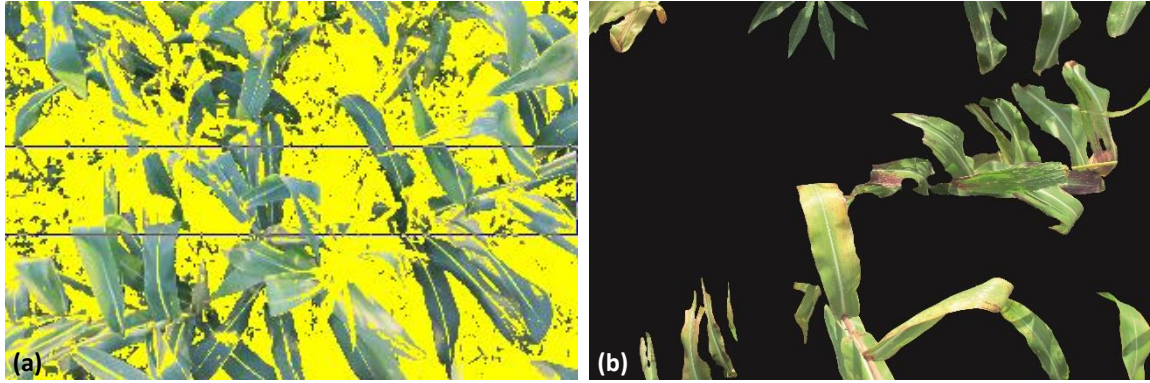


Figure 9. (a) Green canopy cover measured with the GreenCropTracker Tool in field 1. (b) Green canopy cover measured with Photoshop CC 2017 in field 2.

Pictures to determine CC were taken in the beginning of August and just before harvest. In the beginning of August, CC in field 1 was at its maximum. Consequently, the CC determined from those pictures is used as the maximum green canopy cover (CC_x). But, senescence already started in field 2 when the pictures were taken leading to a lower CC than CC_x . Therefore, CC_x of field 2 is determined with ratios between field 1 and field 2. The difference in CC between field 1 and field 2 can be represented by maize density and plant size. For both fields, the plant size was measured when the canopy cover reached its maximum, by measuring the diameter and length of the leaves. The average CC_x of field 2 ($CC_{x,avg,F2}$; %) can be determined with eq. 31 by using the plant density ratio, the plant size ratio and the average CC_x of field 1.

$$CC_{x,avg,F2} = \left(\frac{\rho_{maize,F2}}{\rho_{maize,F1}} \right) \left(\frac{S_{F2}}{S_{F1}} \right) CC_{x,avg,F1} \quad (eq. 31)$$

Where $\rho_{maize,F2}$ is the maize density of field 2 (plants ha^{-1}), $\rho_{maize,F1}$ is the maize density of field 1 (plants ha^{-1}), S_{F2} is the plant size of field 2 (cm^2), S_{F1} is the plant size of field 1 (cm^2) and $CC_{x,avg,F1}$ is the average CC_x of whole field 1 (%). To convert the average CC_x of field 2 ($CC_{x,avg,F2}$; %) to the CC_x for each subplot ($CC_{x,i}$; %), the ratio between the CC of the plot and the average CC of the field measured in August is used:

$$CC_{x,i} = \frac{CC_i}{CC_{avg}} CC_{x,avg,F2} \quad (eq. 32)$$

Where CC_i is the measured CC for plot i of field 2 in August (%) and CC_{avg} is the average measured CC of whole field 2 (%). Besides using the CC measurements of August for determining the CC_x , it was also used to determine the simulated average canopy decline in AquaCrop. In addition, also the plant height was measured for both fields in August by measuring randomly chosen plants with measuring tape.

The canopy cover just before harvest was totally dried, so only the total (yellowish) canopy cover was determined, which was not used in AquaCrop. Furthermore, the time when green canopy cover became 0% was observed for field 2. With proportions between length of growing stages between field 1 and field 2 the time when green canopy cover was 0% for field 1 was estimated. This is used to determine the canopy decline in AquaCrop, which determines the canopy decline coefficient (CDC).

Effective rooting depth

The maximum effective rooting depth, defined as the maximum depth at which roots take up the majority of the water, is measured after excavating a column of soil. When the rooting depth was deeper than the soil depth, the soil depth was taken as the maximum effective rooting depth because it is unlikely that roots can take up water below the soil effectively. The maximum effective rooting depth is measured when the crop reached its maximum canopy cover (Biazin and Stroosnijder, 2012). The time it takes after sowing to reach the maximum root depth is estimated by determining the day when the canopy cover reached its maximum. The minimum effective rooting depth is set equal to the shallowest measured soil depth, because the soil is shallower than the recommended minimum effective rooting depth of maize (FAO, 2012). Besides the effective rooting depth, AquaCrop also uses the water extraction pattern to simulate the root system, since most crops do not extract water uniformly throughout their rooting depth (Kranz et al., 2008). The water extraction pattern of maize follows the 4-3-2-1 rule, which means that 40% of the water is taken up in the top quarter of the soil, 30% in the second quarter, 20% in the third quarter and 10% in the bottom quarter of the soil (Kranz et al., 2008). The maximum root extraction can also be specified in AquaCrop. The recommended 3 mm day⁻¹ for each 0.10 m of rooting depth with a maximum value of 15 mm day⁻¹ for the entire root zone by the FAO is used (Raes et al., 2010).

Biomass and yield

The aboveground biomass and yield per m² were estimated for each subplot by oven drying the biomass samples and air drying the yield samples (Biazin and Stroosnijder, 2012). The aboveground biomass is estimated by cutting the crops at the ground level in a sample area of 2 m by 2 m. The total biomass is weighed in the field and a smaller sample is taken to dry in an oven for 24 to 48 hours at approximately 70 °C (Lievens, 2014). After oven drying the biomass samples, the percentage moisture loss is determined. The biomass measured in the field contained moisture, so to get the total biomass for the sample area the percentage moisture loss needs to be subtracted from the total biomass weighed in the field. To get the total biomass per m² the total biomass without moisture is divided by the sample area. The biomass harvested at the end of the crop cycle can be considered as an expression of the soil fertility level (Biazin and Stroosnijder, 2012).

The yield is estimated for the same sample area as the biomass. After weighing the biomass, the kernels of all the ears in the sample area are removed and weighed to get the total yield of the sample area. A smaller sample of the total yield is taken and air dried in the laboratory for approximately 3 weeks (Biazin and Stroosnijder, 2012). In the 3th week, the yield samples are weighed multiple times to see if the weight still decreases. After air drying the yield samples, the moisture loss is determined and subtracted from the total yield weighed in the field to get the total yield without moisture. To get the total yield per m² the total yield without moisture is divided by the sample area. Unfortunately, most of the yield samples were compromised due to maize eating insects resulting in many unreliable yield measurements. Hence, AquaCrop is calibrated for the measured dried aboveground biomass instead of the measured yield. The soil fertility stress was used to calibrate the biomass in AquaCrop for each subplot. Moreover, to simulate the biomass for previous years with the least uncertainty, the soil fertility stress calibrated for 2016 for each subplot is averaged for the whole field. The average soil fertility stress is used for all subplots.

3.3.3 Soil data

The soil component of AquaCrop allows up to five horizons of variable depths (Steduto et al., 2009). Each horizon has its own texture class with its own hydraulic characteristics, consisting of the saturated hydraulic conductivity (K_{sat}) and the moisture content at saturation (θ_{sat}), field capacity (θ_{FC}) and at permanent wilting point (θ_{pwp}) (Raes et al., 2011). However, the soils in the study area are shallow and consist of only one horizon. The thickness of the horizon is measured with a measuring tape and

a few disturbed and undisturbed samples of the soil are taken by using a soil auger to vertically drill into the soil profile and by using a core sampler, respectively. These samples are used to determine the bulk density, the gravimetric soil moisture content, the soil texture and the organic matter content. The saturated hydraulic conductivity is then determined by pedotransfer functions using the soil texture and the organic matter content. Furthermore, groundwater levels are often very low in African countries (Bonsor and MacDonald, 2011). Therefore, the groundwater level is assumed to be too low to interfere with the water balance of the root zone, so it does not need to be measured.

Bulk density

The bulk density is measured in the laboratory after soil samples at different locations and different depths were taken in the field with a core sampler, which has a volume of 385 cm². The soil samples were dried for 48 hours at 105 °C (Lievens, 2014). Afterwards, the bulk density is determined by dividing the mass of the dried soil in grams by the bulk volume of the soil sample in cm³ (Lievens, 2014).

Percentage texture class

The percentage sand, silt and clay are measured in the laboratory with the hydrometer method proposed by Buoyoucos (1936) and later improved by Buoyoucos (1962). The hydrometer method is simple and quick to use and is based on Stokes' law, which defines a relationship between soil particle sizes and their settling time (Beretta et al., 2014). The hydrometer method uses the difference in settling velocities of sand, silt and clay particles to determine the percentage of sand, silt and clay particles in the suspension. The sand particles, which are the largest, are assumed to settle almost immediately, while the clay particles are the only particles still in suspension after more or less 2 hours (Beretta et al., 2014). A detailed overview of the hydrometer method is given in Appendix 3. When the percentage sand, silt and clay were calculated, the soil texture class is determined with the soil texture triangle of the USDA (Daddow and Warrington, 1983).

Organic matter content

The organic matter content is measured in the laboratory with the Walkley and Black method proposed by Walkley and Black (1934). The method determines the soil organic carbon by using a strong oxidizing agent (potassium dichromate), which reacts with the organic carbon in the soil (Schumacher, 2002). The percentage organic carbon is then determined from the difference between total potassium dichromate and what is left unreacted after oxidation of carbon (Mylavarapu, 2014). After determining the total organic carbon in the soil it can be easily converted to soil organic matter content with the assumption that soil organic matter contains 58% carbon (Schulte and Hoskins, 2009). The procedure of the Walkley and Black method is given in Appendix 4.

Saturated hydraulic conductivity

The saturated hydraulic conductivity can be estimated with pedotransfer functions (PTFs). In recent years, PTFs have been widely used to estimate the hydraulic conductivity from easy to measure soil properties, such as bulk density, particle size distribution and organic matter content (Rasoulzadeh, 2011). Many PTFs have been developed to estimate the saturated hydraulic conductivity, each using similar and slightly different soil properties (e.g. Brakensiek et al., 1984; Campbell, 1985; Saxton et al., 1986; Vereecken, 1990; Wösten et al., 1997; Wösten et al., 1999; Saxton and Rawls, 2006). Hence, many studies reviewed the credibility and accuracy of the PTFs and found different results (Tietje and Hennings, 1996; Wagner et al., 2001; Gijsman et al., 2002; Rasoulzadeh, 2011; Yao et al., 2015). For example, Wagner et al. (2001) indicate that the PTF by Wösten et al. (1997) is the 'best' PTF, while Gijsman et al. (2002) conclude that the PTF by Saxton et al. 1986 performs best and Yao et al. (2015) found the PTFs by Saxton et al. (1986) and Wösten et al. (1997) most capable. However, there is no PTF suitable for all soils (Yao et al., 2015). Therefore, the best PTF for this research was chosen based on their results compared to the expected conductivity based on the soil texture class. Wösten et al. (1999) overestimated the saturated hydraulic conductivity, while Saxton et al. (1986) gave reasonable to low results. Fortunately, in 2006, Saxton and Rawls improved the PTF by Saxton et al. (1986), including adjustments for organic matter content, bulk density and the estimation of soil water

characteristics (Saxton and Rawls, 2006). The improved PTF leads to better results and is used in the computer model SPAW (Soil, Plant, Air, Water), which simulates daily hydrologic water budgets of agricultural landscapes (Saxton and Willey, 2006). Therefore, SPAW can be used to determine the saturated hydraulic conductivity with the PTF of Saxton and Rawls (2006). The equations scheme of Saxton and Rawls (2006) to determine the saturated hydraulic conductivity is given in Appendix 5. In addition, the PTF of Saxton and Rawls (2006) gives the option to account for the effect of small variations between the calculated and the measured bulk density by including a density adjustment factor (DF). Based on their research, Saxton and Rawls (2006) suggest a DF in the range of 0.9 to 1.3. To get similar calculated bulk densities by SPAW and measured bulk densities in the laboratory DF was set at 0.9 for all plots.

Soil moisture content at saturation, field capacity and permanent wilting point

The soil moisture content at saturation is assumed equal to the porosity, which can be easily calculated with eq. 26 using the bulk density (ρ_b ; g cm⁻³) and the particle density (ρ_s ; g cm⁻³) (Sterk and van der Meijden, 2007). The particle density is assumed to be 2.65 g cm⁻³ (Bittelli et al., 2008). And, the bulk density is measured for all subplots, so the porosity, and hence the soil moisture content at saturation, could be determined for all subplots.

$$\phi = \theta_{SAT} = 1 - \frac{\rho_b^d}{\rho_s} \quad (eq. 26)$$

The soil moisture content at field capacity is also measured in the field with a frequency domain reflectometer (FDR). A small area on each subplot is irrigated until the soil profile is saturated (Walker, 1989). After covering the plot with a plastic sheet to prevent evaporation, the soil moisture content measured the next day represents the soil moisture at field capacity. The soil moisture content at field capacity and at saturation are used to calibrate AquaCrop for the measured actual soil moisture content. Therefore, the values used in AquaCrop can differ slightly from the measured and calculated values for field capacity and saturation, respectively.

Moreover, AquaCrop gives indications of the hydraulic characteristics for each soil texture class. The soil moisture content at permanent wilting point could not be measured or calculated, so the indication given by AquaCrop is used. The soil moisture content at permanent wilting point is predominantly defined by the clay- and organic matter content (Raes et al., 2012). Since the organic matter content was approximately the same for all samples and the clay content in the samples was only in a small range of values, the soil moisture content at permanent wilting point was kept equal for all plots and both fields.

Actual soil moisture content

To measure the gravimetric soil moisture content, six soil samples from each field were taken to the laboratory in August to determine the gravimetric soil moisture content. The wet soil samples were weighed and afterwards dried in an oven at 105 °C for 24 hours and weighed again. Then, the dry weight moisture fraction (W ; g g⁻¹) can be calculated with (Walker, 1989):

$$W = \frac{\text{wet weight} - \text{dry weight}}{\text{dry weight}} \quad (eq. 33)$$

W is converted to the gravimetric moisture content (θ_{grv} ; %vol) with eq. 34, which only requires the bulk density (ρ_b ; g cm⁻³) and the density of water (ρ_w ; 1 g cm⁻³), which are both known parameters.

$$\theta_{grv} = \rho_b \frac{W}{\rho_w} \quad (eq. 34)$$

Furthermore, the actual soil moisture content is measured in the field. The soil moisture content is measured in the field with a Frequency Domain Reflectometer (FDR) (figure 10a). The Theta Probe Soil

Moisture Sensor ML3 with the read-out and data storage device HH2 Moisture Meter with an accuracy of 1 %vol was used (Delta-T Devices, Cambridge, England). FDRs make use of radio frequencies and the electrical capacitance of the soil to determine the dielectric permittivity. When the stainless steel rods of the ML3 probe are inserted in the soil, power is applied to the probe and a 100 MHz waveform is formed. The difference in charge between the probes creates an electromagnetic field (Campbell, 2014). When an electromagnetic field is created, polar molecules, like water, tend to reorganize themselves and store some of the charge that is produced in the soil (figure 10b). The FDR measures the charge storing ability of the soil as an output voltage (V; volts), which can be used to estimate the square root of the apparent dielectric permittivity, which is called the refractive index ($\sqrt{\epsilon}$) (Delta-T Devices Ltd, 2017):

$$\sqrt{\epsilon} = 1.0 + 6.175V + 6.303V^2 - 73.578V^3 + 183.44V^4 - 184.78V^5 + 68.017V^6 \quad (eq. 35)$$

Each material has its own dielectric permittivity. For example, air has a dielectric permittivity of 1, organic matter and soil materials between 2 and 5 and liquid water has a dielectric permittivity of approximately 80 (Campbell, 2014). Therefore, liquid water has a much higher ability to store charge than other materials found in natural soils. Over time, the organic material and soil minerals are constant in the soil and only air and water change. Air stores almost no charge, while water stores a large amount of charge. Hence, if the change in dielectric permittivity is measured it tells something about the soil moisture content (Campbell, 2014). One of the most widely used equations to calculate the soil moisture content out of the dielectric permittivity is the Topp equation developed by Topp et al. (1980) (eq. 36) (Yu and Yu, 2006).

$$\theta = 4.3 \times 10^{-6} \epsilon^3 - 5.5 \times 10^{-4} \epsilon^2 + 2.92 \times 10^{-2} \epsilon - 5.3 \times 10^{-2} \quad (eq. 36)$$

Where θ is the actual soil moisture content (%vol) and ϵ is the dielectric permittivity.

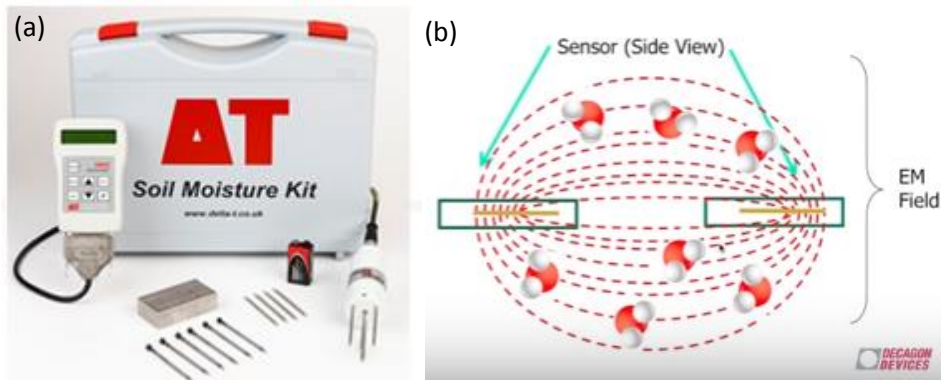


Figure 10. (a) Soil moisture kit used for this study. (b) Working of the FDR: the rods of the probe are inserted in the soil and create an electromagnetic (EM) field (Campbell, 2014).

To calibrate the soil moisture contents measured with the FDR, the values need to be multiplied by a correction factor. The correction factor can be determined by comparing the soil moisture contents measured by the FDR with the gravimetric soil moisture contents. The soil moisture content of the samples which were used to determine the gravimetric soil moisture contents is also measured with the FDR in the field. To determine the correction factor, the gravimetric moisture content is divided by the volumetric moisture content measured with the FDR for each sample. Then, the average of the ratios for each sample of field 1 and field 2 is taken as the correction factor, which is 0.764 for field 1 and 0.690 for field 2. Lastly, all FDR measurements are multiplied by these correction factors to get the calibrated soil moisture contents.

To calibrate AquaCrop for the measured soil moisture contents, the soil moisture content at field capacity and at saturation and the Readily Available Water (REW) are changed by trial and error until the simulated soil moisture content fits the measured soil moisture content best. Therefore, it is

possible that the soil moisture at field capacity and at saturation are slightly different from the measured and calculated values. REW is kept more or less constant for all plots on the whole field with a value of 6 mm for field 1 and 9 mm for field 2, but some plots have slightly higher or lower values. The soil moisture contents are calibrated for 2016 and the same soil moisture content at field capacity and at saturation is used for the simulation of previous years.

Experimental setup of the actual soil moisture measurements

The actual soil moisture content is measured every other day for field 1 and every three days for field 2 for 2.5 weeks in August and once more for both fields in October. The soil moisture measurements are conducted every 2 m along a profile line perpendicular to the soil bunds, which is in the middle of the plots and goes from the upper to the lower part (see profile line in figure 3). In addition, to get a more specific and detailed soil moisture profile, the soil moisture measurements for one plot on each field (plot 1 on field 1 and plot 2 on field 2) are 0.5 m apart when the profile line is close to the soil bunds.

Initial soil moisture conditions

The initial soil moisture conditions are also needed in AquaCrop. Daily temperature and rainfall data is available for the period of 2005 to 2016. Therefore, the initial soil moisture conditions in the beginning of 2016 are estimated based on the temperature and rainfall in the end of 2015. However, for the simulation of all years between 2005 and 2016, the initial soil moisture conditions cannot be estimated from the previous year, since there is no data available for 2004. Therefore, the initial conditions used for 2016 are also used for 2005. However, this probably does not affect the soil moisture content during the growing period. The years after 2005 take their initial soil moisture conditions from the end of the previous year.

Soil moisture statistics

The statistically significant difference in soil moisture between the fields, between the plots within the fields and between locations within the plots is determined by using IBM SPSS Statistics 20 to compare the soil moisture contents between fields, plots and locations within a plot. To determine the difference in soil moisture content between fields, soil moisture contents measured for both fields on the same date (16, 19, 24, 26, 28 August) are compared with the independent samples t-test. The independent t-test compares the means between the two fields of the soil moisture content measured on the same dates. There are six assumptions that need to be met before the independent t-test can be used. The dependent variable should be measured on a continuous scale, the independent variable should consist of two independent groups, there should be independence of observations, there are no significant outliers, the dependent variable needs to be normally distributed and there needs to be homogeneity of variances (Lund and Lund, 2013). The first three assumptions depend on the study design and the last three assumptions are tested in SPSS. For the soil moisture data of both fields, all assumptions are met and the independent t-test is used to determine the significance between the fields. However, to determine the statistically significant difference in soil moisture content between plots and within plots, the one-way ANOVA test (ANalysis Of VAriance) is used. The one-way ANOVA test is similar to the independent t-test, but is used if more than two groups need to be compared (Lund and Lund, 2013). The assumptions are the same as for the independent t-test, so the one-way ANOVA test can be used to determine the statistically significant difference in soil moisture content between plots and locations within plots. For all statistical tests, the difference in soil moisture content is significant if p is lower than 0.05 ($p < 0.05$).

To determine the difference in soil moisture content between plots, the soil moisture measurements of each plot are compared to the other plots for each measurement date using the one-way ANOVA test. The test tells whether there are differences between plots on a certain date or not, but not which plots have significantly different soil moisture contents from each other (Lund and Lund, 2013). If the one-way ANOVA shows an overall statistically significant difference in soil moisture content between

plots on a certain date, a post hoc test is run to confirm for which plots these differences occur. For this study, the Least Significant Difference (LSD) post hoc test is used. The LSD test is developed by R. Fisher in 1935 and explores all possible pair-wise comparisons of means comprising a factor using the equivalent of multiple t-tests (Stevens, 1999). On the whole, the one-way ANOVA test indicates for which dates the plots have a statistically significant difference in soil moisture from each other and the post hoc test indicates which plots have a statistically significant different soil moisture from each other on these dates.

To indicate which plots and locations within these plots are most appropriate for the within plot simulations, e.g. which plots have the largest difference in soil moisture content between locations within the plot, the one-way ANOVA test is used to determine the overall difference in soil moisture content between the locations within a plot for each subplot. The one-way ANOVA test indicates which subplots could be used for the within plot simulation and the LSD post hoc test indicates which locations within the chosen subplots could be used. If possible, one location at the top, the middle and the bottom of the plot were chosen.

Runoff: Curve Number method

It is assumed that the surface runoff on fields with contour soil bunds is zero. Therefore, the runoff is only important for the control plots, which is measured by Mrs Shannon de Roos in a separate accompanying study in the same experimental fields over the period from 1-7-2016 to 19-8-2016. This period contains 19 days with rain, so the total precipitation and the total runoff of the period is divided by 19. Then, the averages of one rain day are used to determine CN. First, the potential maximum storage (S ; mm) is determined with eq. 6 by trial and error. Then, CN is calculated by rewriting eq. 7 into eq. 37.

$$CN = \frac{100}{\left(\frac{S}{254}\right) + 1} \quad (eq. 37)$$

Water balance

The only imposed difference in AquaCrop between plots with and without bunds is the prevention of runoff on plots with bunds. To see the effect of runoff on other parameters of the water balance, the water balance of plots with bunds is compared with the water balance of plots without bunds. The water balance is given in eq. 38.

$$P = D + R + E + Tr + \Delta S \quad (eq. 38)$$

Where P is the amount of water added by rainfall (mm), D is the amount of water lost by drainage (mm), R is the amount of water lost by runoff (mm) E is the amount of water lost by soil evaporation, Tr is the amount of water lost by transpiration (mm) and ΔS is the amount of water stored in the soil (mm), which is assumed to be insignificantly small. Capillary rise is not included in the water balance because the groundwater table is too deep to influence the soil processes.

3.3.4 Management aspects

The height and the dimension of the contour soil bunds are measured with measuring tape. There is no mulch used on the fields. The level of soil fertility is not measured, but it is assumed that the aboveground biomass and the green canopy cover are an expression of the level of soil fertility. Therefore, the measured aboveground biomass and green canopy cover are used to estimate the level of soil fertility stress in the fields. Furthermore, there are no irrigation methods used in the Bokole watershed, so all the crops are rain-fed.

Besides, the slope of each subplot is measured with an inclinometer, which measures the slope in degrees and in percentage. The slopes of the subplots are not included in AquaCrop, but are used to evaluate the results.

4. Results

4.1 Measured data

The measured data is divided in weather conditions, soil properties, soil moisture measurements and crop and yield measurements. The measured total temperature and rainfall over the growing period for each year over the period 2005 to 2016 is presented in figure 11. The important soil properties are given in table 4. Furthermore, the average soil moisture measurements are displayed as graphs in figure 12 to 16 and a complete overview of all soil moisture measurements of field 1 and field 2 can be found in Appendix 6 and 7, respectively. Lastly, the important crop and yield parameters are given in table 7. All parameters in table 4 and 7, except for the soil moisture content at field capacity (θ_{FC}) are assumed to be constant in space within the plot. And, the bund height, CC_x , K_{sat} , the porosity, θ_{FC} , the number of plants per m^2 and the slope are assumed to be constant in time. An overview of all soil, crop and yield measurements is given in Appendix 9.

4.1.1 Weather conditions

The daily temperature and rainfall measured by the weather station is summed over the growing period for each year between 2005 and 2016 and is shown in figure 11a for field 1 and figure 11b for field 2. The temperature is represented by growing degree days (GDD), which is a measure of heat accumulation that can be used by crops. Therefore, a high GDD is better for crop development. The weather conditions differ between the fields because the start and length of the growing period is different for field 1 and field 2. The growing period of field 1 begins at 19 April and takes 157 days, while the growing period of field 2 start at 25 March and has a length of 170 days. The longer growing period of field 2 results in higher totals. But, the pattern between years is similar between the fields, with the exception of 2006, which has a relatively lower amount of rainfall in field 2, and 2005 and 2014, which have a relatively higher amount of GDDs in field 2. The year of 2016 has the most GDDs by far, while the least amount of GDDs is found in 2007. However, the amount of rainfall of 2016 is fairly average for both fields. The highest rainfall is found in 2007 and 2014 and the lowest rainfall is found in 2006.

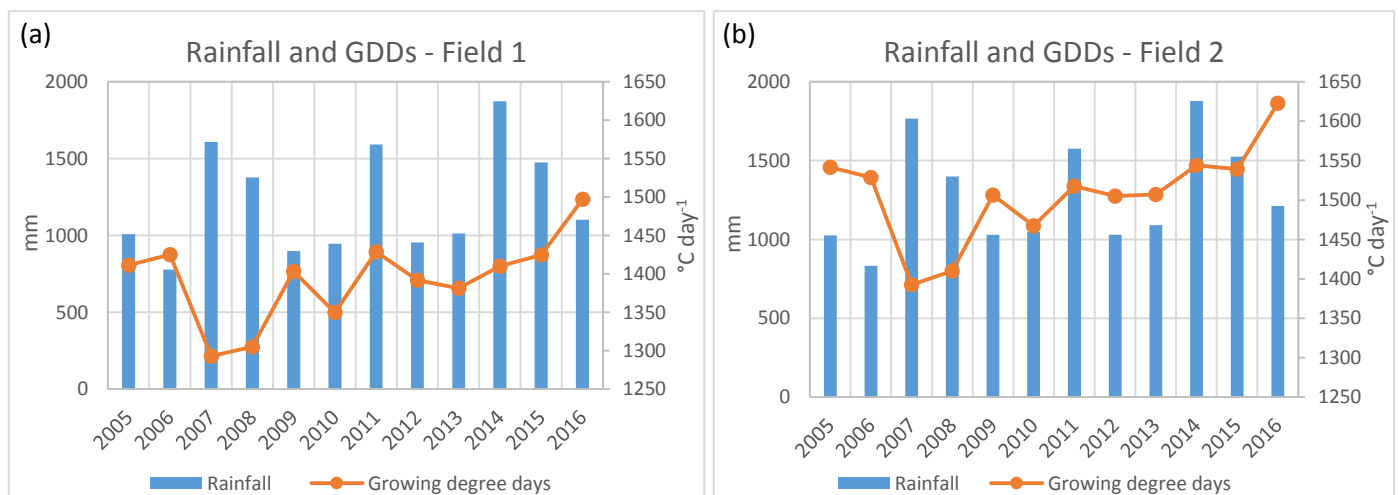


Figure 11. Total amount of rainfall and growing degree days (GDDs) for the growing period of each year for (a) field 1 and (b) field 2.

4.1.2 Soil properties

For both fields, K_{sat} changes fairly much between plots, but no pattern with regard to plots with and without bunds or upper and lower plots can be found. On the contrary, the porosity does not differ much between plots. Furthermore, it can be seen that θ_{FC} is higher in field 1 than in field 2, but the porosity is similar between the fields, which results in a smaller gap between θ_{FC} and θ_{SAT} in field 1. Furthermore, θ_{FC} changes slightly between plots, with a maximum difference of 7.3% in field 1 and

9.5% in field 2. It looks like θ_{FC} is slightly lower for the lower plots than the upper plots in field 1, but in field 2, the values of θ_{FC} are more or less similar, except for one outlier. Moreover, the soil depth between plots changes from 0.10 m to 0.62 m for field 1 and from 0.10 m to 0.19 m for field 2, which is a much lower and smaller range than for field 1. However, for both fields, there is no significant difference in soil depth between upper and lower plots or control plots and plots with soil bunds. But, the rooting depth changes more between plots and it can be noted that the rooting depth is slightly higher for control plots in field 1, while the rooting depth is slightly lower for control plots in field 2.

Table 4. Important calculated and measured soil properties for field 1 and field 2. The control plots are plot 2 and 5 for field 1 and plot 3 and 5 for field 2. K_{sat} is the saturated hydraulic conductivity and θ_{FC} is the soil moisture content at field capacity.

Soil properties										
Plot	Field 1					Field 2				
	Root depth	Soil depth	K_{sat}	Porosity	θ_{FC}	Root depth	Soil depth	K_{sat}	Porosity	θ_{FC}
	m	m	mm day ⁻¹	-	%vol	m	m	mm day ⁻¹	-	%vol
1a	0.23	0.16	440	0.540	47.5	0.30	0.12	585	0.577	39.4
1b	0.40	0.11	764	0.504	45.9	0.35	0.13	640	0.556	39.9
2a	0.60	0.62	563	0.473	45.5	0.29	0.19	578	0.496	47.2
2b	0.54	0.34	715	0.540	45.3	0.35	0.16	613	0.550	38.0
3a	0.22	0.13	685	0.554	41.9	0.40	0.14	571	0.581	38.4
3b	0.48	0.40	666	0.555	41.1	0.29	0.10	585	0.580	38.0
4a	0.32	0.25	767	0.574	42.2	0.40	0.12	503	0.572	37.7
4b	0.34	0.13	698	0.574	45.3	0.35	0.10	558	0.541	38.4
5a	0.31	0.20	848	0.618	45.0	0.23	0.13	435	0.595	38.2
5b	0.45	0.14	730	0.567	41.7	0.24	0.16	531	0.530	38.4
6a	0.32	0.10	848	0.560	44.7	0.37	0.19	435	0.593	38.9
6b	0.45	0.34	730	0.598	40.2	0.29	0.12	531	0.557	39.7

4.1.3 Soil moisture measurements

The actual soil moisture content (θ) is measured for several locations within the plots for 2.5 weeks in August and once more in October. The measurements begin at 0 m, which is just below the upper or middle soil bund for upper and lower plots, respectively, and end just above the middle and lower soil bunds for upper and lower plots, respectively. Only for the soil moisture measurements, the control plots are not divided in an upper and lower plot. So, the measurements begin at the upper boundary (0 m) and end at the lower boundary of the plot. All soil moisture measurements for field 1 and field 2 can be found in Appendix 6 and 7, respectively, of which the averaged soil moisture contents of most plots are evaluated here.

The independent t-test determined that the soil moisture contents of field 1 are significantly higher than θ of field 2 ($p = 0.000$) (table 5). This can also be seen in figure 12 and 13, where θ of field 1 is clearly higher than θ of field 2. However, there is less difference between the plots within the fields. For field 1, only plot 5 is statistically significant different in θ compared to plot 2, 3 and 6 (table 6). Plot 5 is a control plot and is different from the other plots because it has a lower average θ . And for field 2, only plot 4 has a statistically significant different θ than all the other plots, which is due to its lower average θ (table 6). The low θ of plot 4 is probably caused by the abundance of stones in the soil which makes it harder to contain moisture. Small stones were found in other plots in field 2 as well, but never as abundant as in plot 4. The soil moisture contents of the other plots are not statistically significant different from each other. So, in general, there is no large significant difference in θ between plots of a field.

Table 5. Statistically significant difference in soil moisture content between field 1 and field 2 measured in both fields on 16 August and determined with the independent t-test with the conditions $t(127) = 14.642$, $p = 0.000$.

	Average	Standard deviation
	%vol	%vol
Field 1	37.893	5.168
Field 2	26.511	3.805

Table 6. Statistically significant difference in soil moisture content between plots of field 1 and between plots of field 2 determined with a LSD post hoc test. The date of soil moisture content measurements used for the LSD post hoc test is determined by the one-way ANOVA test, which is 19 August for field 1 and 11 August for field 2. A bold significance means that $p < 0.05$ and there is a significant difference in soil moisture content between the plots. The soil moisture contents of field 2 are higher than of field 1 because they are measured on a different date.

	Average	Standard deviation	Significance p					
	%vol	%vol	Plot 1	Plot 2	Plot 3	Plot 4	Plot 5	Plot 6
Field 1 (one-way ANOVA (F(5, 67) = 1.687, p = 0.150 on 19 August)								
Plot 1	28.515	3.913	-	0.192	0.253	0.766	0.224	0.190
Plot 2	31.240	3.001	0.192	-	0.946	0.183	0.031	0.996
Plot 3	29.200	4.485	0.253	0.946	-	0.227	0.047	0.943
Plot 4	28.183	2.611	0.766	0.183	0.227	-	0.458	0.181
Plot 5	27.280	3.042	0.224	0.031	0.047	0.458	-	0.031
Plot 6	30.357	4.607	0.190	0.996	0.943	0.181	0.031	-
Field 2 (one-way ANOVA (F(5, 43) = 4.197, p = 0.003 on 11 August)								
Plot 1	35.717	3.024	-	0.556	0.388	0.006	0.652	0.889
Plot 2	37.000	5.527	0.556	-	0.756	0.000	0.263	0.425
Plot 3	37.490	4.551	0.388	0.756	-	0.000	0.157	0.271
Plot 4	28.986	2.944	0.006	0.000	0.000	-	0.015	0.005
Plot 5	34.657	3.002	0.652	0.263	0.157	0.015	-	0.734
Plot 6	35.400	4.494	0.889	0.425	0.271	0.005	0.734	-

Furthermore, the one-way ANOVA test also determined which plots had statistically significant differences in θ between locations within the plot. For field 1, the plots with statistically significant differences in θ between locations are plot 1a, 1b, 3b, 5a, 5b and 6b. And, for field 2, it is only plot 2a and 4a. The other plots have no statistically significant differences in θ between locations. The overview of the statistic results of the one-way ANOVA test and the LSD post hoc test to determine the significance in θ between locations within the plots can be found in Appendix 8. Nevertheless, for most plots, a pattern can be recognized between θ and location within the plot. Figure 12 shows the average θ of all locations of plots with soil bunds of field 1 and 2. In all plots with bunds, except for plot 6 of field 2, θ decreases from the upper bund to the middle bund. However, for the lower plot, the pattern in θ is more divided. For plot 6 of field 1, θ gently decreases towards the lower bund, but for plot 3 and 4 of field 1 and plot 4 of field 2, θ decreases towards the center of the lower plot and increases again towards the lower bund. Overall, θ in plots with bunds generally decrease downward in the upper part and increase after the middle bund, after which it decreases towards the middle of the lower plot and increases again towards the lower bund. Figure 13 shows the average θ of all locations of the control plots of field 1 and 2. It can be seen that there is less variation in θ between the locations than for plots with bunds. The control plots of field 1 follow similar patterns, θ increases towards the middle of the plot. The control plots of field 2 have a less clear pattern and θ slightly increase and decrease between locations for both control plots. But, in plot 5 there is a sudden increase in θ around 6 m and a sudden decrease in θ around 8 m. Due to the location of this sudden difference in θ it might still be caused by the presence of an obsolete soil bund, which was still visible in the field in plot 5 of field 2. On the whole, the presence of soil bunds is visible in the soil moisture patterns of the plots of field 1, but not in the plots of field 2. In addition, figure 14 and 15 give the soil moisture

pattern of the plots which were measured in more detail close to the soil bunds of field 1 and field 2, respectively. For plot 1 of field 1, there is no pattern in the upper part, but the soil moisture steadily decreases from the middle to the lower bund. And, plot 2 of field 2 shows a lot of variation in soil moisture between the locations, but the effect of the presence of the bunds is not visible. This variation can be caused because some measurement locations were located on a small pile of soil which is a results of plowing and results in lower soil moistures. Moreover, it is important to keep in mind that figure 12 to 15 give average soil moistures per location for each plot, canceling out the possible difference in pattern between dry and wet measurement dates. In general, the dry days had a different soil moisture pattern than wet days. Appendix 6 and 7 contain graphs of soil moisture along the profile line for each day.

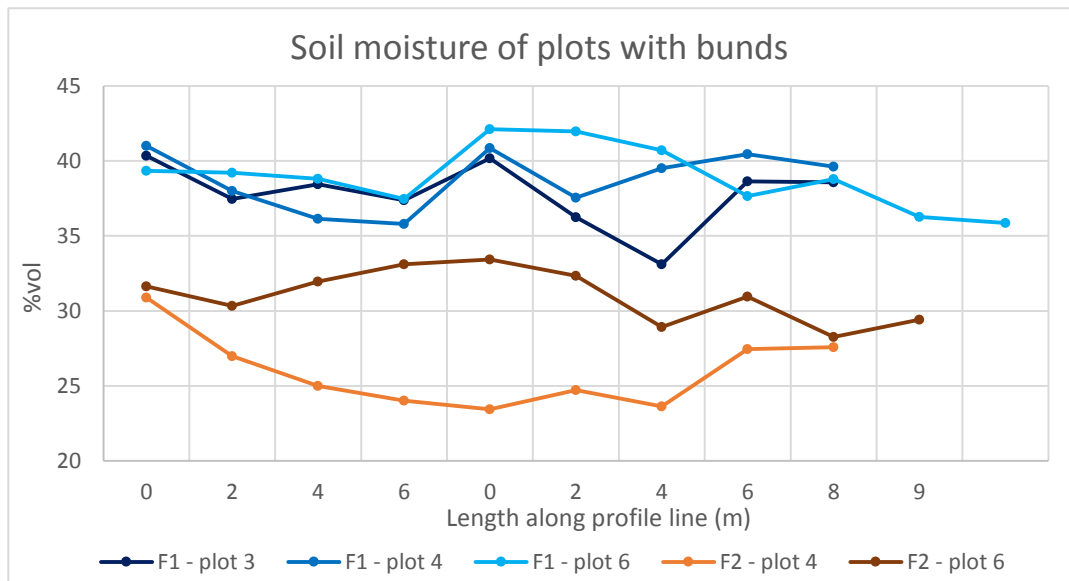


Figure 12. Average measured soil moisture contents of plots with soil bunds of field 1 and field 2. The upper soil bunds are located at the first measurements, the middle soil bunds are located at the middle 0 m and the lower soil bunds are located at the end of the profile lines.

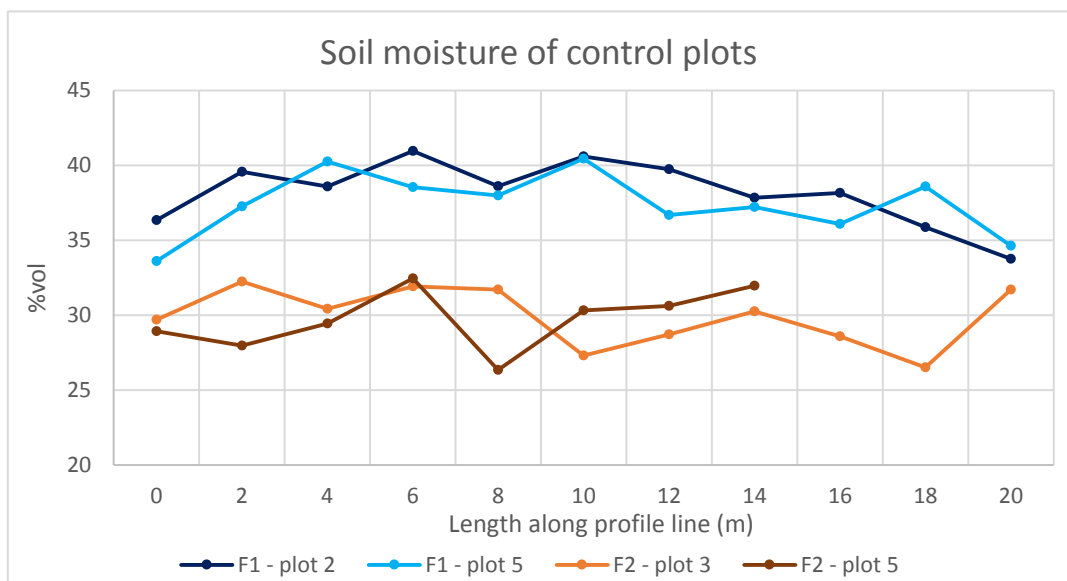


Figure 13. Average measured soil moisture contents of the control plots of field 1 and field 2.

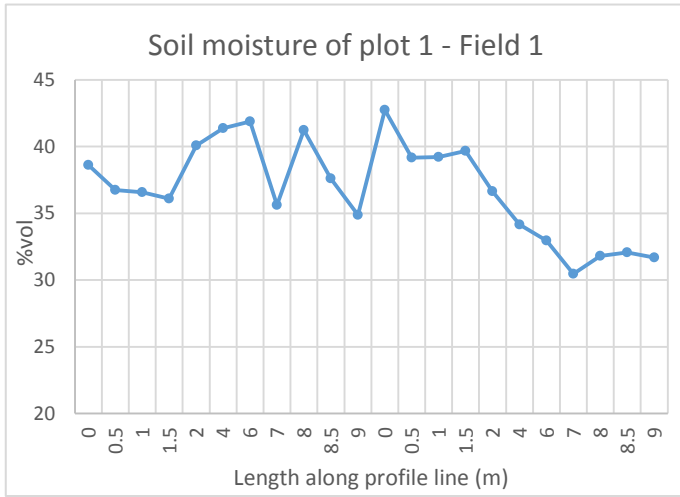


Figure 14. Measured soil moisture content of plot 1 of field 1, where the soil moisture measurements are closer together in the vicinity of the soil bunds. The vertical lines represent the location of the soil bunds.

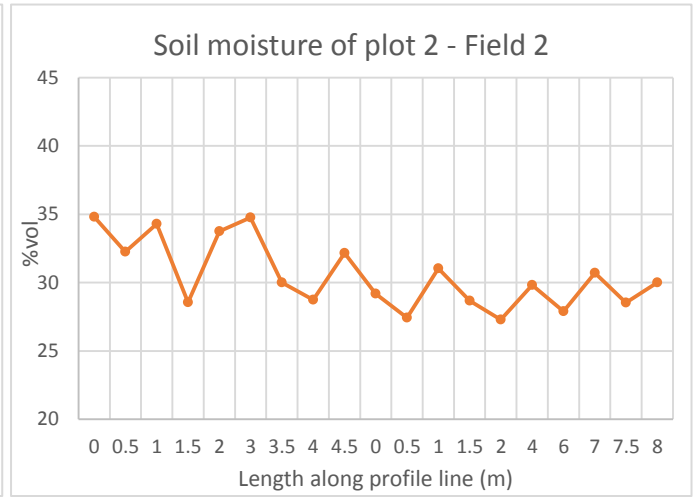


Figure 15. Measured soil moisture content of plot 2 of field 2, where the soil moisture measurements are closer together in the vicinity of the soil bunds. The vertical lines represent the location of the soil bunds.

Besides soil moisture patterns between fields, between plots and within plots, there is also a pattern in soil moisture in time. Figure 16 shows the average θ for all locations of plot 1a of field 1 plotted against the date of measurement. The grey area indicates the range of soil moisture contents measured at the different locations of plot 1a. The grey area between 19 and 22 August is dashed because the pattern of the range of soil moisture contents is uncertain due to a data gap. It can be seen that the soil moisture follows the pattern of rainfall. Just before the beginning of the measurement period there were multiple days with rainfall, leading to a high θ . Afterwards, there was a dry period which resulted in a decrease of θ . After 19 August there were multiple rainy days leading to an increase in θ . It can be seen that the decrease of θ takes days, but the increase in θ after rainfall is much faster. In addition, it is noticeable that the range of higher soil moisture contents is smaller than the range of lower soil moisture contents, which could indicate that infiltration is more evenly distributed within the plot than drainage.

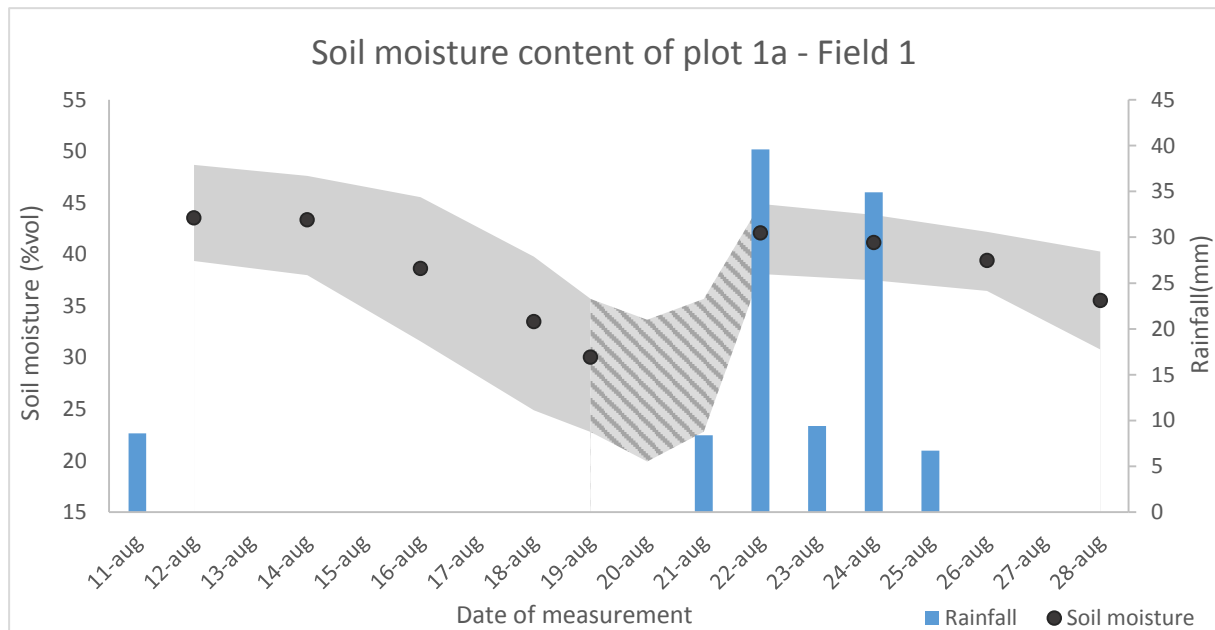


Figure 16. The average measured soil moisture content for all location of plot 1a of field 1 plotted against the date of measurement. The grey area indicates the minimum and maximum boundaries of the measured soil moisture of all locations of plot 1a. The dashed grey area indicates an uncertainty, because there are no measurements between 19 and 22 August.

4.1.4 Crop and yield measurements

The maximum canopy cover (CC_x) is higher in field 1 than in field 2, with an average higher CC_x of 10.5%. Within the fields, the CC_x differs fairly much between plots. For field 1, CC_x is higher for the upper plots and, generally, CC_x of the control plots is slightly lower than for plots with bunds, except for control plot 2a, which has the highest CC_x . For field 2, there is no significant difference in CC_x between upper and lower plots, but the CC_x of the lower control plots is slightly lower than for lower plots with bunds and CC_x of the upper control plots is similar to higher than for the upper plots with bunds. The biomass and the yield become higher over time and the values in table 7 represent the total biomass and yield measured during harvest. Since AquaCrop is calibrated for the measured total biomass, the simulated biomass of the default simulation is more or less similar to the measured biomass. However, the small differences between the measured and the simulated biomass can lead to confusion. Therefore, the simulated biomass and yield will be used and differences in biomass and yield will be discussed during the evaluation of the default simulation.

Almost all parameters in table 7 are lower in field 2 than in field 1, except for the bund height and the slope. The height of the soil bunds is similar for both fields and between plots. Besides, the height of the soil bund only matters when the ponding water on the plot is higher than the bunds, but this did not happen during the study. On average, the slopes of field 1 and 2 are similar, but field 2 has a larger range of slopes with a difference of almost 13° between the steepest and the gentlest slope, while the slopes of field 1 only differ 8.5° . For both fields, the slope is steeper on the lower plots. Similar to CC_x , the number of plants per m^2 are also higher in field 1. However, the number of plants per m^2 does not seem to be related to CC_x . The number of plants per m^2 differ between plots and is generally higher in the lower plots. Converting the number of plants per m^2 to the number of plants per ha gives a maize density of 46 042 plants ha^{-1} for field 1 and 29 167 plants ha^{-1} for field 2.

Table 7. Important calculated and measured crop and yield parameters for field 1 and field 2. The control plots have no soil bunds. Control plots are plot 2 and 5 for field 1 and plot 3 and 5 for field 2. CC_x is the maximum canopy cover.

Crop and yield parameters												
Plot	Field 1						Field 2					
	Biomass	Yield	Bund height	CC_x	Plants per m^2	Slope	Biomass	Yield	Bund height	CC_x	Plants per m^2	Slope
	$ton\ ha^{-1}$	$ton\ ha^{-1}$	m	%		$^\circ$	$ton\ ha^{-1}$	$ton\ ha^{-1}$	m	%		$^\circ$
1a	5.307	1.682	0.11	53.8	4.3	8.5	2.859	1.107	0.19	35.1	3.0	6.2
1b	4.395	1.912*	0.05	47.3	5.5	15.0	4.663	1.673	0.02	40.7	3.3	19.0
2a	7.473	2.689*	-	59.2	4.5	8.0	4.103	2.172	0.06	51.2	2.5	14.5
2b	5.712	2.411*	-	41.0	4.0	14.5	3.613	1.706	0.08	37.4	2.5	16.8
3a	4.957	2.767*	0.05	51.9	3.8	11.9	3.881	1.676	-	41.8	1.8	8.5
3b	4.831	2.280*	0.03	46.6	4.0	16.5	5.165	2.074	-	34.8	3.3	14.5
4a	13.100	5.295*	0.08	52.5	6.3	11.9	3.131	2.364	0.08	28.8	1.8	6.2
4b	5.331	1.579*	0.03	43.8	4.8	12.3	3.070	1.209*	0.14	33.6	2.6	6.2
5a	4.911	2.880*	-	43.2	4.0	8.5	1.256	0.574	-	32.3	1.8	9.0
5b	3.780	1.162*	-	40.6	3.0	10.0	5.522	1.413*	-	30.8	3.8	18.2
6a	7.321	4.163*	0.14	45.5	6.3	8.2	4.185	1.968	0.19	36.7	2.5	7.2
6b	4.110	1.096*	0.18	40.7	5.0	10.0	3.838	1.213*	0.09	37.1	3.5	16.0

* Indicates which yield samples were compromised by maize eating insects

4.2 AquaCrop simulations: effect of soil bunds

For all AquaCrop simulations, the soil fertility stress is constant over the growing period, but the other stresses differ daily and the average value over the growing period is given in this study. The temperature stress, water stress and stomatal closure are given by a percentage of time when stress occurred averaged over the growing period. Moreover, the daily runoff, infiltration, drainage, soil evaporation, transpiration and evapotranspiration are also displayed as an average over the growing period. The shown biomass and yield are the total biomass and yield at harvest time. Furthermore, the harvest index is similar between plots, which results in a similar conversion of the amount of biomass into yield between plots (appendix 10). Therefore, only the biomass will be evaluated knowing that the yield follows the same pattern. However, the harvest index of field 2 is 45.6%, which is higher than the 42.3% of field 1. This means that field 2 converts more biomass into yield than field 1. All these parameters will be used to evaluate the effect of soil bunds and the biomass production.

The default AquaCrop simulation is calibrated for biomass by imposing soil fertility stress. However, the calibration of the AquaCrop simulation for biomass of plot 5a of field 2 was not possible due to the low measured biomass, which is probably a result of an error in the field. Instead, the simulation of plot 5a was calibrated on the canopy cover measured in August, which is assumed to be related to the biomass. As a result, the simulated biomass for plot 5a is very different from the measured biomass in table 7. The simulations of the other plots are all calibrated for the measured biomass. The default simulation is used to see the differences between plots with bunds and plots without bunds. In addition, the within plot simulation is used to determine which locations are most beneficial within the plots and their position with regard to the soil bunds.

4.2.1 Effect of treatment: bunds versus no bunds

To illustrate the possible difference in parameters between plots with and without bunds figure 17 to 19 show the range of soil moisture, biomass and parameters of the water balance for plots with bunds and without bunds (control plots). In addition, for the soil moisture and the biomass, the plots are also divided in upper and lower plots because the possible difference between upper and lower plots could make the difference between plots with bunds and control plots less clear.

Soil moisture content

Figure 17a shows the θ_{avg} for control plots and plots with bunds for field 1. For the upper plots, the plots with bunds have a small range of θ_{avg} and θ_{avg} of control plot 5a is in the same range, only θ_{avg} of control plot 3a is a bit lower. And for the lower plots, the control plots are in the same range as the plots with bunds. In general, there is only a small difference in soil moisture between upper and lower plots and plots with and without bunds in field 1. This can also be seen in figure 17b, which shows θ_{avg} for control plots and plots with bunds for field 2. In general the soil moisture does not differ much, but it can be seen that, θ_{avg} of the upper plots is slightly higher than θ_{avg} of the lower plots. The control plots are in the same range as plots with bunds, except for control plot 5b, which has a slightly higher θ_{avg} than the lower plots with bunds.

Biomass

Furthermore, figure 18a compares the biomass of the control plots with plots with bunds of field 1. The biomass of the control plots is not unanimously lower or higher than plots with bunds, because control plot 2 has a slightly higher biomass than plots with bunds and control plot 5 has a slightly lower biomass than plots with bunds. This difference is probably due to differences in soil fertility stress, since control plot 2 has, on average, a lower soil fertility stress and control plot 5 a higher soil fertility stress. Figure 18b compares the biomass of control plots and plots with bunds for field 2. It seems that the upper control plots are in the same range as the upper plots with bunds, but the lower control plots are fairly higher than the range of lower plots with bunds. This is because plot 3b and 5b have the lowest soil fertility stress resulting in a high biomass. Furthermore, the lower plots have a higher

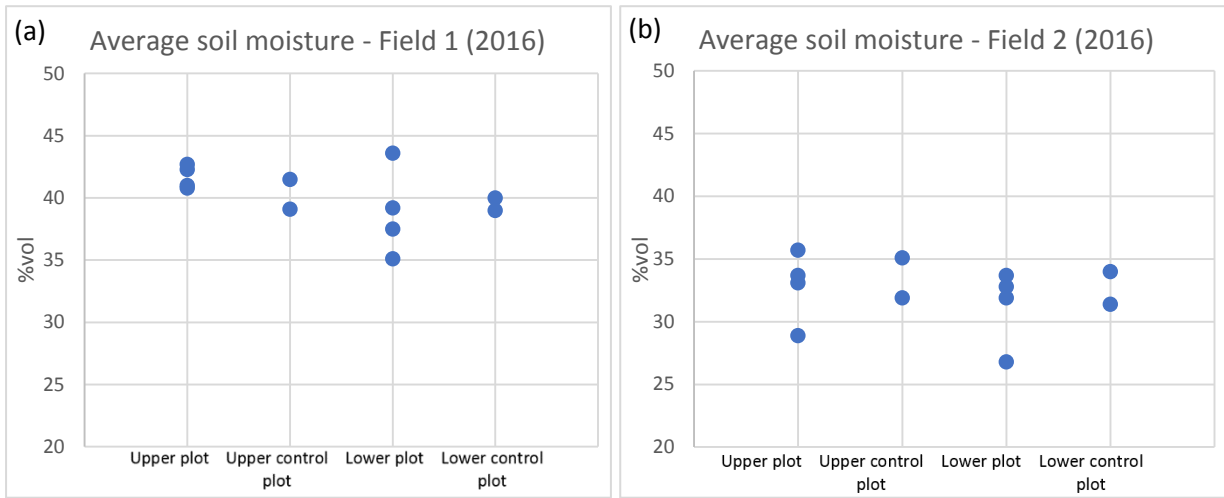


Figure 17. Simulated average soil moisture content of the growing period for upper plots with soil bunds, upper control plots without soil bunds, lower plots with soil bunds and lower control plots without soil bunds. Soil moisture content simulated for the center of the plots of field 1 (a) and field 2 (b).

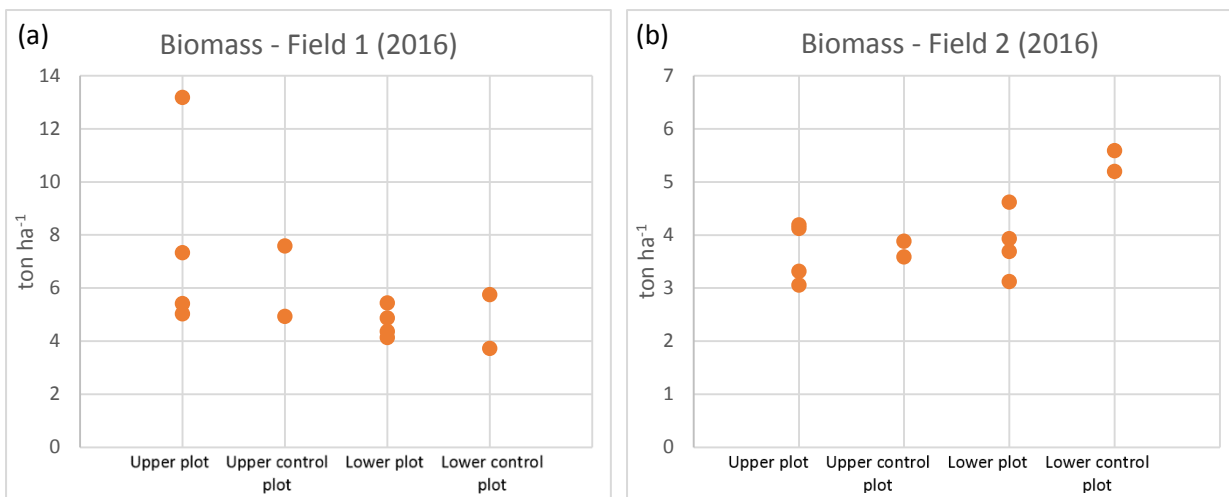


Figure 18. Comparison of the biomass of the upper plots with soil bunds, the upper control plots, the lower plots with soil bunds and the lower control plots of field 1 (a) and field 2 (b). All measured values are plotted on one line, so the differences between the different plots can be seen.

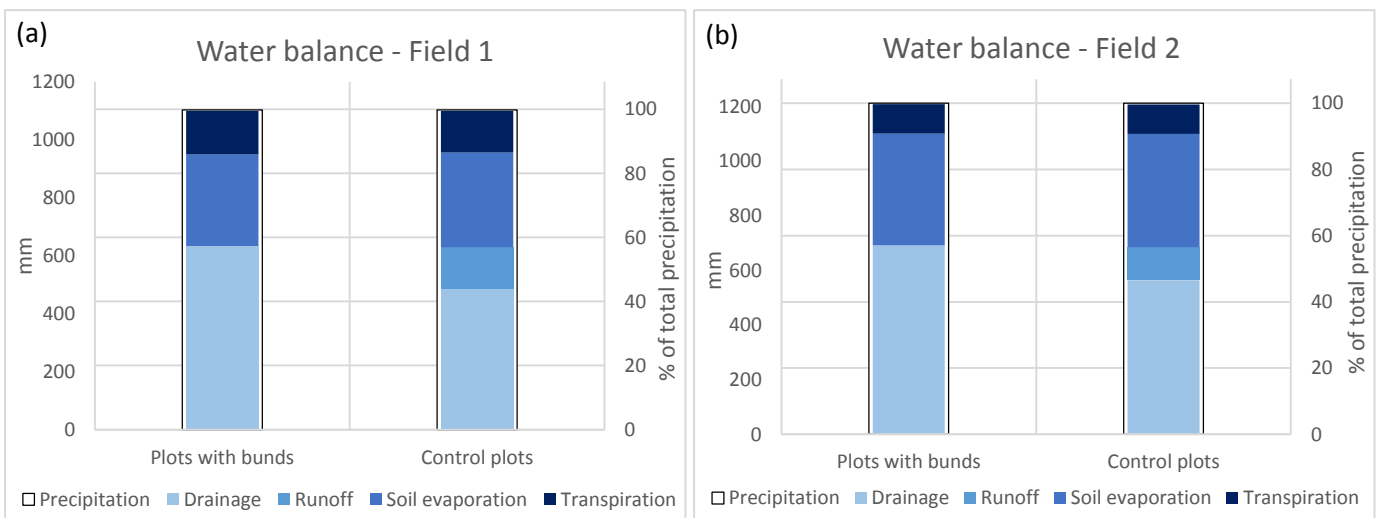


Figure 19. The average water balance over the growing period in mm and in percentage of the total amount of precipitation for field 1 (a) and field 2 (b). The precipitation is given by the black line and is equal to the sum of drainage, runoff, soil evaporation and transpiration.

biomass than the upper plots, even though the lower plots have higher slopes. However, the soils of the lower plots are, in general, slightly deeper than the soils of the upper plots. This can lead to the lower soil fertility stress found in the lower plots, which is, on average, 8% lower than in the upper plots, which most likely leads to the difference in biomass between upper and lower plots.

The water balance

Figure 19 shows the water balance of field 1 and field 2 in mm and in percentage of the total amount of rainfall over the growing period. Comparing the components of the water balance between the fields it can be seen that the percentage drainage is similar, but the percentage soil evaporation is higher in field 2 and the transpiration is higher in field 1. Furthermore, the percentage runoff is higher in field 1. When comparing the components of the water balance between plots with and without bunds it can be seen that there is almost no difference in soil evaporation and transpiration. Plots with bunds have only a slightly higher transpiration and a slightly lower soil evaporation than plots without bunds. The largest effect of the presence of bunds on the water balance can be seen in the drainage and the runoff. In AquaCrop, the only difference between plots with bunds and control plots is that runoff is completely stopped in plots with bunds and only the control plots have runoff. The amount of water used for runoff in the control plots is approximately equal to the reduction in drainage in control plots compared to plots with bunds. Therefore, soil bunds have almost no effect on the amount of soil evaporation and transpiration and have the most effect on drainage and runoff.

4.2.2 Effect of location within the plot

Several locations with significant differences in soil moisture content within a plot are simulated in AquaCrop to determine if the locations within the plot have an effect on the soil moisture content (within plot simulation). If it does, this simulation can also be used to determine which locations within the plot are most beneficial regarding the biomass production. The only difference between the locations within a plot in the simulation are θ_{FC} and θ_{SAT} , which influence the actual soil moisture content, the amount of stress and eventually also the biomass and the yield. The chosen θ_{FC} and θ_{SAT} and the results of the simulation can be found in table 8. The soil moisture content, the amount of stress, the biomass and the yield differ slightly between locations within the plot.

Pattern between soil moisture and different locations within the plot

With this simulation it is possible to determine if there is a pattern between soil moisture and location within the plot, e.g. is the highest soil moisture consequent at the top, middle or bottom of the plot. For field 1, it can be noted that the upper plots (plot 1a and 5a) have other patterns in θ_{avg} than the lower plots (plot 1b, 3b, 5b and 6b), but in general the soil moisture is highest around the middle bund, which means a high θ_{avg} at the bottom of the upper plots and a high θ_{avg} at the top of the lower plots. However, the locations with the lowest θ_{avg} differ between the plots and are mostly around the lower bund and in the middle of the subplots. The findings of the within plot simulation are consistent with the measured soil moisture of field 1 (figure 12), which also indicates that the soil moisture is highest around the middle bunds. This was expected because the measured soil moisture contents were used to calibration AquaCrop for the within plot simulation. For field 2, there are only upper plots in this simulation and θ_{avg} is highest around the upper bund, decreases downward and is lowest around the middle bund, which contradicts the findings in field 1. The measured soil moisture (figure 12) shows that the pattern between plots is less consistent in field 2 than in field 1. Together with the lack of lower plots of field 2 in this simulation, it is difficult to determine a pattern in θ_{avg} in field 2. On the whole, it can be concluded that there is no consistent pattern between soil moisture and the location within the plot, but most of the plots have the highest θ_{avg} around the middle bund in field 1 and around the upper bund in field 2.

Table 8. The input parameters (soil moisture at field capacity (θ_{FC}) and at saturation(θ_{SAT})), the different stresses (canopy expansion stress, stomatal closure and soil fertility stress) and the output parameters (simulated average actual soil moisture content over the growing period (θ_{avg}), biomass and yield) are given for the locations with significantly different soil moisture contents within a plot. The temperature stress is not given because it is the same for all plots. The first column indicates the plot and the second column indicates the location of the soil moisture measurement and hence the location of the simulation. 0m is the most upper part of the plot, directly below the upper bund and the locations with higher meters are located more downward on the plot.

Field 1										
Location		Soil depth	θ_{FC}	θ_{SAT}	θ_{avg}	Canopy expansion	Stomatal closure	Soil fertility	Biomass	Yield
Plot	m	m	%vol	%vol	%vol	%	%	%	ton ha ⁻¹	ton ha ⁻¹
1a	0	0.16	42.0	51.0	37.4	7	5	73	5.747	2.473
1a	1	0.16	42.0	48.0	36.5	7	8	73	5.580	2.401
1a	4	0.16	47.0	51.0	40.8	5	12	73	5.412	2.328
1a	9	0.16	40.0	47.0	34.9	8	7	73	5.584	2.404
1b	0	0.11	49.5	56.0	44.5	4	7	75	4.449	1.915
1b	1	0.11	46.5	52.0	41.0	7	7	75	4.405	1.898
1b	4	0.11	45.0	50.4	39.2	8	8	75	4.364	1.881
1b	8	0.11	40.0	49.0	35.3	10	6	75	4.303	1.857
1b	9	0.11	40.5	49.0	35.6	10	6	75	4.305	1.858
3b	0	0.40	49.0	56.0	43.1	0	3	76	4.815	2.071
3b	4	0.40	40.0	50.0	35.1	1	2	76	4.875	2.069
3b	8	0.40	44.0	53.0	38.8	0	2	76	4.862	2.091
5a	0	0.20	44.0	50.0	37.2	6	6	73	4.817	2.024
5a	6	0.20	48.0	56.0	41.5	4	3	73	4.929	2.070
5a	10	0.20	49.0	58.0	42.1	4	3	73	4.970	2.088
5b	10	0.14	49.0	55.0	42.9	6	7	80	3.657	1.537
5b	14	0.14	44.0	54.0	39.0	8	3	80	3.724	1.566
5b	19	0.14	42.5	55.0	38.0	8	3	80	3.731	1.569
6b	0	0.34	49.0	57.0	43.9	0	3	78	4.067	1.708
6b	6	0.34	41.2	55.0	37.5	1	1	78	4.140	1.739
6b	10	0.34	42.5	55.0	38.5	1	1	78	4.130	1.735
Field 2										
Location		Soil depth	θ_{FC}	θ_{SAT}	θ_{avg}	Canopy expansion	Stomatal closure	Soil fertility	Biomass	Yield
Plot	m	m	%vol	%vol	%vol	%	%	%	ton ha ⁻¹	ton ha ⁻¹
2a	0	0.19	40.0	49.6	35.3	8	6	80	4.158	1.967
2a	2	0.19	39.0	46.5	33.7	9	7	80	4.125	1.952
2a	4	0.19	34.0	44.0	29.7	11	7	80	4.097	1.936
4a	0	0.12	37.0	50.0	33.9	11	7	74	3.397	1.567
4a	2	0.12	31.5	45.0	28.9	14	8	74	3.317	1.473
4a	6	0.12	29.0	42.0	26.5	16	10	74	3.256	1.425

Pattern between biomass and different locations within the plot

The same can be evaluated for the biomass. If only field 1 is considered, there is no consistent pattern in biomass within the plots. Plot 1 has its highest biomass in the downward vicinity of the bunds, but plot 3b and 6b have the lowest biomass just downward of the middle bund, which contradicts the findings of plot 1. The highest biomass in plot 3b and 6b is found in the middle of the plot, but the biomass close to the lower bund is only slightly lower. Besides, the control plot shows a different pattern in biomass. The biomass is lowest at the upper boundary and increases towards the middle of the plot, which is repeated in the lower control plot. If only field 2 is considered, both plots follow the same pattern. The biomass is highest around the upper bund and decreases downward towards the middle bund. However, when the patterns of the two fields are combined it can be concluded that there is no dominant pattern between biomass and the location within the plot.

4.3 AquaCrop simulations: effect of soil moisture

To determine the effect of soil moisture on biomass the within plot simulations are used. First, the overall effect of soil moisture on biomass between the plots is evaluated (figure 20). Then, the relation between soil moisture and biomass within the plots is evaluated to determine if the highest soil moisture always results in the highest biomass or vice versa. This is done by comparing θ_{avg} with the biomass within each plot, which are given in table 8.

4.3.1 The effect of soil moisture on biomass between the plots

To determine the overall effect of soil moisture on biomass, θ_{avg} and the biomass are plotted for each plot in figure 20. The upper two graphs are the soil moisture and the biomass of field 1. It can be seen that θ_{avg} is more or less in the same range, while the biomass differs between plots. The small differences in the range of θ_{avg} between plots do not result in the pattern of the biomass. For example, plot 1a and 3b have similar ranges of θ_{avg} , but the biomass of plot 1a is much higher than the biomass of plot 3b. Furthermore, plot 5b and 6b have a low biomass, while the range of θ_{avg} of plot 5b and 6b is the same as plot 5a, which has a much higher biomass. The lower two graphs are the soil moisture and the biomass of field 2. Since field 2 has only two plots with significant locations it is difficult to see patterns between θ_{avg} and the biomass. The only pattern that can be seen is that plot 2a has a higher range of θ_{avg} than plot 4a, which results in a higher biomass.

4.3.2 The effect of soil moisture on biomass within the plots

The relation between soil moisture and biomass within a plot can also be evaluated. For half of the plots of field 1, the decrease in soil moisture positively influences the biomass, while for one-third of the plots the increase in soil moisture positively influences the biomass. Only one plot, plot 1a, has the highest biomass with an intermediate soil moisture content. However, field 2 has the same pattern for both plots, the increase in soil moisture positively influences the biomass, which is different from the dominant pattern of field 1. Therefore, it can be concluded that there is no consistent pattern between soil moisture and biomass. However, the difference in patterns between plots can be explained by θ_{FC} and θ_{SAT} and the soil depth of the plots. θ_{FC} is much lower for field 2, which means that an increase of soil moisture results in less water stress, but does not cause much aeration stress, resulting in an increase of biomass. The other way around, when the soil moisture decreases, there is more water stress resulting in less biomass. This leads to a more consistent pattern in field 2. However, for field 1, the average θ_{FC} is higher and an increase in soil moisture can easily trigger aeration stress leading to a lower biomass. In addition, when the gap between θ_{FC} and θ_{SAT} is small, aeration stress is more easily triggered. As a result of the high θ_{FC} of field 1, the gap between θ_{FC} and θ_{SAT} is often small (figure 25), leading to a negative influence on the biomass when soil moisture increases. However, a decrease in soil moisture leads to a decrease in aeration stress and is often not low enough to cause water stress, which results in a positive influence on the biomass. In addition, plots with deeper soils, like plot 3b and 6b, are more resistant to changes in soil moisture, leading to only very small changes in biomass within the plot. The shallow plots, like plot 1a, 1b and 5b are more vulnerable to changes

in soil moisture and how it influences the biomass. Hence, the biomass of all three plots with shallow soils react different to changes in soil moisture. On the whole, it can be concluded that the soil moisture content has little effect on the amount of biomass produced. However, it seems like the soil moisture content does influence the water and aeration stress, which might lead to small differences in the amount of biomass produced.

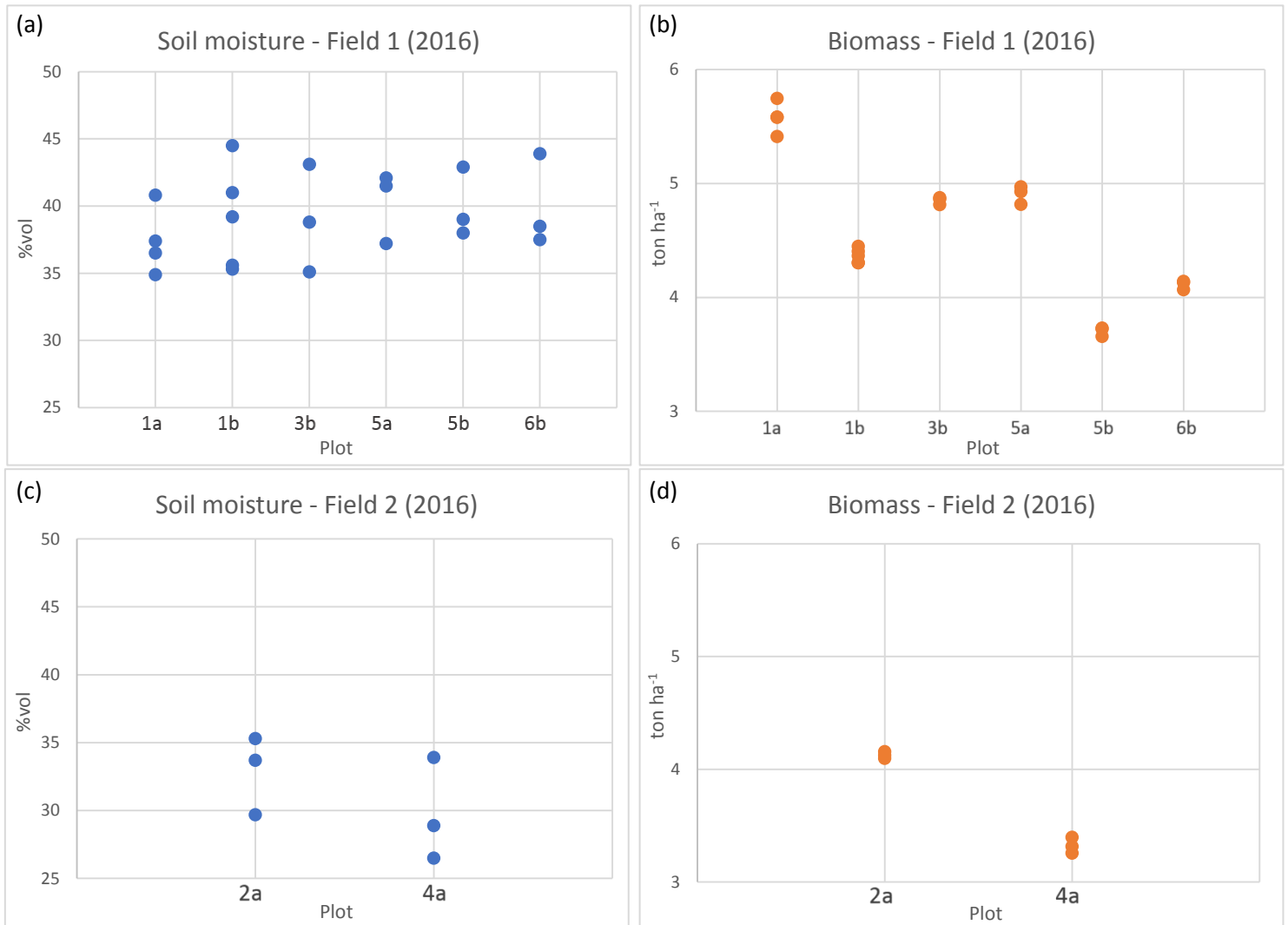


Figure 20. Boxplots of the simulated average soil moisture content over the growing period and the biomass for all locations with significant different soil moisture contents. All locations within a plot are plotted together for each plot, making it possible to see the range of values within a plot. (a) range of soil moisture content within the plots of field 1. (b) range of biomass produced within the plots of field 1. (c) and (d) are the same as (a) and (b), respectively, but than for field 2.

4.4 AquaCrop simulations: effect of soil fertility

To determine the effect of soil fertility stress on the biomass, the default simulation, the within plot simulation, the average fertility simulation and the average fertility within plot simulation are used. The default simulation is used to determine the relation between the amount of soil fertility stress and the biomass between the plots, which have variable soil fertility stresses. Moreover, the variation of water and aeration stress, soil moisture content and evaporation between the plots and their influence on the biomass is also evaluated. An overview of the simulated parameters from the default simulation is given in Appendix 10. Furthermore, the within plot simulation and the average fertility within plot simulation are compared to see the effect of soil fertility stress on biomass. Then, the average fertility simulation is used to determine which other parameters possibly significantly affect the biomass, because the variation in soil fertility is eliminated making the influence of other parameters on the biomass better visible.

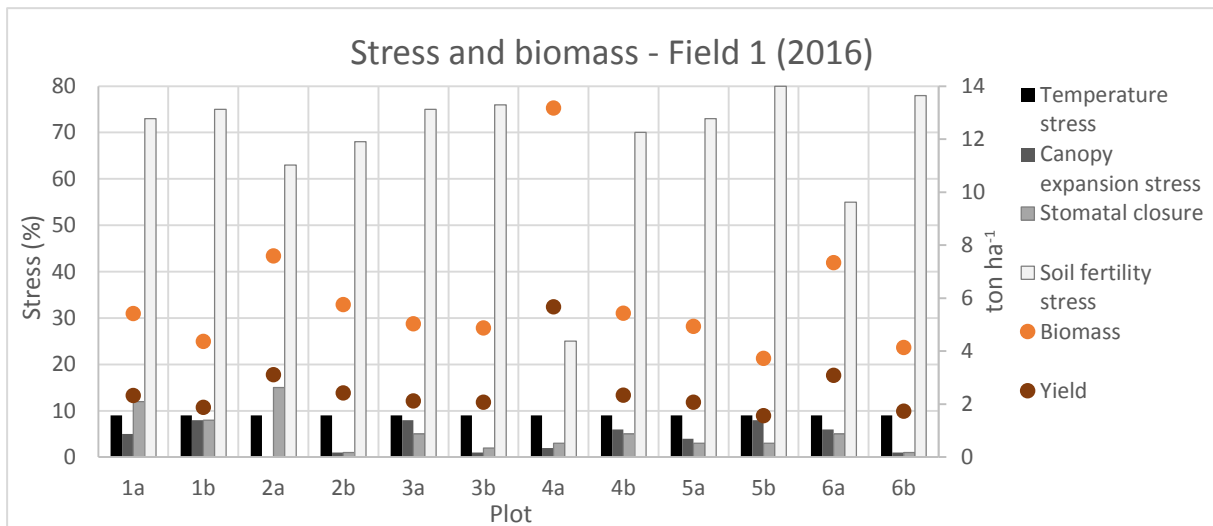


Figure 21. Comparison of the amount of stress, given as a percentage of time when stress occurred during the growing period and total biomass and yield, given in ton ha⁻¹ between the subplots for field 1. Parameters simulated by AquaCrop for the center of the plots with variable soil fertility stress for each subplot.

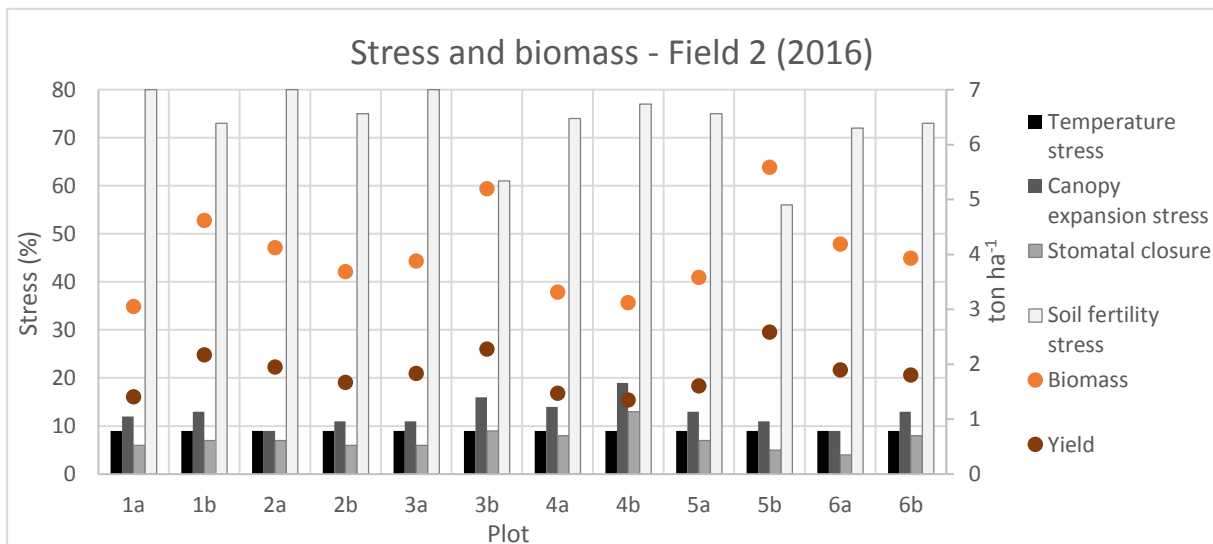


Figure 22. Comparison of the amount of stress and total biomass and yield between the subplots for field 2. Parameters simulated by AquaCrop for the center of the plots with calibrated soil fertility stress for each subplot.

4.4.1 Variable soil fertility stress

Stress and biomass

Figure 21 and 22 show the amount of different stresses and total biomass and yield for field 1 and field 2, respectively. The biomass and yield differ greatly between plots for both fields. But, the biomass and yield in field 2 are significantly lower than in field 1. In addition, the stresses in field 2 are higher than in field 1, except for the temperature stress, which depends on the air temperature, which is the same in both fields. The lower biomass in field 2 is probably a result of the lower soil depths and the less dense canopy cover found in field 2 (table 4 and 7). For both fields it can be seen that the soil fertility stress is the most severe stress and is mostly around 70%. On average, the soil fertility stress is slightly less in field 1 than in field 2.

Within field 1, the highest biomass is found in plot 2a, 4a and 6a and the lowest biomass in plot 1b, 5b and 6b. And for field 2, the highest biomass is found in plot 3b and 5b, which are both control plots, and the lowest biomass is found in plot 1a and 4b. Furthermore, the canopy expansion stress and the stomatal closure also differ between plots and range between 0 – 8% and 1 – 15% in field 1,

respectively, and between 9 – 19% and 4 – 13% in field 2, respectively. For both fields it can be seen that the soil fertility stress is the most severe stress and ranges between 25% and 80% in field 1 and between 56% and 80% in field 2. As a result of the severe impact of the soil fertility stress, the biomass is highly related to the soil fertility stress. When the soil fertility stress is lowest, for example in plot 4a of field 1, the biomass is highest and when the soil fertility stress is highest, for example in plot 1a of field 2, the biomass is lowest. However, it can be noted that the soil fertility stress is not the only factor which causes the difference in biomass and yield between plots. For example, plot 1a and 4b of field 1 have similar total biomasses, but the soil fertility stress is higher for plot 1a. And, plot 2a and 6a of field 2 have similar biomasses, but plot 2a has a more severe soil fertility stress. Therefore, the soil fertility stress is not the only parameters affecting the biomass production.

Soil moisture content

The soil moisture content at field capacity (θ_{FC}), the soil moisture content at saturation (θ_{SAT}) and the simulated average actual soil moisture content over the growing period (θ_{avg}) are given in figure 23a and 23b for field 1 and field 2, respectively. Comparing the soil moistures in field 1 with the soil moistures in field 2 it can be seen that θ_{FC} and θ_{avg} are fairly higher in field 1, but θ_{SAT} is similar between the fields. Thereby, θ_{FC} is much closer to θ_{avg} in field 2, creating a larger gap between θ_{FC} and θ_{SAT} than in field 1 (figure 25). Furthermore, the variation in soil moisture between plots within the fields is larger in field 2 than in field 1. θ_{avg} ranges between 35.1% and 43.6% in field 1, while θ_{avg} ranges between 26.8% and 35.7% in field 2. Sometimes it seems like there is a pattern between soil moisture and biomass, but often there is not. For example, plot 1b and 2a of field 1 have similar soil moisture contents, but plot 2a has a much higher biomass. And, plot 5b and 6b of field 2 have the same soil moisture, but the biomass of plot 5b is much higher. But, plot 1a and 3a of field 1 have a similar soil moisture content and a similar biomass. However, this is probably due to a similar CC_x and a similar soil depth and not the similar soil moisture contents.

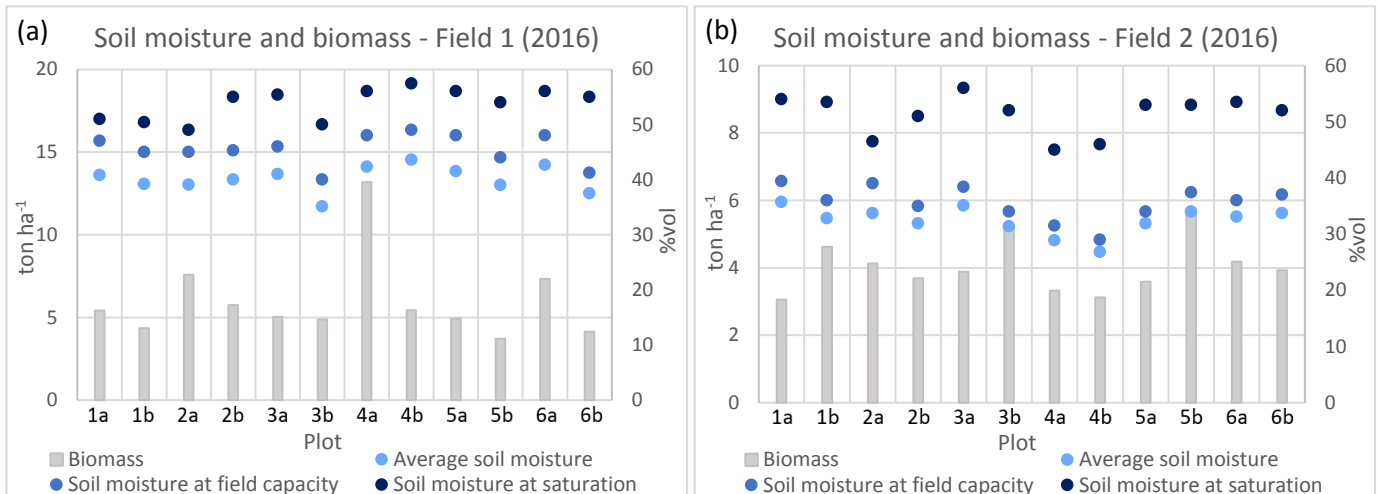


Figure 23. The soil moisture content at field capacity, the soil moisture content at saturation and the simulated average soil moisture content over the growing period are plotted together with the biomass. The parameters are all simulated with AquaCrop for the center of the plots of field 1 (a) and field 2 (b).

Figure 24 and 25 show the total available water (TAW) and the gap between θ_{FC} and θ_{SAT} with the canopy expansion stress and the stomatal closure, respectively. For field 1, it can be seen that TAW does not influence the stress significantly. For example, plot 1b and 2b have similar values for TAW, but plot 1b has much higher stresses. However, the gap between θ_{FC} and θ_{SAT} seems to have more influence on the stress, where low gaps result in high stresses, for example plot 1b and high gaps result in low stresses, for example plot 6b. On the contrary, field 2 shows the opposite. The gap between θ_{FC} and θ_{SAT} seems to have little influence on the stress. For example, plot 2a has a small gap between

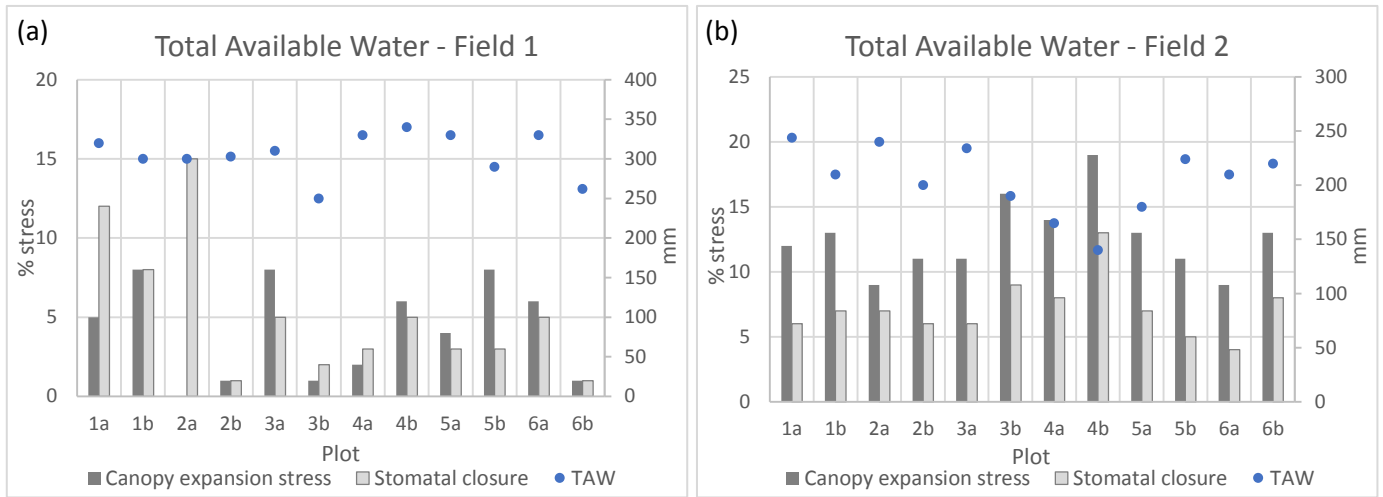


Figure 24. The total available water (TAW), expressed in mm, plotted with the canopy expansion stress and stomatal closure for field 1 (a) and field 2 (b). The stress is given as a percentage of time when stress occurred averaged over the growing period.

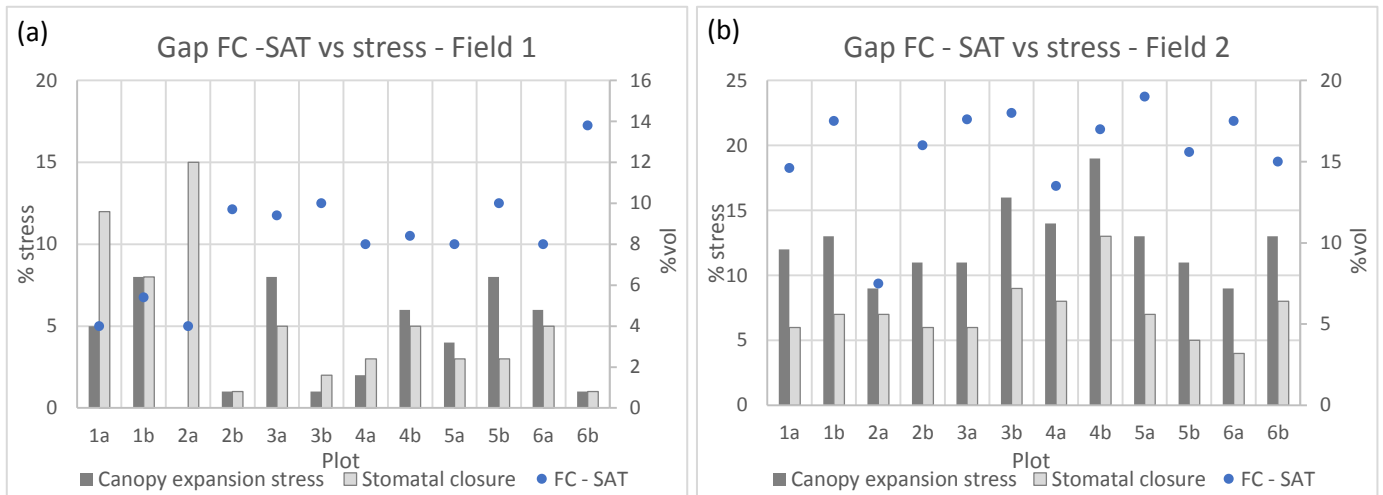


Figure 25. The gap between θ_{FC} and θ_{SAT} , expressed in %vol, plotted with the canopy expansion stress and stomatal closure for field 1 (a) and field 2 (b). The stress is given as a percentage of time when stress occurred averaged over the growing period.

θ_{FC} and θ_{SAT} , but the stress is similar to other plots which have a larger gap between θ_{FC} and θ_{SAT} . However, the amount of TAW has more influence on the stress. For example, plot 4a and 4b have low TAWs and high stresses. But, when the TAW is high it has less influence on the stress. On the whole, the TAW and the gap between θ_{FC} and θ_{SAT} only influence the stress when they are small. As a result of the high value of θ_{FC} in field 1, the gap between θ_{FC} and θ_{SAT} is small and enhances the stress, but the low value of θ_{FC} in field 2 results in a low TAW, which enhances the stress. Therefore, a small increase in soil moisture enhances the stress in field 1, but reduces the stress in field 2 resulting in different effects of variation in soil moisture on biomass.

Evaporation

Field 2 has a lower CC_x than field 1, which results in a higher soil evaporation (E) and a lower transpiration (Tr) in field 2. In addition, the total evapotranspiration (ET) is also higher in field 2 than in field 1. In both fields, E, Tr and ET differ slightly between plots. Since E, Tr and ET are related to the canopy cover, differences in canopy cover between plots cause minor differences in E, Tr and ET between plots. However the small differences between the plots cannot cause the differences in biomass between plots.

On the whole, the soil fertility stress has the largest influence on the biomass production. However, it can be seen that the soil fertility stress is not the only parameter which significantly affects the biomass. After evaluating the results of the soil moisture content and the evaporation of the default simulation it is clear that they did not lead to the difference in biomass between plots.

4.4.2 Average soil fertility stress

Figure 26 shows the biomass for the significant location of the within plot simulation with variable and average soil fertility stress for field 1 and field 2. It can be seen that the biomass simulated with the average soil fertility stress is higher. For field 1, the variation in biomass between the plots is smaller due to the average soil fertility stress. However, there is still difference in biomass between the plots, which confirms that soil fertility stress is not the only parameter causing the difference in biomass between plots. Comparing the biomass of the average fertility simulation with the soil moisture content it is noted that the variation in biomass between plots is not caused by the soil moisture content (figure 20). On the contrary, for field 2, the variation in biomass became larger. This is due to the high calibrated soil fertility stress of plot 2a, which decreased with 7% in the average fertility simulation leading to a higher biomass, while plot 4a had only a decrease of 1% in soil fertility stress. Besides, it has to be noted that the soil fertility stress did not decrease in all plots when the average soil fertility stress was taken. For some plots, the soil fertility stress increased in the average fertility simulation leading to a lower biomass. The average biomass of the whole field is approximately equal to the simulations with variable soil fertility stress, only the proportions between the plots change.

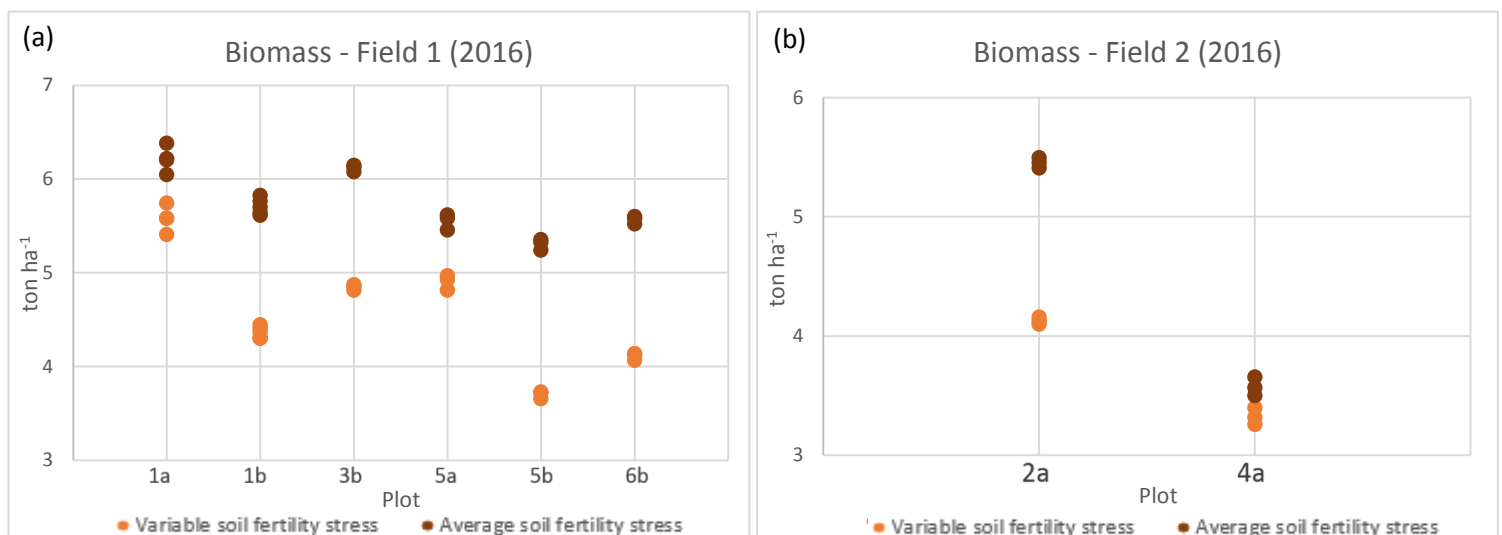


Figure 26. Boxplots of the biomass for all locations with significant different soil moisture contents simulated with the default simulation (variable soil fertility stress) and the average fertility simulation (average soil fertility stress) for field 1 (a) and field 2 (b). All locations within a plot are plotted together for each plot, making it possible to see the range of values within a plot.

From figure 26 and the default simulation it can be concluded that there are other parameters which influence the biomass besides the soil fertility stress. The average fertility simulations do not result in changes in soil moisture and stress, with the small exception of plot 1a, 4a and 6a of field 2, which have slightly different stresses. The evaporation changes slightly between the simulations. In general, a higher soil fertility stress results in a small increase in soil evaporation, a small decrease in transpiration and a small decrease in evapotranspiration. But, the major changes are in the biomass and the yield. The total range of biomass for the center of the plots of field 1 changes from 4.1 – 13.2 to 5.3 – 6.6 ton ha⁻¹ and the total range of biomass for the center of the plots of field 2 changes from 3.1 – 5.6 to 3.5 – 5.5 ton ha⁻¹ due to the change in soil fertility stress. The biomass of field 1 is still higher than the biomass of field 2, but the ranges are closer together. To be able to identify the parameters affecting the biomass the results of the average fertility simulations will be evaluated. This will be done for each field separately, beginning with the plot with the highest biomass and ending with the plot with the

lowest biomass. Table 9 gives the important parameters in the order of the highest biomass for field 1 and field 2.

Field 1

Similar to the default simulation, plot 4a has the highest biomass and yield, but now it is only slightly higher than the second highest biomass. Plot 4a has a high CC_x , CGC and CDC, but since plot 1a and 2a have a larger CC_x , CGC and CDC this cannot be the sole reason for the high biomass. Furthermore, plot 4a has an intermediate soil depth, but a high θ_{FC} , θ_{SAT} and θ_{avg} resulting in little water stress. The gap between θ_{FC} and θ_{SAT} is 8%, which is large enough to have little aeration stress. The combination of all these factors ensures the highest biomass for plot 4a. The second highest biomass is found in control plot 2a. While plot 2a has the highest CC_x and the deepest soil, it does not have the highest biomass. Plot 2a has an average θ_{FC} , but it has the lowest θ_{SAT} resulting in a gap of only 4%. Although the average θ_{FC} and the deep soil result in no water stress, the biomass is lower than in plot 4a due to the small gap between θ_{FC} and θ_{SAT} , which leads to the highest aeration stress of field 1. Plot 3a has the third highest biomass. It has a very low soil depth and an intermediate θ_{FC} , resulting in a lot of water stress, but the fairly high θ_{SAT} leads to an intermediate aeration stress. This in combination with the fourth highest CC_x results in the third highest biomass. On the contrary, plot 3b has the fourth highest biomass, but the second highest soil depth and a CC_x which is below average. In addition, plot 3b has the lowest θ_{FC} and the second lowest θ_{SAT} , but it has the largest gap between θ_{FC} and θ_{SAT} . The deep soil ensures little water stress, while the small gap between θ_{FC} and θ_{SAT} results in little aeration stress. Therefore, even though plot 3b has fairly low canopy cover the biomass is still high. Furthermore, plot 1a has the second highest CC_x and the second deepest soil, but ends with the fifth highest biomass. This is mostly due to the fairly low soil depth and the small gap between θ_{FC} and θ_{SAT} , which result in an intermediate canopy expansion stress and high aeration stress. Plot 1b and 6a have an intermediate biomass, because they both have average parameters. Furthermore, plot 6b has the fifth lowest biomass, while it has the second lowest CC_x . Although CC_x is low, the deep soil leads to barely any water stress and the large gap between θ_{FC} and θ_{SAT} results in the lowest aeration stress. In addition, the REW is slightly lower for plot 6b, which results in less water lost by evaporation. All of this combined gives plot 6b the fifth lowest biomass even though it had to be much lower based on its CC_x . Plot 4b has the fourth lowest biomass, because all parameters are average except for the low soil depth causing the biomass to be below average. The parameters of plot 5a are all just below average resulting in the third lowest biomass. On the contrary, plot 2b has the second lowest biomass even though it has a large soil depth, an average θ_{FC} and θ_{SAT} and a large gap between θ_{FC} and θ_{SAT} resulting in little water and aeration stress. The only reason for the low biomass can be the low CC_x , but it is only the third lowest which does not completely explain the low biomass. An explanation can be found by comparing plot 2b with the plots with higher biomasses. Plot 2b is very similar to plot 6b. They have the same CC_x , the same soil depth and the same amount of stress, but plot 6b has a slightly higher biomass due to its lower REW. Plot 4b and 5a probably have a higher biomass than plot 2b because of their higher CC_x . Lastly, plot 5b has the lowest biomass, because it has the lowest CC_x , a low soil depth and an intermediate θ_{FC} , θ_{SAT} and θ_{avg} . The shallow soil easily triggers water stress and even though the gap between θ_{FC} and θ_{SAT} is large, the shallow soil makes it easier to trigger aeration stress resulting in an intermediate stomatal closure. As a result of the scarce canopy cover, the transpiration is low and the soil evaporation is higher. All of these parameters combined result in the lowest biomass for plot 5b.

In general, it is clear that the biomass follows the pattern of CC_x , a high CC_x leads to a high biomass and when the CC_x decreases, the biomass decreases as well. However, if the plot has a deep soil, the biomass can be higher than plots which have a higher CC_x and a shallower soil. On the contrary, when the plot has a shallow soil, the biomass will be lower than assumed with the pattern of CC_x . It is a logical conclusion that the canopy cover has the largest influence on the biomass, after the soil fertility, since the canopy cover represents the crop development, but it needs to be known which parameters influence the canopy cover. There is no clear pattern between CC_x and the other parameters, but plots

with a high CC_x often have a gentle slope. However, there are also many plots with a high CC_x which have a steep slope. The same can be said about the rooting and soil depth, sometimes it seems like deeper soils result in a higher CC_x , but often this is not the case. In addition, the gap between θ_{FC} and θ_{SAT} can also influence the biomass. If the plot has a small gap, the biomass will be lower than another plot with the same CC_x but a larger gap. Moreover, a high biomass leads to a low soil evaporation and a high transpiration and vice versa, which is a feedback from the CC_x .

Field 2

As can be seen in table 9, the biomass of field 2 follows the pattern of the CC_x better than in field 1. Plot 2a has the highest CC_x , which leads to the highest biomass, plot 3a has the second highest CC_x , which leads to the second highest biomass, etc. The biomass follows the pattern of CC_x more tightly in field 2 because the other parameters differ less between plots. As is mentioned before, θ_{FC} of field 2 is much lower than θ_{FC} of field 1, while θ_{SAT} is more or less similar. This results in a large gap between θ_{FC} and θ_{SAT} for all plots of field 2, which makes it an unimportant parameter for determining the biomass since it is only important if the gap is small. Nevertheless, due to the lower θ_{FC} the TAW becomes more important for biomass production. This can be seen in table 9, where the pattern in biomass almost perfectly follows the pattern in TAW. Furthermore, the soil depth only differs from 0.10 m to 0.19 m, while it differs from 0.10 m to 0.62 m in field 1. Consequently, the soil depth has only little influence on the biomass production. However, there are a few plots of which the biomass does not follow the pattern of CC_x . According to the pattern of CC_x , plot 6b should have a higher biomass than plot 6a, but plot 6a has a significantly deeper soil leading to low canopy expansion stress and stomatal closure, which results in a slightly higher biomass for plot 6a than for 6b. Moreover, plot 2b has a lower biomass than plot 6b, while they have the same CC_x , but all the other parameters of plot 2b are more convenient than in plot 6b. The reason why plot 2b has a lower biomass cannot be explained with this study, but a accompanying study of S. de Roos indicated that plot 2b experienced the most erosion, which might be a reason for the lower biomass of plot 2b. Furthermore, plot 5a has the third lowest CC_x , but the sixth lowest biomass. This is probably because all the other parameters are very average for plot 5a and the plots with a lower biomass all have low soil depths leading to high water stress. So, plot 5a has a higher biomass than other plots with a higher CC_x because these other plots have shallower soils. Lastly, plot 5b has the second lowest CC_x , but the third lowest biomass. This is due to the deep soil and the high TAW of plot 5b, while the other plots with low biomass all have shallow soils and lower TAWs. The plot with the lowest biomass is plot 4a, which has the lowest CC_x , a low soil depth, a low θ_{FC} , θ_{SAT} and θ_{avg} and high canopy expansion stress and stomatal closure. However, the plot with the second lowest biomass has the highest canopy expansion stress and stomatal closure, but due to the higher CC_x , plot 4b has a slightly higher biomass than plot 4a.

Similar to field 1, the biomass generally follows the pattern of CC_x . There are only small exceptions, mostly due to a difference in soil depth. For field 2, there is a clearer pattern between CC_x and soil depth. Often, a deeper soil leads to a higher CC_x , but this is still not always the case. The relation between CC_x and the slope is less clear than in field 1, sometimes it even seems that a high slope leads to a higher CC_x . However, it is noticeable that the plots with a high biomass generally have a high θ_{FC} and plots with a low biomass a low θ_{FC} . But, the same is not true for the θ_{avg} , which seems randomly divided, only the two plots with the lowest biomass also have the lowest θ_{avg} . The pattern of the evaporation is the same as for field 1.

The overall conclusion of the average fertility simulation is that, next to the soil fertility stress, the maximum green canopy cover is the most important parameter in determining the biomass. However, it is unclear which parameters have the largest effect on CC_x and, consequently, on the biomass. Another important parameter is the soil depth, which positively influence the biomass when it is high and negatively influence the biomass when it is low. In addition, when the gap between θ_{FC} and θ_{SAT} is small, it becomes more important for determining the biomass, because it makes it easier to trigger stomatal closure which has a negative effect on the biomass. Furthermore, the parameter which

seemed to have very little effect on the biomass production is the saturated hydraulic conductivity. Besides, the control plots of field 1 almost all have the lowest biomass, while in field 2 this is not the case. Control plot 3a even has the second highest biomass, but the other control plots have lower biomasses, namely the third, fourth and sixth lowest.

Table 9. Input and output parameters of the average fertility simulation for the center of the plots ordered from highest biomass to lowest biomass. CC_x is the maximum green canopy cover, θ_{FC} is the soil moisture content at field capacity, θ_{SAT} is the soil moisture content at saturation, θ_{avg} is the simulated average soil moisture content over the growing period, K_{sat} is the saturated hydraulic conductivity, TAW is the total available water, REW is the readily evaporable water, Exp stress is the canopy expansion stress, Sto stress is the stomatal closure.

Field 1													
	CC _x	Soil depth	θ_{FC}	θ_{SAT}	θ_{avg}	K _{sat}	TAW	REW	Slope	Exp stress	Sto stress	Biomass	Yield
Plot	%	m	%vol	%vol	%vol	mm day ⁻¹	mm	mm	°	%	%	ton ha ⁻¹	ton ha ⁻¹
4a	52.5	0.25	48.0	56.0	42.3	767	330	6	11.9	2	3	6.567	2.824
2a	59.2	0.62	45.0	49.0	39.1	563	300	6	8.0	0	15	6.396	2.622
3a	51.9	0.13	46.0	55.4	41.0	685	310	6	11.9	8	5	6.221	2.616
3b	46.6	0.40	40.0	50.0	35.1	666	250	6	16.5	1	2	6.147	2.643
1a	53.8	0.16	47.0	51.0	40.8	440	320	6	8.5	5	12	6.050	2.542
6a	45.5	0.10	48.0	56.0	42.7	848	330	6	8.2	6	5	5.706	2.401
1b	47.3	0.11	45.0	50.4	39.2	764	300	6	15.0	8	8	5.701	2.457
6b	40.7	0.34	41.2	55.0	37.4	730	262	4	10.0	1	1	5.601	2.408
4b	43.8	0.13	49.0	57.4	43.6	698	340	6	12.3	6	5	5.596	2.408
5a	43.2	0.20	48.0	56.0	41.5	848	330	10	8.5	4	3	5.586	2.347
2b	41.0	0.34	45.3	55.0	40.0	715	303	6	14.5	1	1	5.510	2.314
5b	40.6	0.14	44.0	54.0	39.0	730	290	6	10.0	8	4	5.328	2.294
Field 2													
	CC _x	Soil depth	θ_{FC}	θ_{SAT}	θ_{avg}	K _{sat}	TAW	REW	Slope	Exp stress	Sto Stress	Biomass	Yield
Plot	%	m	%vol	%vol	%vol	mm day ⁻¹	mm	mm	°	%	%	ton ha ⁻¹	ton ha ⁻¹
2a	51.2	0.19	39.0	46.5	33.7	578	240	9	14.5	9	7	5.454	2.580
3a	41.8	0.14	38.4	56.0	35.2	571	234	9	8.5	11	6	4.824	2.280
1b	40.7	0.13	36.0	53.5	32.8	640	210	9	19.0	13	7	4.516	2.123
6a	36.7	0.19	36.0	53.5	33.4	435	210	9	7.2	9	4	4.202	1.903
6b	37.1	0.12	37.0	52.0	33.7	531	220	9	16.0	14	8	4.118	1.889
2b	37.4	0.16	35.0	51.0	31.8	613	200	7	16.8	11	6	4.110	1.861
5a	32.3	0.13	34.0	53.0	31.9	435	180	8	9.0	13	7	3.910	1.790
1a	35.1	0.12	39.4	54.0	35.7	585	194	9	6.2	13	7	3.855	1.737
3b	34.8	0.10	34.0	52.0	31.4	585	190	9	14.5	16	9	3.838	1.680
5b	30.8	0.16	37.4	53.0	33.9	531	224	9	18.2	11	5	3.758	1.740
4b	33.6	0.10	29.0	46.0	26.7	558	140	9	6.2	19	13	3.693	1.598
4a	28.8	0.12	31.5	45.0	28.9	503	165	6	6.2	14	9	3.566	1.584

4.5 AquaCrop simulations: effect of inter-annual variability

The all year default and within plot simulations are not only conducted for 2016, but also for all years from 2005 to 2016 to see the effect of weather conditions on the biomass and yield production. The simulations between years only differ from each other in temperature and rainfall, which affect other parameters, such as soil moisture, stress and yield. However, the all year simulations of field 2 with the same crop development, soil characteristics and field management practices of 2016 resulted in many harvest failures. This problem only occurred for field 2 and not field 1 due to the earlier sowing date of field 2. In many previous years, it was still very dry in the end of March resulting in severe water stress in the beginning of the crop cycle leading to crop failure. In mid-April, when field 1 was sowed, the driest period was over and the crops could develop. To give the crops of field 2 a chance to grow, the sowing date in AquaCrop is changed for some years. This is probably the most realistic, because a farmer does not start sowing when it is still too dry. Table 10 gives an overview of the changes in sowing dates for field 2. The sowing date of field 1 remains 19 April for all subplots.

Figure 11 shows that the amount of rainfall in the growing period varies between 833 mm in 2006 and 2614 mm in 2014 and the number of GDDs in the growing period varies between 1293 °C day⁻¹ in 2007 and 1623 °C day⁻¹ in 2016. It is noticeable that 2007 and 2014 have approximately the same amount of rainfall, but 2014 has a much higher GDD. By comparing the simulation of 2007 and 2014 the effect of temperature on biomass production can be determined. In addition, 2007 and 2008 have similar GDDs, but 2007 has more rainfall than 2008. Comparing the simulation of 2007 and 2008 can determine the effect of rainfall on biomass production. Therefore, it is interesting to evaluate the results of the simulation of 2006, because it is the driest year, 2014, because it is the wettest year and 2008 and 2007 to evaluate the effect of rainfall and temperature.

Table 10. Adjusted sowing dates for field 2 for each year.

Year	Sowing date	Year	Sowing date	Year	Sowing date
2005	12 April	2009	6 May	2013	25 March
2006	20 April	2010	25 March	2014	25 March
2007	25 March	2011	29 March	2015	27 April
2008	23 April	2012	15 March	2016	25 March

4.5.1 Effect of temperature and rainfall on soil moisture and biomass

The significant locations of field 1 for some specific years (2006, 2007, 2008 and 2014) are compared and evaluated to determine the effect of rainfall and temperature on the soil moisture and biomass production. Only the significant locations of field 1 will be discussed here, because field 2 has only two plots with significant locations. Figure 27 shows θ_{avg} and the biomass of the significant locations for each year. The pattern of the soil moisture follows the amount of rainfall for each year. The lowest soil moisture is found in the driest year, 2006, and the highest soil moisture is found in the wettest year, 2014. The proportions of soil moisture between plots remain similar between the years, with the highest soil moisture for plot 6b and the lowest soil moisture for plot 1a. Furthermore, also the proportion of biomass between the plots remains the same over the years, with the highest biomass in plot 3b and the lowest in plot 5b. The range of biomass does change between the years. The highest range of biomass is found in 2014, but it is almost the same as in 2006. So, the wettest and the driest year both produce the same amount of biomass. Furthermore, 2007 and 2008 have approximately the same range of biomass, but in 2008 there is one location with no biomass, which results in a slightly higher average biomass in 2007. When comparing the changes in soil moisture with the changes in biomass, it can still be seen that the differences in soil moisture content have little influence on the differences in biomass between plots. The soil moisture contents of 2007 and 2014 are very similar due to their similar amount of rainfall. However, the biomass production is higher in 2014. On average for all locations, the biomass in 2014 is 0.410 ton ha⁻¹ higher than the biomass in 2007, which is a difference of 8.5%. Therefore, it can be concluded that a higher amount of GDDs result in a higher

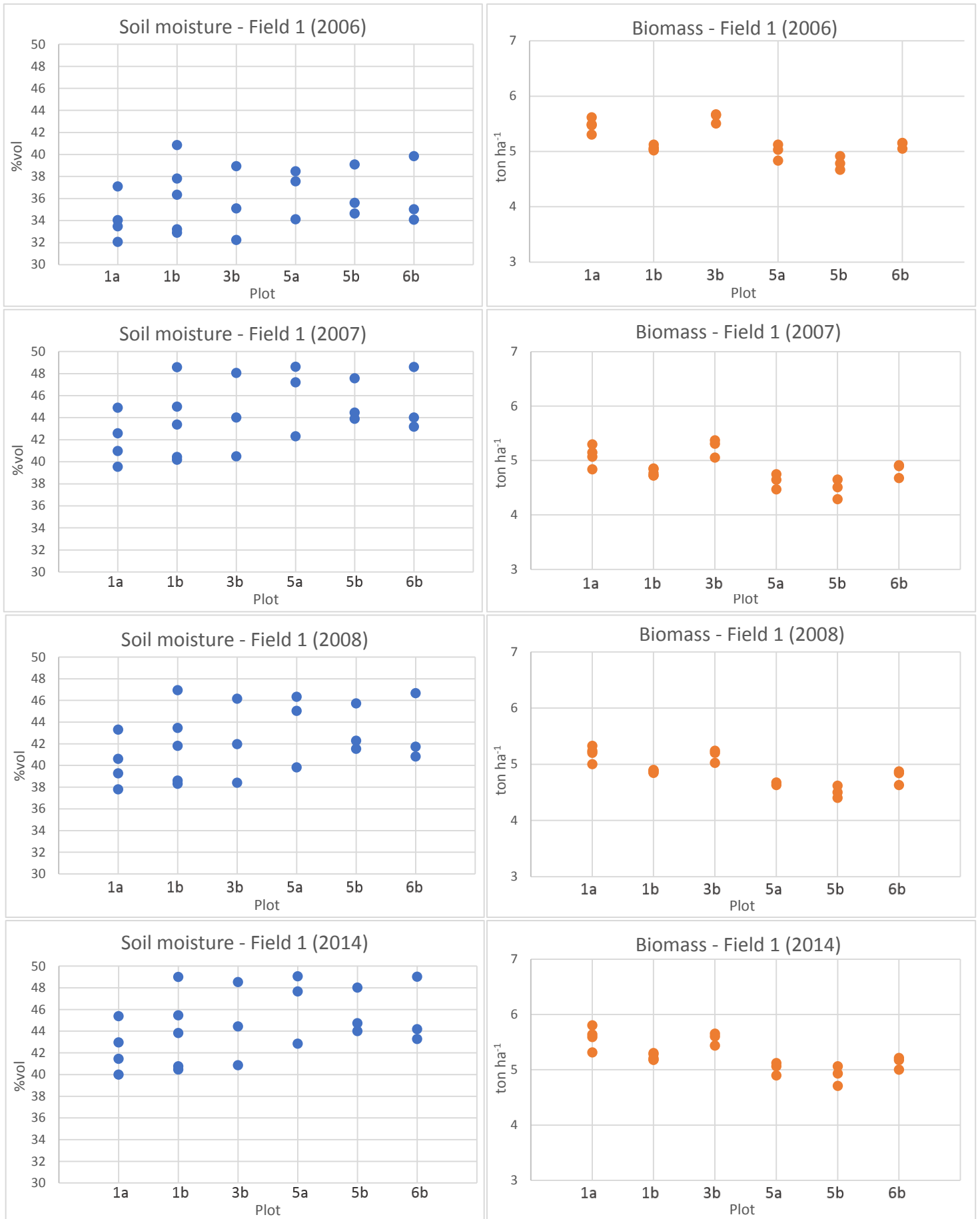


Figure 27. The simulated average soil moisture content over the growing period and the biomass plotted for all significant locations of field 1 for 2006, 2007, 2008 and 2014. All locations within a plot are plotted together for each plot.

biomass. Furthermore, the soil moisture contents of 2007 are, on average, 2% higher than in 2008 due to the higher amount of rainfall in 2007. But, there is no significant difference between the biomass of 2007 and the biomass of 2008.

To better indicate the differences in biomass between years, figure 28 gives the ranges of θ_{avg} and biomass of all measurement locations of each year over the period 2005 to 2016 for field 1 and field 2. The soil moisture differs between the years, with the lowest soil moisture in 2006 and the highest soil moisture in 2007, 2011 and 2014, which is in agreement with the amount of rainfall (figure 11). The biomass changes relatively more between the years than the soil moisture. For field 1, the highest biomass is found in 2016 and the lowest in 2007 and 2008, which follows the pattern of GDDs between the years (figure 11). However, for field 2, the highest biomass is found in 2015 and 2016, while the lowest biomass is found in 2005 and 2012, which does not relate to the pattern in GDDs or rainfall. It is most likely that a combination between temperature and rainfall causes the low yields in 2005 and 2012. For both fields, there are a few years where some locations did not produce any biomass. In field 2, this was mostly plot 4, which is also the plot with the statistically significant lower soil moisture content (table 6). On the whole, it can be concluded that temperature has a larger effect on the biomass than rainfall according to the weather conditions in the Bokole watershed. This conclusion is only applicable for the ranges of temperature and rainfall in the Bokole watershed, where even the driest year recorded in 11 years is still sufficient enough to produce biomass and yield.

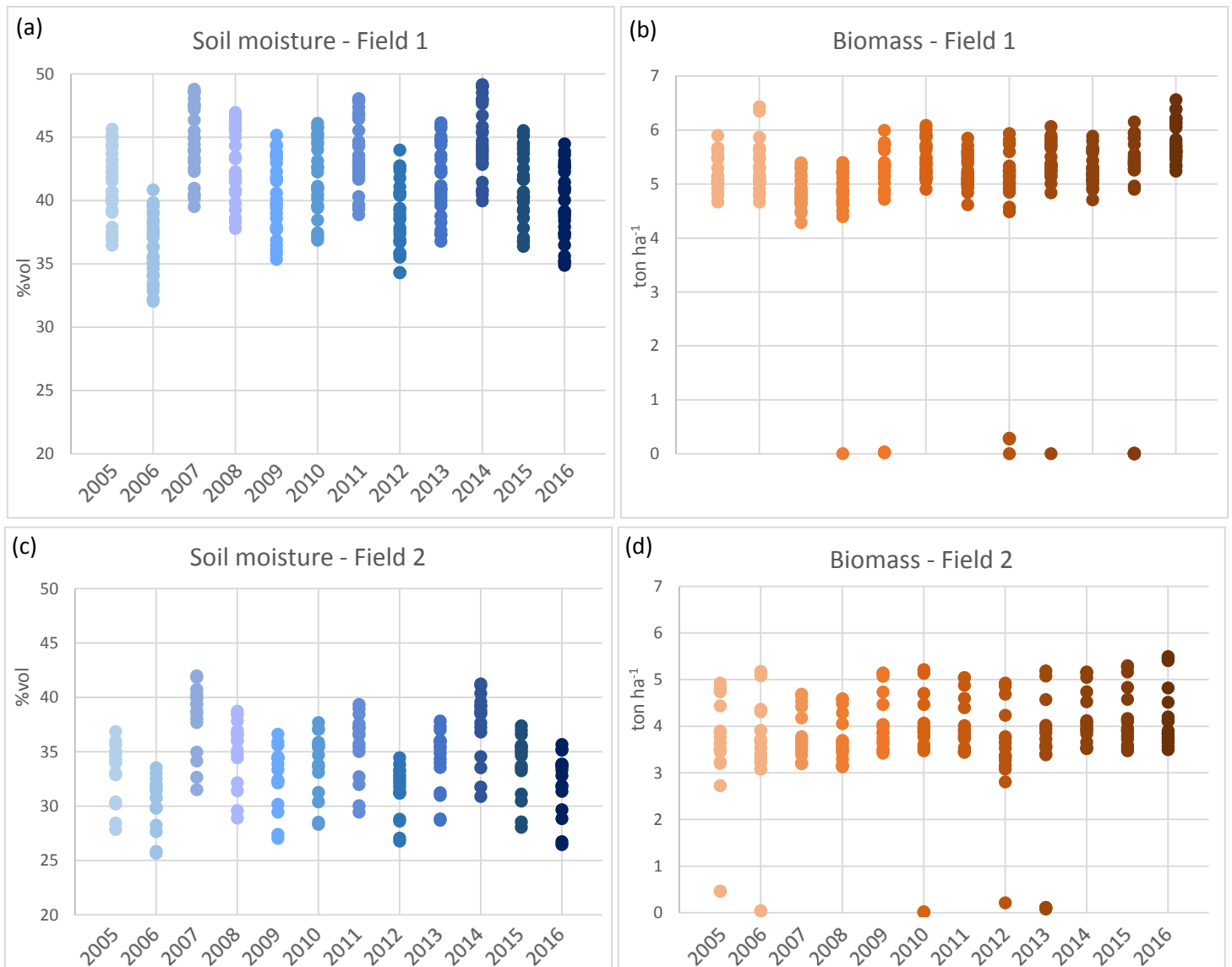


Figure 28. The averaged actual soil moisture content for all measurement locations plotted for each year for field 1 (a) and field 2 (c) and the biomass for all measurement locations plotted for each year for field 1 (b) and field 2 (d).

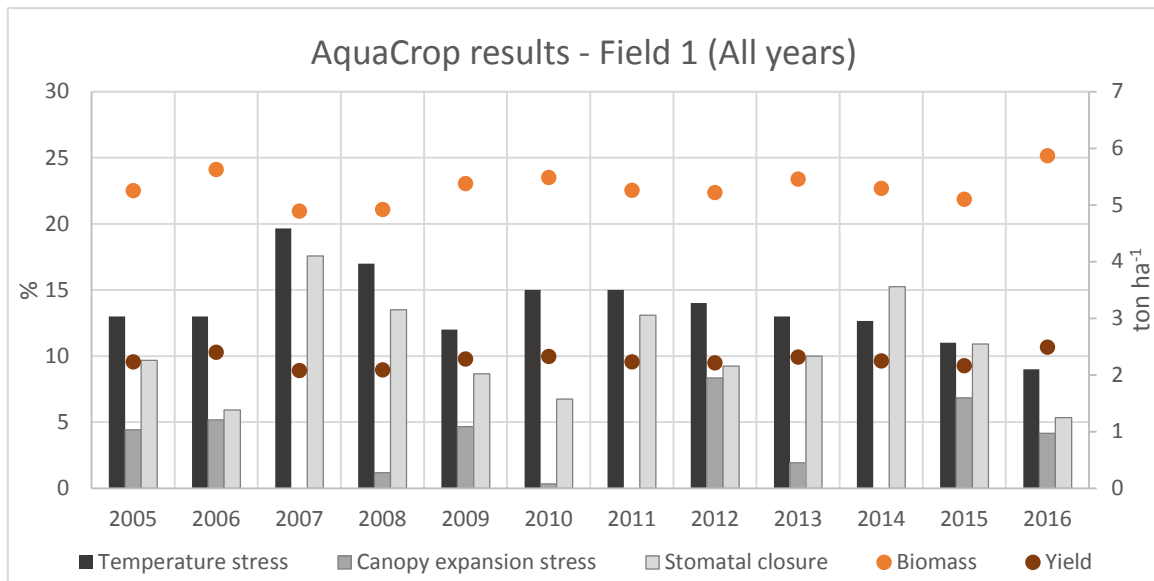


Figure 29. The amount of temperature stress, canopy expansion stress, stomatal closure, biomass and yield per subplot, averaged over the entire field for each year. The amount of stress is given as an average stress over the growing period.

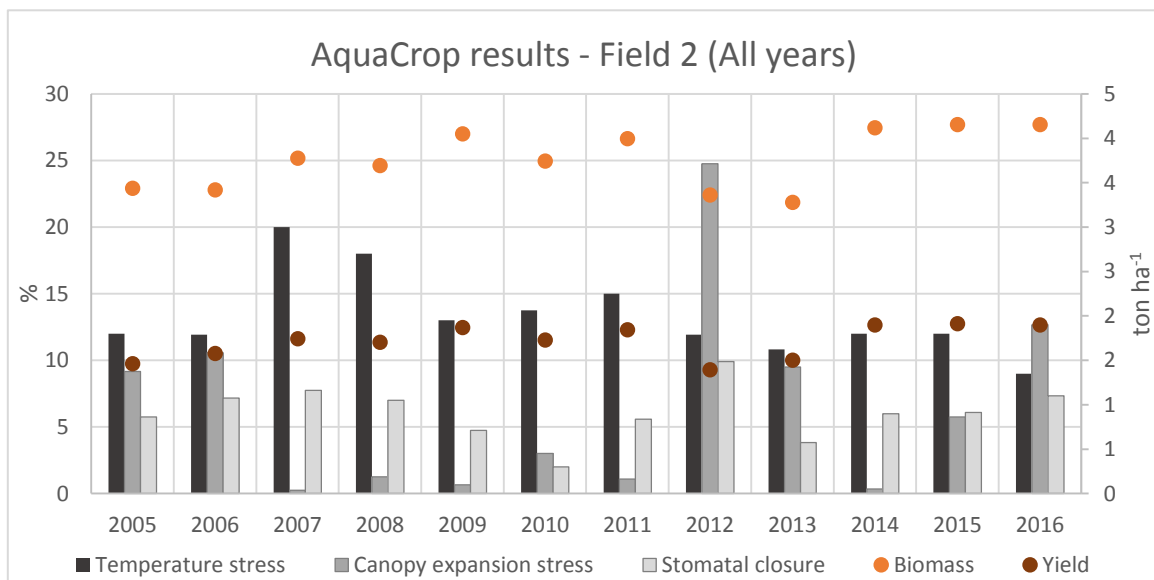


Figure 30. The amount of temperature stress, canopy expansion stress, stomatal closure, biomass and yield per subplot averaged over the entire field for each year. The amount of stress is given as an average stress over the growing period.

4.5.2 Effect of temperature and rainfall on stress conditions and biomass

The all year simulations are conducted for each subplot for each year. Then, the average values of the stresses, biomass and yield of all plots are taken for each year to get the values for each year for the whole field, which are shown in this paragraph. The average stresses, biomass and yield of field 1 for each year are given in figure 29. The amount of temperature stress ranges from 9% to 20% and follows the GDD pattern of figure 11. For example, the highest temperature stress is found in 2007, which also has the least GDDs, and the lowest temperature stress is found in 2016, which has the most GDDs. The canopy expansion stress ranges between 0 – 8% of which the years with the most rain (2007, 2011 and 2014) have no canopy expansion stress. However, the years with the least rain do not necessarily have the highest canopy expansion stress. Furthermore, the range of stomatal closure is between 5 – 18%. The highest stomatal closures are found in the years with the most rain, because a high amount of rain saturates the soil more easily, which leads to aeration stress and stomatal closure. However, the

stomatal closure does not necessarily follow the pattern of the rainfall of figure 11. For example, the stresses of 2005 and 2006, which have similar rainfall and GDD values, but the stomatal closure in 2005 is higher than in 2006. This is probably because 2005 has more contiguous days of rain, giving the soil less time to remove the excessive water, which leads to aeration stress. The number of contiguous days of rain is probably also the reason that the years with the least rain do not necessarily have the highest canopy expansion stress. Moreover, the biomass changes slightly between the years. The range of average biomass of all years is from 4.9 to 5.9 ton ha⁻¹ of which the highest biomass is found in 2016 and the lowest in 2007. The biomass is low in 2007 due to the large temperature stress and stomatal closure, while 2016 has the lowest temperature stress and stomatal closure, only the canopy expansion stress is average.

Figure 30 gives the average stresses, biomass and yield for all plots of field 2 for each year. It can be seen that there is biomass production for each year. However, some plots for some years still have no biomass production (figure 28). The temperature stress is similar to field 1. But, the canopy expansion stress is often much higher. It ranges between 0 – 25%, of which the highest canopy expansion stress occurs in 2012, but it is also high in 2006 and 2016. Similar to field 1, the years with the most rainfall, 2007 and 2014, have no canopy expansion stress, but the pattern of the canopy expansion stress does not necessarily follow the amount of rainfall of each year. Furthermore, the stomatal closure is significantly lower than for field 1. It ranges from 2 – 10%. But, the highest stomatal closure is now found in 2012 and the lowest in 2010. This can differ from field 1 due to the difference in dates of growing stages. Furthermore, the biomass differs slightly between years. The range of average biomass of all years is between 3.3 and 4.2 ton ha⁻¹. The highest biomass is found in 2009, 2014, 2015 and 2016. Most likely, 2009 and 2014 have a high biomass because both years have a low amount of stress and an average to high amount of GDDs. However, 2015 and 2016 do not have the least amount of stress, but they have a high amount of GDDs and an average amount of rainfall, which can lead to a better canopy development and a higher biomass production. The lowest biomass is found in 2013, but also 2005, 2006 and 2012 have low biomasses. The low biomass of 2012 is due to the high canopy expansion stress and stomatal closure. The year of 2013 has a very similar amount of rainfall and GDDs to the year of 2012, also leading to a low biomass.

On the whole, it can be concluded that weather conditions influence the biomass production. Rainfall influences the severity of water stress and aeration stress. However, not only the amount of rainfall, but also the number of contiguous days of rain is important. If the rainy days are more equally divided over the growing period, there is less water and aeration stress resulting in a higher biomass than when the number of rainy days is less equally divided. Therefore, a year with a low amount of rainfall can still have less water stress than a year with more rainfall, but less equally divided over the growing period. The temperature influences the temperature stress. For the weather conditions of the Bokole watershed, it can be concluded that the temperature has a larger effect on the biomass than rainfall. For the most extreme weather conditions in the Bokole watershed of the past 11 years, the average range of biomass is 4.5 – 6.6 ton ha⁻¹ and 2.7 – 5.5 ton ha⁻¹ for field 1 and field 2, respectively. So, even with more extreme weather conditions, the biomass will not be lower than 4.5 ton ha⁻¹ for field 1 and 2.7 ton ha⁻¹ for field 2. It has to be kept in mind that there is always a chance on harvest failure, but those were not included in these ranges.

5. Discussion

5.1 Evaluation of methods

A variety of methods is used to determine the results in the present study, with all their own uncertainties of which the most important uncertainties are evaluated here. The soil moisture content was measured with a FDR in the fields, which is sensitive to changes in temperature and to the electrical conductivity in the soil (Campbell, 2014). Changes in temperature change the availability of water to be polarized by the electromagnetic field (Campbell, 2014). The soil moisture content was measured on the same location for 10 and 7 days for field 1 and field 2, respectively. The exact temperature was not measured, but the time of the soil moisture measurements differed between the days, so it is most likely that there were changes in temperature between the measurements. This leads to deviations in the measured soil moisture content between days which is not due to differences in the soil moisture content. Moreover, polar molecules in the electromagnetic field change how charge is stored and, hence, can change the relationship between the sensor output and the soil moisture content (Campbell, 2014). Furthermore, the canopy cover is measured by taking digital camera pictures of the maize almost vertically towards the ground. In August, when the pictures were taken, the maize was approximately 1.7 m high, of which some plants exceeded 2 m (see plant height in Appendix 9). Therefore, it was difficult to take good pictures vertically towards the ground, but the best pictures were chosen for the calculation of the canopy cover. The method of measuring the total biomass and yield was accurate enough, but other factors caused some uncertainties in the biomass and the yield. Just before harvest, monkeys came to eat the maize in field 1, especially in plot 1 because it is the border of the field. It was tried to take the sample areas on undisturbed places in the plots, but the monkeys could have caused an underestimation of the biomass and the yield. In addition, the yield samples were compromised by maize eating insects and were therefore not used in the present study. The rainfall and temperature were measured by a weather station located 5 km northwest of the fields and 400 to 450 m higher in altitude. This can result in differences between the measured rainfall and temperature and the actual rainfall and temperature in the experimental fields. Especially the rainfall is variable in space, which makes it harder to link the measured soil moisture in the experimental fields to the rainfall data.

To see the effect of soil fertility stress, the simulations were run again but with an average soil fertility stress. In addition, when the variation in soil fertility stress between the plots was eliminated, the effect of other parameters on the biomass and yield could be evaluated. This is not done for the soil depth because it was assumed that the small variation in soil depth between the plots was too small to have a large effect on the variation of biomass and yield between the plots. However, after assessing which parameter had the largest influence on the biomass and yield it seemed that the soil depth had a rather large influence. Therefore, in further research it is important to determine the sensitivity of biomass and yield to soil depth by conducting an AquaCrop simulation with an average soil depth. Furthermore, the all year simulation simulates the situation of the experimental fields in 2016 for each year in the period of 2005 to 2016, by changing the rainfall and temperature data, while all the other input data remains the same to the situation determined in 2016. Obviously, the crops will respond differently to the different weather conditions, which makes it not entirely realistic that parameters, such as the maximum green canopy cover, do not change over the years. In addition, the farmers will also respond differently to different weather conditions with regard to the sowing date. However, since this simulation is only used to see the effect of changes in rainfall and temperature, based on actual rainfall and temperature data of the past years, on the soil moisture content, stresses, biomass and yield the all year simulation suffices.

5.2 Evaluation of the FAO AquaCrop model

The present study as well as other studies encounter some limitations of the FAO AquaCrop model. It was challenging to simulate the very shallow soils of the Bokole watershed in AquaCrop due to the

minimum restriction of some input parameters and the internal relation of some parameters in AquaCrop. AquaCrop lacks transparency with regard to the internal model structure, which constraints the applicability of the model. AquaCrop changes some parameters internally, like the maximum canopy cover, which makes it difficult to use the model since the user has no control on the parametrization (Paredes et al., 2015). AquaCrop is distributed as a compiled software package, which does not have open access to the source code (Foster et al., 2017). This limits the user to reproduce model calculations, to evaluate the influence of the internal model structure on the simulation outputs, to link AquaCrop directly with other models and to adapt the code to make the model more applicable to the specific purposes of the study (Foster et al., 2017).

Furthermore, AquaCrop only simulates the presence of soil bunds by their inhibition of surface runoff, but does not consider the effect of soil bunds on soil erosion, soil fertility, crop production and the soil water balance (Van Gaelen, 2016). Therefore, the only differences between plots with and without bunds in the present study are the runoff and the potential differences in measured parameters in the field and in the lab, but the simulated processes, except for runoff, remain the same for all plots whether they have bunds or not. Besides, AquaCrop does not consider the slope of the plots which can influence the amount of runoff and infiltration. Since the slopes of the fields in the study area are steep it should be taken into consideration in the simulations of AquaCrop. Furthermore, the rainfall intensity cannot be implemented in AquaCrop. So, AquaCrop distributes the rainfall of one day evenly over the entire day, but in reality it is more likely that the rainfall occurs for only one or two hours. This results in a lower rainfall intensity in AquaCrop than in reality, which affects infiltration and runoff. For the simulations of the present study, almost all rainfall infiltrated in the soil. Furthermore, Van Gaelen (2017) found that AquaCrop only considers the effect of heat stress on pollinations or indirectly through increased potential evapotranspiration, but does not consider the effect of heat stress on flowering and grain filling, which Van Gaelen (2017) found to result in unrealistic maize simulations. In addition, Van Gaelen (2017) found that some processes, such as cold acclimation and vernalization* are absent in the AquaCrop simulations. In addition, the green canopy cover is adjusted for micro-advection in AquaCrop (see 3.1.2 crop development and equation 22). This is determined with an equation with linear and quadratic terms (eq. 22), which does not look like other equations that adjust for micro-advection (Diaz-Espejo et al., 2005; Yuge et al., 2005). Therefore, the present study questions whether equation 16 adjusts for micro-advection.

Moreover, AquaCrop is designed to predict crop yield as a point simulation at the single field scale and assumes the field to be uniform without spatial differences in crop development, transpiration, soil characteristics and management (Raes, 2017). In the present study, the simulations were conducted for an area of approximately 65 m², which is unlikely to have no spatial differences in crop development, transpiration and soil characteristics. Therefore, the simulations used in the present study are based on average parameters, which represent the entire subplot. Furthermore, Greaves and Wang (2016) found the use of a single set of soil characteristics without spatial variability to result in poor predictions of the evapotranspiration when extreme weather variations occurred, such as heavy rainfall, droughts or heat waves. Heavy rainstorms are not unlikely in the Bokole watershed, so it is plausible to consider that the simulation of the evapotranspiration had a lower accuracy during the periods with heavy rainfall. Furthermore, AquaCrop is a one dimensional model and only considers vertical incoming and outgoing water fluxes (rainfall, evaporation, transpiration, deep percolation) and does not consider lateral movement of water fluxes (Raes, 2017). Therefore it is not possible to simulate, for example, the movement of soil moisture from the upper bunds to the lower bunds. To include the spatial gradient in the simulations a two dimensional model is needed.

Despite the limitations, many studies found AquaCrop to be a simple and robust model, which simulates the soil water balance, the crop development, the biomass production and the yield with a fairly well accuracy (Araya et al., 2010; Abedinpour et al., 2012; Biazin and Stroosnijder, 2012; Mkhabela and Bullock, 2012; Van Gaelen et al., 2015; Muluneh et al., 2016). Van Gaelen et al. (2015)

* Vernalization is the cooling of the seed during germination in order to accelerate flowering when it is planted.

report that AquaCrop provides good indicative values for the soil moisture, canopy cover, biomass and maize yield when the crop production is affected by soil fertility and soil water stress in Nepal. Furthermore, Abedinpour et al. (2012) indicate that in spite of the lesser number of input data required, AquaCrop predicts the maize yield with acceptable accuracy in northern India. Moreover, even in Ethiopia there are positive results. Muluneh et al. (2016) indicate that AquaCrop is able to simulate soil water, canopy cover and yields for maize fairly well in southern Ethiopia. In addition, Araya et al. (2010) found similar measured and simulated canopy cover, biomass and yield values and considers AquaCrop as a valid model to simulate yield in northern Ethiopia. And, Biazin and Stroosnijder (2012) conclude that AquaCrop is a good decision support tool for planning and development of appropriate management techniques in southern Ethiopia.

The main difference between the present study and the studies mentioned above is the soil depth, which is extremely low for the study area of the present study. Together with the abovementioned limitations this could have resulted in the less positive results of the FAO AquaCrop model found in the present study. Nevertheless, after calibration of AquaCrop, the soil moisture, the biomass and the canopy cover were simulated well enough in AquaCrop for the majority of the plots. However, it is questionable if the simulation of the effect of soil bunds on soil moisture, crop development and yield in AquaCrop is sufficient enough to see the potential differences in soil moisture and yield between plots with and without soil bunds.

5.3 Maize yield

In the present study, the biomass and yield range between 4.1 – 13.2 ton ha⁻¹ and 1.5 – 5.7 ton ha⁻¹ for field 1, respectively, and between 3.1 – 5.6 ton ha⁻¹ and 1.3 – 2.6 ton ha⁻¹ for field 2, respectively (table 7 and figure 21 and 22). If these yields are compared to, for example, maize yields from the Netherlands, the study area in the Bokole watershed produces approximately 20 times less maize (available on www.melkvee.nl [date of search: 1-5-2017]). But, studies conducted in Africa and in Ethiopia report more similar maize yields to the Bokole watershed (Kang et al., 1981; Fan et al., 2005; Nyakudya and Stroosnijder, 2014; Hadgu et al., 2015; Mourice et al., 2015; Tully et al., 2015; Zeng et al., 2015 and Masvaya et al., 2017). Kang et al. (1981) indicated a yield of 3.8 ton ha⁻¹ in Nigeria, Nyakudya and Stroosnijder (2014) observed a mean yield of 2.7 ton ha⁻¹ in Zimbabwe, Hadgu et al. (2015) measured a maize yield of 3.81 ton ha⁻¹ in northern Ethiopia, Mourice et al. (2015) found maize yields ranging from 0.05 – 3.6 ton ha⁻¹ in Tanzania, Zeng et al. (2015) found a maize yield of 2.16 ton ha⁻¹ in Ethiopia and Masvaya et al. (2017) found maize yields of 1.99 ton ha⁻¹ in Zimbabwe. However, some other studies conducted in Africa and in Ethiopia measured higher yields (Das et al., 2010 and Akumaga et al., 2017). For example, Das et al. (2010) found yields in the range of 5.15 – 8.13 ton ha⁻¹ in eastern Ethiopia. The studies which report higher yields have better slope and soil conditions than in the present study. Even for the studies with similar maize yields, the maize yields of the present study are often slightly lower.

When the soil fertility stress is averaged for the whole field and the simulation is conducted for each year between 2005 and 2016 the range of biomass and yield which could be produced in other weather conditions ranges between 4.5 – 6.6 ton ha⁻¹ and 1.9 – 2.8 ton ha⁻¹ for field 1 and 2.7 – 5.5 ton ha⁻¹ and 0.8 – 2.6 ton ha⁻¹ for field 2, respectively (figure 29 and 30, respectively). In general, the ranges of yield between the fields are more similar. But, these ranges are still in the lower range of the yields mentioned above.

5.4 Effect of soil bunds on soil moisture and maize yield

The presence of soil bunds can influence soil properties, soil hydraulic characteristics, crop development, crop yield, soil loss, nutrient loss and erosion. In the present study, the soil and rooting depth are similar to higher for control plots in field 1 and similar to lower for control plots in field 2 (table 4). In addition, there is generally no difference in slope between plots with and without bunds

for both fields. The same is observed for the maximum canopy cover of field 2, but the maximum canopy cover of field 1 is, generally, slightly lower for control plots. It is noticeable that the difference between plots with and without bunds is not similar for field 1 and field 2. But in general, it can be concluded that there is no significant difference in soil depth, slope and maximum canopy cover between plots with and without soil bunds (see table 4). Wolka et al. (2016) came to the same conclusion for the Bokole watershed, reporting that only the cation exchange capacity was higher in fields without bunds, while the other soil properties were not different between fields with and without soil bunds.

The simulations by AquaCrop and the field measurements are used to evaluate the effect of soil bunds on soil moisture, biomass and maize yield. The measured soil moisture contents indicate that only plot 5 of field 1, which is a control plot, and plot 4 of field 2, which is a plot with bunds, have statistically different soil moisture contents (table 6). The other plots all have similar soil moisture contents. However, when the simulated actual soil moisture content over the growing period is evaluated it can be seen that plot 5 of field 1 is not significantly different from the other plots anymore (figure 23a). But, plot 4 of field 2 is still significantly different from the other plots (figure 23b). The low θ of plot 4 is probably caused by the abundance of stones in the soil which makes it harder to contain moisture. Small stones were found in other plots in field 2 as well, but never as abundant as in plot 4. On the whole, it can be concluded that the soil bunds have no effect on the soil moisture content for both fields. Vancampenhout (2003) found that stone bunds enhance soil moisture contents close to the bund, but the effect was most visible at greater depths of approximately 1.0 m to 1.5 m. However, the soil depth in the experimental fields of the present study varies between 0.10 m and 0.60 m.

The simulated maize yield shows no difference between plots with and without bunds for field 1, but for field 2 the lower control plots have a higher yield than plots with bunds (figure 18). However, when the soil fertility stress is averaged for the whole field (e.g. results of the average fertility simulation) there is no difference in yield between plots with and without bunds for field 2, but for field 1 the yield of the control plots is slightly lower than the yield of plots with bunds (table 9). Therefore, it can be concluded that soil bunds do not significantly influence the maize yield in the Bokole watershed for this growing season. Nyssen et al. (2007) indicates the potential short-term benefits of bunds to be the reduction of the slope length and the creation of little retention basins for runoff and sediment, which reduce the volume and eroding capacity of the overland flow immediately after construction, which in turn reduces soil and nutrient loss. The reduction in runoff and soil loss due to bunds in Ethiopia is reported by many studies, with an average reduction of 28% and 64%, respectively (Hengsdijk et al., 2005; Gebremichael et al., 2005; Vancampenhout et al., 2006; Nyssen et al., 2007; Teshome et al., 2013; Adimassu et al., 2014; Wolka et al., 2011; Wolka et al., 2016). Moreover, Adimassu et al. (2014) found that soil bunds significantly reduce nutrient losses by approximately 50%. However, Nyssen et al. (2007) found the amount of phosphorus, nitrogen and organic matter highly variable between plots but it was not a result of bunds. Furthermore, according to Nyssen et al. (2007), the medium and long term effects of bunds are the reduction in slope angle by progressive terrace formation and the development of vegetation cover on the bunds. For example, Gebremichael et al. (2005) observed a gradual average 3% reduction in slope angle due to bunds in approximately 9 years. In addition, Gebremichael et al. (2005) also found that the soil loss rate decreases with the increasing age of bunds. The combination of the short and long term effects of bunds are likely to enhance crop yields. Many Ethiopian studies report a positive effect of contour soil and stone bunds on crop yield (Vancampenhout et al., 2006; Nyssen et al., 2007; Teshome et al., 2013; Wolka et al., 2016). Although, Teshome et al. (2013) only indicate a 10% – 15% increase in crop yield from the third year after constructing the bunds. And likewise, Wolka et al. (2016) observe improved crop yields after approximately 1 to 2 years after construction of the bunds in the Bokole watershed. However, the studies of Hengsdijk et al. (2005) and Adimassu et al. (2014) both observe no effect of bunds on yield or even a decrease in yield. They both found that the bunds had no effect on the yield, but due to the reduction in cultivatable area for the construction of the bunds, the total yield in plots with bunds is

lower. Similar to the present study, the bunds in these studies were constructed shortly before the study. Therefore, it can be assumed that the effect of the soil bunds is not yet noticeable after one growing season, which explains the different results of the effect of bunds on yield in previous studies. But, when the bunds are not properly maintained, the age of the bunds can have a negative influence on the crop yield.

The difference in stress between plots with and without bunds can indicate the effect of soil bunds with regard to water conservation. For field 1, plots with bunds have an average canopy expansion stress of 4.6% and an average stomatal closure of 5.1%, while plots without bunds have an average canopy expansion stress of 3.3% and an average stomatal closure of 5.5%. This suggests that the presence of bunds increases water stress and decreases stomatal closure in field 1. However, the reason for the high stomatal closure in control plots can also be attributed to the small gap between θ_{FC} and θ_{SAT} (figure 25). However, in field 2, plots with bunds have an average canopy expansion stress of 12.5% and an average stomatal closure of 7.4%, while plots without bunds have an average canopy expansion stress of 12.8% and an average stomatal closure of 6.8%. This suggests that the presence of bunds slightly reduces water stress and increases stomatal closure, which was expected based on the findings of previous studies. Adimassu et al. (2014) pointed out that the positive effect of bunds on crop yield is only found in moisture-deficit areas. In moisture-deficit areas the presence of bunds help the conservation of water and decreases the water stress of the crops, which is beneficial for crop yield. However, when an area has a considerably high amount of rainfall, like in the Bokole watershed, the prevention of runoff due to bunds increases the water logging hazard. Maize is moderately sensitive to water logging and reaches its anaerobiotic point when the soil moisture content is 5% below the soil moisture content at saturation (Biazin and Stroosnijder, 2012). Water logging causes aeration stress and stomatal closure and, hence, reduces biomass production and yield.

Most likely, the combination of the age of the soil bunds and the additional water availability result in no observed effects of soil bunds on the maize yield and other parameters. Nevertheless, it is proven by previous studies that bunds prevent runoff, reduce soil and nutrient loss and decrease the slope angle, which will prevent further shallowing of the already shallow soil of the study area. Therefore, it is important to remain and maintain the soil bunds in the study area even though it seems like the yield does not increase, because when more soil is lost the maize yield will definitely decrease rapidly.

5.5 Effect of soil fertility, canopy cover, soil depth and slope on maize yield

When the simulation in AquaCrop is conducted without implementing soil fertility stress, the simulated biomass and maize yield are much higher than measured in the experimental fields. It is assumed that this gap between the measured and the simulated biomass and maize yield is caused by the soil fertility level. To overcome this gap, the soil fertility stress is implemented in AquaCrop to calibrate the biomass. Likewise, Mourice et al. (2015) found an average maize yield gap of 79% in Tanzania and indicates that a major soil fertility improvement is needed to narrow the gap. The soil fertility stress is quite variable within the fields, ranging from 25% to 80% (figure 21 and 22). According to the results, the level of soil fertility stress has the most influence on the maize yield. Therefore, the high levels of soil fertility stress are the most dominant reason for the low yields found in the study area. The high variation in level of soil fertility between plots is also observed by Nyssen et al. (2007), who suggest it is caused by differences in small scale soil and environmental features, plot history and management. In addition, previous studies also report that the low yield is mainly caused by a high soil fertility stress and the absence of sustainable fertility management practices (Fan et al., 2005; Erkossa et al., 2011; Alemu and Kidane, 2014; Bedada et al., 2014; Jemo et al., 2015; Mourice et al., 2015; Tully et al., 2015; Akumaga et al., 2017; Masvaya et al., 2017). Fan et al. (2005) found an increase in yield of 145% after 6 years of annually adding equal amounts of farmyard manure (M), nitrogen (N) and phosphorus (P). But, if only N was added the yield increased with 32% and if only M was added the yield increased with 92%. Hence, different treatments have different effects on the crop yield. Furthermore, Mourice et al. (2015) indicate that the small scale crop production in Africa is characterized by nutrient leaching as a

result of insufficient input of fertilizers and organic matter, which they suggest, is the main reason for the low yields. Besides, Tully et al. (2015) found that fertilizers have a larger effect on yield if there is sufficient rainfall, otherwise the moisture availability becomes more important and has a greater effect on the yield than fertilizers. Since the rainfall in the study area has been sufficient for the last 11 years, this does not apply to the study area and the main reason for the low yields is most likely the soil fertility level. Besides, there is no consistent pattern recognized between the soil depth and slope of the fields and the soil fertility stress. However, Tefera and Sterk (2010) report that steep fields tend to have shallow soils and a low soil fertility level and in order to sustain yield levels the application of fertilizers is a necessity. In addition, Phiri et al. (1999) observed soils of steep plots to have a limited soil fertility and indicate that it is the main reason for the observed lower yield on the steeper plots.

As is noted in the results and can be seen in figure 21 and 22 the soil fertility stress is not the only parameter affecting the biomass and maize yield. In the simulations with an average soil fertility stress the variation in maize yield due to soil fertility stress is eliminated and the effect of other parameters can be determined. From these simulations, it can be concluded that the maximum canopy cover and the soil depth have the largest effect on the maize yield (table 9). In addition, when the gap between θ_{FC} and θ_{SAT} is small, it also has a large influence on the maize yield, because aeration stress is more easily triggered. For field 1, plot 1a and 2a even have a gap lower than 5%, which means that if the soil is at field capacity aeration stress is already triggered (figure 25). It was expected that the maximum canopy cover has a large influence on the maize yield, since it is related to the biomass. Therefore, it is also interesting to look at the parameters which influence the maximum canopy cover. In general, the soil depth, the rooting depth and the slope have the largest influence on the maximum canopy cover and consequently also the maize yield (table 9).

The variation in soil depth does not directly result in the variation of maize yield, but deep soils often lead to higher yields than shallow soils (table 4 and 7). Even though field 2 has less variation in soil depth, the relation between soil depth and biomass is clearer than in field 1. This is probably because the gap between θ_{FC} and θ_{SAT} also influences the maize yield in field 1 due to its small gaps. Field 2 has larger gaps between θ_{FC} and θ_{SAT} , which does often not influence the maize yield (figure 25). However, for field 2, the TAW had a larger effect on the maize yield (figure 24). Many studies report that shallow soils result in lower maize yields than deeper soils (Calviño and Sadras, 1999; Calviño et al., 2001; Sadras and Calviño, 2001 and Mhizha et al., 2014). For example, Calviño and Sadras (1999) found a 58% reduction in crop yield when the soil decreases from 1.0 m depth to 0.5 m depth. In addition, Sadras and Calviño (2001) found maize yield to be most affected by soil depth, with a measured decrease in biomass from 14 ton ha⁻¹ in deep soils of 1 m to a biomass of 8.5 ton ha⁻¹ in shallow soils of 0.35 m. It has to be kept in mind that most of the soils in the experimental fields are even shallower than the soils in the studies discussed above. Consequently, yield can respond differently to soil depth in the study area. Furthermore, Mhizha et al. (2014) report that the larger storage capacity of deep soils allows for later sowing dates than for shallow soils, which results in higher yields because the uncertainty at the beginning of the rain season can be avoided. This can also be seen in the present study, where the deeper soils of field 1 allow a later sowing date and result in less water stress in the beginning of the growing period and a higher yield than in field 2.

Besides the soil depth, the rooting depth was also very shallow for the study area. But, the rooting depth is in almost all plots larger than the soil depth (table 4). The relation between the maximum canopy cover and the rooting depth is less clear than its relation with the soil depth. This is probably because the roots cannot efficiently take up water below the soil and, hence, the effective rooting depth is likely to be equal to the soil depth. The rooting depth influences the amount of water and nutrients the crop can extract (Nyakudya and Stroosnijder, 2014). Vogel (1993) reports that a deeper root penetration improves plant water and nutrient uptake and, consequently, enhances crop yield. In addition, Nyakudya and Stroosnijder (2014) report that an increase in rooting depth increases yield, but only until a certain depth. They observed that an increase of rooting depth from 0.60 m to 0.80 m

did not increase yield, but if the rooting depth increases in combination with increasing plant density the yield became higher. Besides, Nyakudya and Stroosnijder (2014) indicate that a larger rooting depth results in a higher canopy cover.

Moreover, the slope of the fields also influence the canopy cover and, hence, the maize yield. The slopes of the plots vary between 12% and 34% with an average of 21% (table 7). In general, a gentler slope leads to a lower biomass. However, this is only true in field 1 and cannot be recognized in field 2. Phiri et al. (1999) studied the effect of slope on maize yield by examining the crop development on plots with a gentler slope of less than 12% and on steep plots with slopes above 12%. They found the soils of the steep plots to lower yields. It has to be noted that the plots in the study area are remarkably steeper than in the study by Phiri et al. (1999).

5.6 Effect of weather conditions on maize yield

Based on the results of the present study it can be concluded that weather conditions influence the maize yield. It was clear that the temperature had more influence on the maize yield than the rainfall, where a higher amount of GDDs results in a higher maize yield (figure 11 and 28). The rainfall has less influence on the maize yield because the rainfall in the study area is sufficient enough, of which even the driest year over the past 11 years had a total rainfall of 833 mm in the growing period. However, the amount of rainfall and especially the amount of contiguous days of rainfall influence the water and aeration stress, which result in small changes in the yield.

Other studies also found weather conditions to influence the yield and indicate that temperature has a larger effect on maize yield than rainfall (Muchow et al., 1989; Abraha and Savage, 2006; Walker and Schulze, 2006; Lobell et al., 2011; Sun and van Kooten, 2014 and Ye et al., 2017). Sun and van Kooten (2014) and Ye et al. (2017) also found that the yield increases as the amount of GDDs increase in northern China and Kansas, respectively. However, Abraha and Savage (2006) and Walker and Schulze (2006) found that an increase in temperature negatively affects the maize yield in the eastern part of South Africa. This difference is probably due to the difference in climate, since the eastern part of South Africa has an average maximum temperature which is approximately 3.5°C higher than in the Bokole watershed and the total amount of rainfall is approximately half of the total amount of rainfall in the Bokole watershed for 2016. Therefore, an increase in temperature causes heat stress more easily in the eastern part of South Africa resulting in a decrease in maize yield. Furthermore, Lobell et al. (2011) report that each degree day spent above 30°C reduces the yield more under drought conditions. So, higher temperatures are more harmful for yield production when there is less rainfall, which is the case in the eastern part of South Africa. In addition, Ye et al. (2017) also found that temperatures above 30°C negatively influence the maize yield. Besides, Sun and van Kooten (2014) indicate that the importance of rainfall depends on time of the year, for example during the peak or in the beginning of the growing period.

The temperature in the study area has never been above 30°C during the growing period for at least the past 11 years and, therefore, does not negatively influence the maize yield in the study area. Furthermore, the lowest temperature observed in the last 11 years is 9.8 °C, which is above the base temperature of maize and, hence, does not negatively influence the maize yield either. In the study area, the number of contiguous days of rainfall and the time of the year when rainfall occurs have more influence on the maize yield than the total amount of rainfall. Therefore, years with the same amount of rainfall and GDDs can have different yields due to differences in contiguous days of rainfall and in differences in the timing of the year when rainfall occurs. For example, no rainfall in the beginning of the growing period leads to water stress, which results in lower yields, but the total amount of rainfall over the growing period can still be high. This cannot be seen in total amount over the growing period and, therefore, it is important to also evaluate the distribution of rainfall over the year.

6. Conclusion

Due to the enormous amount of soil loss on cultivated fields, contour soil bunds and stone bunds are widely constructed in Ethiopia to serve as a soil and water conservation measure. Contour bunds prevent runoff, reduce the erosive capacity of the runoff and decrease the slope angle of the fields. Previous studies indicate that the effects of bunds enhance the crop yield. For the study area, the Bokole watershed in western Ethiopia, Wolka et al. (2016) observed an increase in crop yield due to contour bunds, but did not find significant differences in soil properties between fields with and without contour bunds and suggest that the enhanced crop yield might be a result of the effect of contour bunds on soil moisture availability. Therefore, the main objective of the present study is to quantify the influence contour soil bunds have on soil moisture conservation and how it affects maize yield on a hillslope scale in the Bokole watershed. The data for the study was obtained by conducting lab and field measurements and from the literature. Furthermore, the FAO AquaCrop model was used to simulate the daily soil water balance, the crop development and the total attainable maize yield. After calibration, the FAO AquaCrop model simulates the soil moisture and the biomass well with the regard to the measured parameters. The effect of soil bunds is evaluated by comparing the results of the plots with soil bunds and the plots without soil bunds. To determine the main objective of the present study, the sub-objectives are answered first and afterwards a main conclusion is given.

To quantify the amount of increased soil moisture content, aboveground dried biomass and maize yield due to contour soil bunds

The amount of soil moisture content, the aboveground dried biomass and the maize yield were quantified on plots with and without soil bunds by conducting measurements in the field. The soil moisture measurements were conducted for 2.5 weeks in the field and the total biomass and yield were measured at harvest time. AquaCrop makes it possible to quantify the soil moisture content by simulating the soil moisture content for the growing period on a daily basis.

To simulate the soil moisture content and crop production with FAOs AquaCrop for plots with and without contour soil bunds

After AquaCrop was calibrated for the measured soil moisture content and total biomass the results between plots with and without bunds could be evaluated. The average actual soil moisture, the soil moisture at field capacity and the soil moisture at saturation do not differ between plots with and without soil bunds, only the soil moisture content at saturation is slightly higher for the plots without bunds in field 2 (3.3%). Hence, the soil bunds had no effect on the soil moisture content. In AquaCrop, the only difference between plots with and without bunds is the inhibition of runoff in plots with bunds. The water balance indicates that there is almost no difference in soil evaporation and transpiration between plots with and without bunds and the water lost by runoff in the plots without bunds is solely compensated by a reduction in drainage.

Furthermore, the biomass and yield differ between plots with and without bunds. For field 1, the biomass and yield are, on average, 0.722 and 0.362 ton ha⁻¹ higher for plots with bunds than for plots without bunds, but for field 2, the biomass and yield are, on average, 0.807 and 0.360 ton ha⁻¹ lower for plots with bunds than for plots without bunds. The difference in biomass and maize yield between plots is dominantly caused by the soil fertility stress, which is 5.1% higher for control plots in field 1 and 7.5% lower for control plots in field 2. When the soil fertility stress is averaged over the whole field, the biomass and yield are slightly higher in the plots with bunds in both fields. Moreover, the canopy expansion stress and the stomatal closure also differ between plots. In field 1, the average canopy expansion stress is slightly higher in plots with soil bunds, but in field 2 there is no significant difference between plots with and without soil bunds. The average stomatal closure is slightly lower in plots with bunds in field 1, but is slightly higher in plots with bunds in field 2. However, the higher stomatal closure in plots without bunds in field 1 is caused by the gap of only 4.0 %vol between the

soil moisture content at field capacity and at saturation and not by the presence of soil bunds. Therefore, the presence of soil bunds does not necessarily decrease water stress, but does have a small positive effect on the aeration stress.

To determine which locations within a plot benefit most from contour soil bunds

The differences between locations within a plot are characterized by differences in the soil moisture content, while the other input parameters do not change between locations. On the whole, there is no consistent pattern between the simulated actual soil moisture content and the locations within the plot, but most of the plots have the highest average actual soil moisture over the growing period around the middle bund in field 1 and around the upper bund in field 2. Besides, the measured soil moisture content gives consistent patterns of soil moisture between the plots for field 1, but for field 2 the patterns in soil moisture are inconsistent between the plots. Furthermore, the biomass between locations within a plot are compared to determine which locations are most beneficial with regard to maize yield. In field 1, there is no consistent pattern in biomass within the plots and the pattern of some plots even contradict each other. However, the biomass within the plots of field 2 is highest around the upper bund and decreases downward. Combining the patterns of biomass within the plot of both fields leads to no dominant pattern between biomass and the location within the plot.

To determine which parameters have the largest influence on the aboveground biomass production, which is related to the maize yield

Unrelated to the soil bunds, the maize yield differs between plots. For field 1, the maize yield ranges from 1.5 to 5.7 ton ha⁻¹ and for field 2 the maize yield ranges from 1.3 to 2.6 ton ha⁻¹. Compared to other studies, the yields for the study area are low, but not uncommon in Africa and Ethiopia. No consistent pattern between the soil moisture and the biomass could be found, but, on average, the soil moisture changes with 9.5% within the plot, while the biomass changes with 2.7%. However, the variation in biomass is caused by differences in the soil moisture content at field capacity, the soil moisture content at saturation and the soil depth between the plots. The size of the gap between the soil moisture content at field capacity and at saturation determines whether an increase in soil moisture can positively or negatively affect the biomass. When the gap is large, an increase in soil moisture leads to less water stress, but does not cause aeration stress, leading to a higher biomass. But, when the gap is small, the increase in soil moisture is more likely to trigger aeration stress, which leads to a lower biomass. In addition, plots with a deeper soil are more resistant to changes in soil moisture leading to almost no changes in the biomass. However, when the soil is shallow, the plot is more vulnerable to changes in soil moisture content resulting in less clear patterns in biomass.

The soil fertility stress has the largest influence on the biomass production in both fields, where a high soil fertility stress results in a low biomass and vice versa. However, the soil fertility stress is not the only parameter which significantly affects the biomass. In the average fertility simulations the biomass follows the pattern of the maximum green canopy cover (CC_x), where a high CC_x leads to a high biomass. But, the soil depth also influences the biomass, where plots with a deeper soil have a higher biomass than assumed with the pattern of CC_x. The effect of soil depth on the biomass is more pronounced in field 1 than in field 2, because the soil depth only varies from 0.10 to 0.19 m in field 2, while it varies from 0.10 to 0.62 m in field 1. Furthermore, in field 1 the plots with a high CC_x generally have a gentle slope, but this pattern is not recognized in field 2.

To determine the effect of rainfall and temperature on the biomass, the average fertility simulations are repeated for each year over the period 2005 to 2016. The rainfall influences the severity of water and aerations stress and the temperature influences the severity of the temperature stress. However, the number of contiguous days is more important than the amount of rainfall for the severity of the water and aeration stress. In the case of the study area in the Bokole watershed, changes in temperature have a larger effect on the maize yield than changes in rainfall. This is due to the sufficient

amount of rainfall in the study area for at least the past 11 years, making the bunds less important for water conservation. The Bokole watershed does know dry periods, but these occur during the off season months when the soil is bare, which does not influence the yield.

Based on the sub-objectives the importance of contour soil bunds on soil moisture and maize yield and the effect of possible other parameters on maize yield, like rainfall, temperature, soil depth, slope and soil fertility could be determined. It can be concluded that the soil bunds have no effect on any measured or simulated parameter, except for the runoff, because AquaCrop inhibits runoff when soil bunds are present. However, when the average soil fertility stress is used the biomass and yield are higher in plots with bunds than in plots without bunds in both fields. In addition, there is no consistent location which benefits more than other locations, with regard to the biomass, from the presence of soil bunds. Furthermore, the actual soil moisture itself is less important for the maize yield, but together with the relation between the soil moisture at field capacity and at saturation it has a larger influence on the maize yield and influences the water and aeration stress, which lead to small differences in the maize yield. However, the variation in maize yield between the plots is mostly due to the variation in soil fertility stress, maximum canopy cover, soil depth, slope and the gap between the soil moisture content at field capacity and saturation between plots. Besides, for the Bokole watershed, the temperature also influences the biomass and yield. Since the temperature is the same for the whole field, this could only be determined by comparing the yields of different years. Therefore, the main conclusion of this study is that the soil bunds had no effect on the soil moisture content, the soil depth, the crop production and the yield in the Bokole watershed in the first season after construction of the soil bunds. However, small differences between the aeration stress of plots with bunds and plots without bunds indicate that the presence of soil bunds increase the stomatal closure.

7. Recommendations

The present study only had one year of experimental data to calibrate and validate the FAO AquaCrop model and evaluate the effect of soil bunds on soil moisture and yield. A better calibration of AquaCrop can be conducted with long-term data of the experimental fields of the Bokole watershed. In addition, a long-term data set can also be used to evaluate the effect of soil bunds over the years, e.g. does the effect of soil bunds on soil moisture and yield change when the soil bunds get older. Furthermore, it is recommended that the soil moisture is also measured earlier in the season, when the channels of the soil bunds are actually filled with rainwater. This might give other results of the influence of soil bunds on the soil moisture content.

By simulating the calibrated and the average soil fertility stress, the sensitivity of maize yield to soil fertility stress could be determined. It is recommended to continue this sensitivity analysis with regard to the maize yield with other parameters which are found to significantly affect the maize yield. For example, the soil depth, the maximum canopy cover and other soil and hydraulic properties. Comparing the maize yield simulated with the measured values per plot and with the average values for the whole field gives a good indication of the level of influence that the parameter has on the maize yield.

For the study area itself, it is recommended to keep constructing and maintaining contour bunds to reduce further soil loss to maintain the already very shallow soils and to reduce nutrient loss to not further aggravate the soil fertility stress. Since the soil fertility stress is the most important reason for the low yields in the study area, it is recommended to measure the severity of the soil fertility stress as well as which nutrients are most limited in order to apply efficient fertility management and increase the soil fertility level. For example, Bedada et al. (2014) found that the combination of adding compost and NP fertilizer had the most positive effect on the yield in south-central Ethiopia. Furthermore, if the soil is low in P, Jemo et al. (2015) found that the crop yield will increase by adding products with high concentrations of P in their formulation, like foliar application of Turbotop or Agroleaf high-P. In addition, Masvaya et al. (2017) found that soils low in N will have enhanced yields with manure application. In addition, Biazin and Stroosnijder (2012) report that an additional supply of nitrogen to maize crops under waterlogged conditions can improve maize yield.

Acknowledgements

There are many people who helped me to accomplish this master thesis. First and foremost I want to thank Shannon, who went on this journey to Ethiopia with me. It is nice to share adventures, experiences and frustrations with a good friend in a foreign country like Ethiopia. We had such a good time together and I enjoyed doing fieldwork together. Even after we came back she was a great help and I could always contact her to discuss the data and problems I encountered.

Furthermore, I want to thank dr. ir. Geert Sterk for making this thesis possible and helping us to prepare for the fieldwork and the journey to Ethiopia. When we arrived in Ethiopia we travelled to the Hawassa University Wondo Genet College of Forestry and Natural Resources. I want to thank the college and especially Kebede Wolka for their kind hospitality. He helped us accustom to the Ethiopian way of life, arranged our fieldwork, tried to teach us about trees and was always available for us when we needed him to discuss thesis related matters or practical and personal matters. Without him we would have been lost, so a lot of thanks goes to Kebede Wolka. Moreover, I want to thank Alex, the kindest driver I have ever met, who brought us to the fieldwork area and back to the college. And, at the end of our journey in Ethiopia, he made sure we made it to the airport in Addis Ababa safely and on time!

During the fieldwork period we stayed in a small village called Ella. For this period, I want to thank the neighbors, who were always ready to help us, whether it was providing fruits, inviting us for coffee, helping us to get water or kill a dangerous spider in our bedroom. In addition, I want to thank the farmers, Cholamo Chondu and Arja Herana and their many children, who let us use their ground as experimental fields, which are used in the study and were always there to help us and borrow us tools. During the fieldwork period, a special thanks goes to Asfaw, who helped us in so many ways. He did not only help us to conduct the fieldwork, but also went grocery shopping with us, learned us a lot about the Ethiopian culture and was eager to learn about the Dutch culture as well and translated a lot for us. Not to forget, I want to thank Asfaw and his wife for cooking for us every morning, afternoon and evening for 3 weeks. We are really thankful for your help and hospitality. Furthermore, I would like to thank the staff of the laboratory in Wondo Genet who helped us determining which methods to use and show us how to use these methods.

Then, I want to thank dr. Rens van Beek for his supervision during my master thesis. Thanks for always helping me with the problems I encountered and discussing new ideas with me. His feedback and advice certainly improved the quality of my thesis.

A last thanks goes to Robin, my family and my friends for always supporting me, listen to my stories about Ethiopia and for occasionally helping me with the problems I encountered during my master thesis.



References

- Abate, T., B. Shiferaw, A. Menkir, D. Wegary, Y. Kebede, K. Tesfaye, M. Kassie, G. Bogale, B. Tadesse and T. Keno (2015) Factors that transformed maize productivity in Ethiopia, *Food Security*, 7(5), 965-981
- Abedinpour, M., A. Sarangi, T.B.S. Rajput, M. Singh, H. Pathak and T. Ahmad (2012) Performance evaluation of AquaCrop model for maize crop in a semi-arid environment, *Agricultural Water Management*, 110, 55 – 66
- Abraha, M.G. and M.J. Savage (2006) Potential impacts of climate change on the grain yield of maize for the midlands of KwaZulu-Natal, South Africa, *Agriculture, Ecosystems & Environment*, 115, 150 – 160
- Adimassu, Z., K. Mekonnen, C. Yirga and A. Kessler (2014) Effect of soil bunds on runoff, soil and nutrient losses, and crop yield in the central highlands of Ethiopia, *Land degradation & development*, 25, 554 – 564
- Akumaga, U., A. Tarhule and A.A. Yusuf (2017) Validation and testing of the FAO AquaCrop model under different levels of nitrogen fertilizer on rainfed maize in Nigeria, West Africa, *Agricultural and Forest Meteorology*, 232, 225 – 234
- Alemu, B. and D. Kidane (2014) The implication of integrates watershed management for rehabilitation of degraded lands: case study of Ethiopian Highlands, *Journal of Agriculture and Biodiversity Research*, 3:6, 78–90
- Allen, R.G., L.S. Pereira, D. Raes and M. Smith (1998) Crop evapotranspiration – Guidelines for computing crop water requirements - FAO irrigation and drainage paper 56, Natural Resources Management and Environment Department, FAO
- Amare, T., A.D. Zegeye, B. Yitafaru, T.S. Steenhuis, H. Hurni and G. Zeleke (2014) Combined effect of soil bund with biological soil and water conservation measures in the northwestern Ethiopian highlands, *Ecohydrology and hydrobiology*, 14, 192 – 199
- Andarzian, B., M. Bannayan, P. Steduto, H. Mazraeh, M.E. Barati, M.A. Barati and A. Rahnema (2011) Validation and testing of the AquaCrop model under full and deficit irrigated wheat production in Iran, *Agricultural Water Management*, 100, 1 – 8
- Araya, A., S.D. Keesstra and L. Stroosnijder (2010) Simulating yield response to water of Teff (*Eragrostis tef*) with FAO's AquaCrop model, *Field Crops Research*, 116, 196 – 204
- Azam-Ali, S.N. and G.R. Squire (2002) *Principles of Tropical Agronomy*, CABI Publishing, Wallingford, United Kingdom
- Bedada, W., E. Karlton, M. Lemenih and N. Tolera (2014) Long-term addition of compost and NP fertilizer increases crop yield and improves soil quality in experiments on smallholder farms, *Agriculture, Ecosystems and Environment*, 195, 193 – 201
- Ben-Dor, E. and A. Banin (1989) Determination of organic matter content in arid zone soils using a simple “loss-on-ignition” method, *Communications in Soil Science and Plant Analysis*, 20, 1675 – 1695
- Bengtsson, L. and M. Enell (1986) Chemical analysis. In Berglund, B. E. (ed.), *Handbook of Holocene Palaeoecology and Palaeohydrology*, John Wiley & Sons Ltd., Chichester, 423 – 451
- Beretta, A.N., A.V. Silbermann, L. Paladino, D. Torres, D. Bassahun, R. Musselli and A. García-Lamohte (2014) Soil texture analyses using a hydrometer: modification of the Bouyoucos method, *Ciencia e Investigación Agraria*, 41(2), 263 – 271

- Bewket, W. (2006) Soil and water conservation intervention with conventional technologies in northwestern highlands of Ethiopia: acceptance and adoption by farmers', *Land Use Policy*, 24 (2), 404–416
- Biazin, B and L. Stroosnijder (2012) To tie or not to tie ridges for water conservation in Rift Valley drylands of Ethiopia, *Soil and Tillage Research*, 124, 83 – 94
- Bonsor, H.C. and A.M. MacDonald (2011) An initial estimate of depth to groundwater across Africa, Groundwater Science Programme: open report OR/11/067, British Geological Survey, Keyworth, Nottingham
- Bouyoucos, G.J. (1936) Directions for Making Mechanical Analysis of Soils by the Hydrometer Method, *Soil Science*, 4, 225 – 228
- Bouyoucos, G.J. (1962) Hydrometer method improved for making particle size analysis of soils, *Agronomy Journal*, 54, 464-465
- Bruin, de, H.A.R. and W.N. Lablans (1998) Reference crop evapotranspiration determined with a modified Makkink equation, *Hydrological Processes*, 12, 1053 – 1062
- Calviño, P.A., F.H. Andrade and V.O. Sadras (2001) Maize yields as affected by water availability, soil depth and crop management, *Agronomy Journal*, 95, 275 – 281
- Calviño, P.A. and V.O. Sadras (1999) Interannual variation in soybean yield: interaction among rainfall, soil depth and crop management, *Fields Crops Research*, 63, 237 – 246
- Critchley, W. and O. Graham (1991) Looking after our land: soil and water conservation in Dryland Africa, FAO, Oxfam, Oxford
- Campbell, C. (2014) Soil moisture 201: water content measurements methods and applications available online on: <https://www.youtube.com/watch?v=jzYCuspFhwo> [date of search: 08-07-2016]
- Daddow, R.L. and G.E. Warrington (1983) Growth-limiting soil bulk densities as influenced by soil texture, WSDG Report, Watershed Systems Development Group, USDA Forest Service
- Das, T.K., P.K. Sakhuja and H. Zelleke (2010) Herbicide efficacy and non-target toxicity in highland rainfed maize of Eastern Ethiopia, *International Journal of Pest Management*, 56:4, 315 – 325
- Dean, W. E. Jr. (1974) Determination of carbonate and organic matter in calcareous sediments and sedimentary rocks by loss on ignition: Comparison with other methods, *Journal of Sedimentary Petrology*, 44, 242 –248
- Delta-T Devices Ltd (2017) User manual for the ML3 ThetaProbe, version ML3-UM-2.1, Delta-T Devices Ltd, Cambridge, UK
- Dingman, S. L. (2015) *Physical hydrology*, third edition, Waveland press, Long Grove, Illinois
- Doorenbos, J. and A.H. Kassam (1979) Yield response to water, *Irrigation and Drainage Paper*, 33, FAO, Rome, Italy, 193 pp
- Erkossa, T., S.B. Awulachew and D. Aster (2011) Soil fertility effect on water productivity of maize in the upper Blue Nile basin, Ethiopia, *Agricultural Sciences*, 2(03), 238
- Estefan G., R. Sommer and J. Ryan (2013) *Methods of soil, plant, and water analysis: A manual for the West Asia and North Africa region*, International Center for Agricultural Research in the Dry Areas (ICARDA), Beirut, Lebanon
- Fan, T., B.A. Stewart, W. Yong, L. Junjie and Z. Guangye (2005) Long-term fertilization effects on grain yield, water-use efficiency and soil fertility in the dryland of Loess Plateau in China, *Agriculture, ecosystems and environment*, 106:4, 313-329

- FAO (1986) Ethiopian highlands reclamation study, Final Report (Volume I and II), Food and Agriculture Organization (FAO)
- FAO (2012) Crop parameters, Reference Manual, Annex III – AquaCrop, Version 4.0
- Foster, T., N. Brozovic, A.P. Butler, C.M.U. Neale, D. Raes, P. Steduto, E. Fereres and T.C. Hsiao (2017) AquaCrop-OS: An open source version of FAO's crop water productivity model, *Agricultural Water Management*, 181, 18 – 22
- Gebreegziabher, T., J. Nyssen, B. Govaerts, F. Getnet, M. Behailu, M. Haile and J. Deckers (2009) Contour furrows for in situ soil and water conservation, Tigray, Northern Ethiopia, *Soil and Tillage Research*, 103, 257 – 264
- Gebremichael, D., J. Nyssen, J. Poesen, J. Deckers, M. Haile, G. Govers and J. Moeyersons (2005) Effectiveness of stone bunds in controlling soil erosion on cropland in the Tigray Highlands, northern Ethiopia, *Soil Use and Management*, 21, 287–297
- Girmay G., B.R. Singh, H. Mitiku, T. Borresen and R. Lal (2008) Carbon stocks in Ethiopian soils in relation to land use and soil management, *Land Degradation & Development*, 19, 351–367
- Greaves, G.E. and Y.M. Wang (2016) Assessment of FAO AquaCrop Model for Simulating Maize Growth and Productivity under Deficit Irrigation in a Tropical Environment, *Water*, 8, 557
- Hadgu, G., K. Tesfaye and G. Mamo (2015) Analysis of climate change in Northern Ethiopia: implications for agricultural production, *Theoretical Applied Climatology*, 121, 733 – 747
- Heiri, O., A.F. Lotter and G. Lemcke (2001) Loss on ignition as a method for estimating organic and carbonate content in sediments: reproducibility and comparability of results, *Journal of Paleolimnology*, 25, 101 – 110
- Hendriks, M.R. (2010) *Introduction to Physical Hydrology*, Utrecht University, Oxford University Press, New York
- Heng, L.K., T. Hsiao, S. Evett, T. Howell and P. Steduto (2009) Validating the FAO AquaCrop model for irrigated and water deficient field maize, *Agronomy Journal*, 101, 488 – 498
- Hengshijk, H., G.W. Meijering and M.E. Mosugu (2005) Modeling the effect of three soil and water conservation practices in Tigray, Ethiopia, *Agriculture, Ecosystems and Environment*, 105, 29 – 40
- Hsiao, T.C., L. Heng, P. Steduto, B. Rojas-Lara, D. Raes and E. Fereres (2009) AquaCrop – the FAO crop model to simulate yield response to water: III. Parameterization and testing for maize, *Agronomy Journal*, 101, 448 – 459
- Jasrotia, P. (2008) Particle size analysis for soil texture determination (hydrometer method), Long-term Ecological Research, KBS LTER, Michigan State University
- Jemo, M., C. Nwoke, P. Pypers and B. Vanlauwe (2015) Response of maize (*Zea mays*) to the application of foliar fertilizers in the Sudan and Guinea savanna zone of Nigeria, *Journal of Plant Nutrition and Soil Science*, 178(3), 374-383
- Kang, B.T., G.F. Wilson and L. Sipkens (1981) Alley cropping maize (*Zea mays* L.) and leucaena (*Leucaena leucocephala* Lam) in southern Nigeria, *Plant Soil*, 63, 165 – 179
- Karlsson, E. (2004) Methods of estimating potential and actual evaporation, Department of Water Resources Engineering
- Kidane, D. and B. Alemu (2015) The effect of upstream land use practices on soil erosion and sedimentation in the upper Blue Nile basin, Ethiopia, *Research Journal of Agriculture and Environmental Management*, 4:2, 55–68

- Kranz, W.L., S. Irmak, S.J. van Donk, C.D. Yonts and D.L. Martin (2008) Irrigation Management for corn, University of Nebraska-Lincoln, Extension Publications
- Lievens, E. (2014) Parameterization and testing of the FAO AquaCrop model to simulate yield response to water in North-eastern Thailand, MSc thesis Universiteit Gent, Faculty of Bioscience Engineering, Gent, Belgium
- Liu, J.G. and E. Pattey (2010) Retrieval of leaf area index from top-of-canopy digital photography over agricultural crops, *Agricultural and Forest Meteorology*, 150, 1485–1490
- Lobell, D.B., M. Bänziger, C. Magorokosho and B. Vivek (2011) Nonlinear heat effects on African maize as evidenced by historical yield trials, *Nature Climate Change*, Vol 1 (April 2011)
- Lund, A. and M. Lund (2013) One-way ANOVA, Laerd Statistics, Lund Research Ltd
available online on: <https://statistics.laerd.com/statistical-guides/one-way-anova-statistical-guide.php> [date of search: 15-03-2017]
- Masvaya, E. N., J. Nyamangara, K. Descheemaeker and K.E. Giller (2017) Tillage, mulch and fertilizer impacts on soil nitrogen availability and maize production in semi-arid Zimbabwe, *Soil and Tillage Research*, 168, 125-132
- Matula, S. and C. Dirksen (1989) Automated regulating and recording system for cylinder infiltrometer, *Soil Science Society of America Journal*, 53, 299 – 302
- Meshesha D.T., A. Tsunekawa, M. Tsubo and N. Haregeweyn (2015) Dynamics and hotspots of soil erosion and management scenarios of the Central Rift Valley of Ethiopia, *International Journal of Sediment Research*, 27 (1), 84–99
- Mhizha, T., S. Geerts, E. Vanuytrecht, A. Makarau and D. Raes (2014) Use of the FAO AquaCrop model in developing sowing guidelines for rainfed maize in Zimbabwe, *Water SA*, 40:2, 233 - 244
- Michel, C., V. Andréassian and C. Perrin (2005) Soil conservation service curve number method: how to mend a wrong soil moisture accounting procedure?, *Water Resources Research*, 41:2
- Mkhabela, M.S. and P.R. Bullock (2012) Performance of the FAO AquaCrop model for wheat grain yield and soil moisture simulation in Western Canada, *Agricultural Water Management*, 110, 16 – 24
- Mourice, S. K., S.D. Tumbo, A. Nyambilila and C.L. Rweyemamu (2015) Modeling potential rain-fed maize productivity and yield gaps in the Wami River sub-basin, Tanzania, *Acta Agriculturae Scandinavica, Section B—Soil & Plant Science*, 65:2, 132-140
- Muchow, R.C., T.R. Sinclair and J.M. Bennett (1989) Temperature and solar radiation effects on potential maize yield across locations, *Agronomy Journal*, 82, 338 – 343
- Muluneh, A., L. Stroosnijder, S. Keesstra and B. Biazin (2016) Adapting to climate change for food security in the Rift Valley dry lands of Ethiopia: supplemental irrigation, plant density and sowing date, *The Journal of Agricultural Science*, 1-22
- Nrm laboratories (2013) Routine estimation of the Organic Matter content of soils by Loss on Ignition, NRM laboratories, Cawood Scientific Group
- Nyakudya, I.W. and L. Stroosnijder (2014) Effect of rooting depth, plant density and planting date on maize (*Zea mays* L.) yield and water use efficiency in semi-arid Zimbabwe: Modelling with AquaCrop, *Agricultural Water Management*, 146, 280 – 296
- Nyssen, J., J. Poesen, D. Gebremichael, K. Vancampenhout, M. D’aes, G. Yihdego, G. Govers, H. Leirs, J. Moeyersons, J. Naudts, N. Haregeweyn, M. Haile and J. Deckers (2007) Interdisciplinary on-site evaluation of stone bunds to control soil erosion on cropland in Northern Ethiopia, *Soil and Tillage Research*, 94, 151 – 163

Nyssen J., J. Poesen, M. Haile, J. Moeyersons and J. Deckers (2000) Tillage erosion on slopes with soil conservation structures in the Ethiopian highlands, *Soil & Tillage Research*, 57, 115–127

SNNPRS-BoFED, 2004. Regional Atlas. Southern Nation, Nationalities and Peoples Regional State, Bureau of Finance and Economic Development, Bureau of Statistics and population, Awassa, Ethiopia

Ogolo, E.O. (2014) The comparative analysis of performance evaluation of recalibrated reference evapotranspiration models for different regional climatic conditions in Nigeria, *Ife Journal of Science*, 16:2

Paredes, P., Z. Wei, Y. Liu, D. Xu, Y. Xin, B. Zhang and L.S. Pereira (2015) Performance assessment of the FAO AquaCrop model for soil water, soil evaporation, biomass and yield of soybeans in North China Plain, *Agricultural Water Management*, 152, 57 – 71

Phiri, A.D.K., G.Y. Kanyama-Phiri and S. Snapp (1999) Maize and sesbania production in relay cropping at three landscape positions in Malawi, *Agroforestry Systems*, 47, 153 – 162

Raes, D. (1982) A summary simulation model of the water budget of a cropped soil, *Dissertationes de Agricultura n° 122*, K.U. Leuven University, Leuven, Belgium, 110 p.

Raes, D., P. Steduto, T.C. Hsiao and E. Fereres (2010) AquaCrop – the FAO cropwater productivity model to simulate yield response to water: III. Calculation procedures (version 3.1), Reference Manual FAO

Raes, D., P. Steduto, T.C. Hsiao and E. Fereres (2011) AquaCrop – the FAO cropwater productivity model to simulate yield response to water: I. Concepts and underlying principle (version 3.1plus), *Agronomy Journal*

Raes, D., P. Steduto, T.C. Hsiao and E. Fereres (2012) AquaCrop – the FAO cropwater productivity model to simulate yield response to water: II. User guide, Reference Manual FAO

Raes, D. (2017) AquaCrop training handbook I. Understanding AquaCrop, Food and Agriculture Organization of the United Nations, Rome

Rallison, R.E. (1980) Origin and evolution of the SCS runoff equation, *Watershed Management Symposium*, ASCE, New York, N.Y., 912-924

Rasoulzadeh, A. (2011) Estimating Hydraulic Conductivity Using Pedotransfer Functions, *Hydraulic Conductivity - Issues, Determination and Applications*, Prof. Lakshmanan Elango (Ed.)

Sadras, V.O. and P.A. Calviño (2001) Quantification of grain yield response to soil depth in soybean, maize, sunflower, and wheat, *Agroclimatology*, 93, 577 – 583

Saxton K.E., W.J. Rawls, J.S. Romberger, and R.I. Papendick (1986) Estimating generalized soil water characteristics from texture, *Soil Science Society of America Journal*, 50, 1301 – 1036

Steduto, P., T.C. Hsiao, D. Raes and E. Fereres (2009) AquaCrop – the FAO crop model to simulate yield response to water: I. Concepts and underlying principle, *Agronomy Journal*, 101, 426–437

Steduto, P., T.C. Hsiao, E. Fereres and D. Raes (2012) FAO Irrigation and drainage paper 66, Crop yield response to water, Food and Agriculture Organization of the United Nations

Sterk, G. and G.M.J. van der Meijden (2007) Physical Aspects of Land Management – Lecture Notes, Erosion and Soil & Water conservation group, Wageningen University, Wageningen, The Netherlands

Stevens, J.J. PhD (1999) Post Hoc Tests in ANOVA, University of Oregon, Department of Educational Methodology, Policy and Leadership, Eugene

Stibinger, J. (2014) Examples of determining the hydraulic conductivity of soils: theory and applications of selected basic methods, *University Handbook on Soil Hydraulics*, Purkyně University in Ústí n. Labem, Faculty of the Environment

- Stoorvogel, J.J. and E.M.A. Smaling (1990) Assessments of Soil Nutrient Depletion in sub-Saharan Africa 1983– 2000, Report 28, The Winand Staring Center for Integrated Land, Soil and Water Research (SC-DLO), Wageningen
- Sun, B.J. and G.C. van Kooten (2014) Weather effects on maize yields in northern China, *Journal of Agricultural Science*, 152, 523 – 533
- Tefera, B. and G. Sterk (2010) Land management, erosion problems and soil and water conservation in Fincha'a watershed, western Ethiopia, *Land Use Policy*, 27, 1027 – 1037
- Tesfahunegn, G.B., L. Tamene and P.L.G. Vlek (2014) Soil erosion prediction using Morgan-Morgan-Finney model in a GIS environment in Northern Ethiopia catchment, *Applied and Environmental Soil Science*, 2014
- Tesfaye M. (2008) Soil conservation experiments on cultivated lands in the Maybar area, Wello region, Ethiopia, Research Report Soil Conservation Research Project No. 16, University of Berne, Switzerland
- Teshome A, D. Rolker and J. de Graaff (2012) Financial viability of soil and water conservation technologies in northwestern Ethiopian highlands, *Applied Geography*, 37, 139–49
- Todorovic, M., R. Albrizio, L. Zivotic, M.T.A. Saab, C. Stockle and P. Steduto (2009) Assessment of AquaCrop, CropSyst, and WOFOST Models in the Simulation of Sunflower Growth under Different Water Regimes, *Agronomy Journal*, 101, 509 – 521
- Topp, G.C., J.L. David, and A.P. Annan (1980) Electromagnetic Determination of Soil Water Content: Measurement in Coaxial Transmission Lines, *Water Resources Research*, 16:3, 574 – 582
- Tsegay, A., D. Raes, S. Geerts, E. Vanuytrecht, B. Abraha, J. Deckers, H. Bauer and K. Gebrehiwot (2012) Unravelling crop water productivity of tef (*Eragrostis Tef* (zucc.) Trotter) through AquaCrop in Northern Ethiopia, *Experimental Agriculture*, 48:2, 222 – 237
- Tully, K. L., S.A. Wood, M. Almaraz, C. Neill and C. Palm (2015) The effect of mineral and organic nutrient input on yields and nitrogen balances in western Kenya, *Agriculture, Ecosystems & Environment*, 214, 10-20
- USDA (1964) Estimation of direct runoff from storm rainfall, *National Engineering Handbook*, Washington DC, USA, Section 4 Hydrology, Chapter 4, 1-24
- Van der Zanden, E.H. (2011) Soil erosion control on sloping olive fields in northwest Syria, MSc thesis, Physical Geohydrology, Utrecht University, The Netherlands
- Vancampenhout, K. (2003) Consequences of stone bund implementation in the highlands of northern Ethiopia, MSc thesis, Department of Land Management, University of Leuven
- Vancampenhout, K., J. Nyssen, D. Gebremichael, J. Deckers, J. Poesen, M. Haile and J. Moeyersons (2006) Stone bunds for soil conservation in the northern Ethiopian highlands: Impacts on soil fertility and crop yield, *Soil & Tillage Research*, 90, 1–15
- Van Gaelen, H., A. Tsegay, N. Delbecque, N. Shrestha, M. Garcia, H Fajardo, R. Miranda, E. Vanuytrecht, B. Abrha, J. Diels and D. Raes (2015) A semi-quantitative approach for modelling crop response to soil fertility: evaluation of the AquaCrop procedure, *The Journal of Agricultural Science*, 153:07, 1218 – 1233
- Van Gaelen, H. (2016) Evaluating agricultural management from field to catchment scale: Development of a parsimonious agro-hydrological model, PHD, Faculty of Bioscience Engineering, KU Leuven
- Vereecken H., J. Maes, and J. Feyen (1990) Estimating unsaturated hydraulic conductivity from easily measured soil properties, *Soil Science*, 149, 1 – 12

- Vogel, H. (1993) Tillage effects on maize yield, rooting depth and soil water content on sandy soils in Zimbabwe, *Field Crops Research*, 33, 367 – 384
- Waelti, C. and D. Spuhler (2013) Bunds, Sustainable Sanitation and Water Management available online on: <http://www.sswm.info/content/bunds> [date of search: 19-05-2016]
- Wagayehu B. and L. Drake (2003) Soil and water conservation decision behavior of subsistence farmers in the Eastern Highlands of Ethiopia: a case study of the Hunde-Lafto area, *Ecological Economics*, 46 (3), 437–451
- Walker, W.R. (1989) Guidelines for designing and evaluating surface irrigation systems, FAO Irrigation and Drainage paper 45, Natural Resources management and Environment Department
- Walker, N.J. and R.E. Schulze (2006) An assessment of sustainable maize production under different management and climate scenarios for smallholder agro-ecosystems in KwaZulu-Natal, South Africa, *Physics and Chemistry of the Earth, part A/B/C*, 31, 995 – 1002
- Wallace, J.S. (2000) Increasing agricultural water use efficiency to meet future food production, *Agriculture, Ecosystems and Environment*, 82, 105 – 119
- Whiting, D., A. Card, C. Wilson and J. Reeder (2015) Estimating soil texture: sand, silt or clayey?, Colorado Master Gardener Program, CMG GardenNotes #214, Colorado State University
- Wolka, K, A. Moges and F. Yimer (2011) Effects of level soil bunds and stone bunds on soil properties and its implications for crop production: the case of Bokole watershed, Dawuro zone, Southern Ethiopia
- Wolka, K., A. Moges and F. Yimer (2013) Farmers' perception of the effects of soil and water conservation structures on crop production: The case of Bokole watershed, Southern Ethiopia, *African Journal of Water Conservation and Sustainability*, 1, 071 – 080
- Wolka, K., G. Sterk, A. Moges, F. Yimer and S.M. de Jong (2016) The effect of contour bunds on soil properties and crop production in the Bokole watershed, Dawuro zone, Southwest Ethiopia, not yet published
- Wösten, J.H.M. (1997) Pedotransfer functions to evaluate soil quality. In: Gegerich, E.G. and Carter, M.R. (Eds.), *Soil Quality for Crop Production and Ecosystem Health, Developments in Soils Science*, 25, Elsevier, Amsterdam, 221-245
- Wösten J.H.M., A. Lilly, A. Nemes, and C. Le Bas (1999) Development and use of a database of hydraulic properties of European soils, *Geoderma*, 90, 169 – 185
- Ye, Q., X. Lin, E. Adey, D. Min, Y.A. Mulisa, D. O'Brien and I.A. Ciampitti (2017) Evaluation of climatic variables as yield-limiting factors for maize in Kansas, *International Journal of Climatology*
- Young, A. (1997) *Agroforestry for soil management*, 2nd edition, CAB International, Wallingford
- Yu, X. and X. Yu (2006) Time Domain Reflectometry Teste of Multilayered Soils, TDR 2006, Purdue University, West Lafayette, USA, Paper ID 3, 16p
- Zeng, D., J. Alwang, G.W. Norton, B. Shiferaw, M. Jaleta and C. Yirga (2015) *Ex post* impacts of improved maize varieties on poverty in rural Ethiopia, *Agricultural Economics*, 46:4, 515 – 526

Appendices

Appendix 1 – Makkink equation to estimate the reference evapotranspiration

The Makkink equation (eq. 1.1) uses a radiation based approach to estimate the reference evapotranspiration. It only requires the air temperature (T ; °C), the incoming shortwave radiation at the earth's surface (S_t ; MJ m⁻² day⁻¹) and the gradient of the saturation vapour pressure curve (Δ ; kPa °C⁻¹) to estimate the reference evapotranspiration (ET_{MK} ; mm day⁻¹):

$$ET_{MK} = C_{MK} \frac{1000}{\rho\lambda} \frac{\Delta}{\Delta + \gamma} S_t \quad (eq. 1.1)$$

Where ρ is the water density (1000 kg m⁻³), λ is the latent heat of vaporization (2.45 MJ kg⁻¹), γ is the psychrometric constant (0.067 kPa °C⁻¹) and C_{MK} is the Makkink coefficient (Hendriks, 2010). Δ is determined with eq. 1.2 (Hendriks, 2010).

$$\Delta = \frac{4098e_s}{(237.3 + T)^2} \quad (eq. 1.2)$$

Where e_s is the saturation vapour pressure (kPa), which depends on the minimum and maximum temperature. Equation 1.3 is used to calculate e_s for the minimum and maximum temperature and, afterwards, e_s is calculated by averaging the results (eq. 1.4) (Hendriks, 2010).

$$e_s = 0.6108 e^{\frac{17.27T}{237.3+T}} \quad (eq. 1.3)$$

$$e_s = \frac{e_s(\min T) + e_s(\max T)}{2} \quad (eq. 1.4)$$

Furthermore, S_t is calculated with eq. 1.5 (Hendriks, 2010).

$$S_t = \left(a_s + b_s \frac{n}{N} \right) S_0 \quad (eq. 1.5)$$

Where a_s is the fraction of S_0 on overcast days, b_s is the fraction of S_0 on clear days, n is the number of bright sunshine hours per day, N is the day length (hour) and S_0 is the sun's shortwave radiation incident at the top of the earth's atmosphere (MJ m⁻² day⁻¹). Since there is no actual solar radiation data available the recommended values by the FAO, $a_s = 0.25$ and $b_s = 0.5$ are used (Allen et al., 1998). Furthermore, S_0 can be determined with figure 8, which only requires the latitude and the day of the year (Hendriks, 2010).

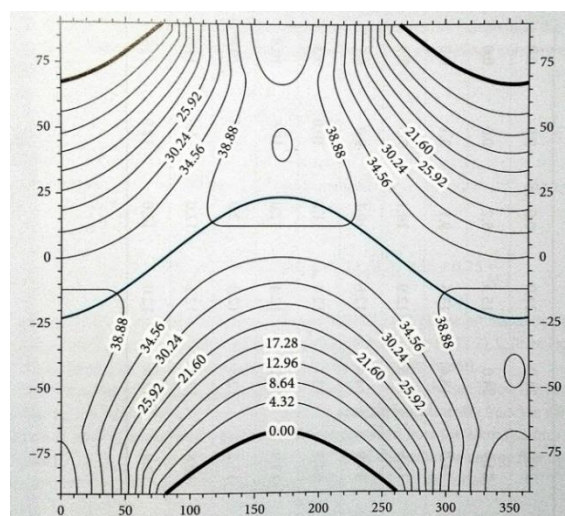


Figure 1.1. The sun's shortwave radiation incident at the top of the earth's atmosphere (S_0) as a function of latitude (vertical axis) and day of the year (horizontal axis) (Hendriks, 2010)

Appendix 2 – Crop and water stress parameters

Table 2.1. Crop and water stress parameters from the Reference Manual, Annex III from FAO (2012).

<i>a. Crop phenology</i>	<i>Value</i>	<i>Unit</i>
Base temperature (T_{base})	8.0	°C
Upper temperature (T_{upper})	30.0	°C
Number of plants per hectare ¹	50,000-100,000	#plants ha ⁻¹
Soil surface covered by an individual seedling at 90% emergence (CC_0)	6.50	Cm ² plant ⁻¹
Maximum canopy cover (CC_x) ¹	65-99	%
Canopy growth coefficient (CGC)	0.012-0.013	fraction GDD ⁻¹
Canopy decline coefficient (CDC)	0.010	fraction GDD ⁻¹
Time from sowing to emergence ¹	60-100	GDD
Time from sowing to start senescence ¹	60-100 + 1150-1500	GDD
Time from sowing to maturity ¹ (length of crop cycle)	60-100 + 1450-1850	GDD
Time from sowing to flowering ¹	60-100 + 600-900	GDD
Length of flowering stage	150-200	GDD
Minimum effective rooting depth ¹	0.3	m
Maximum effective rooting depth ¹	up to 2.80	m
Shape factor describing root zone expansion	1.3	-
<i>b. Crop transpiration</i>		
	<i>Value</i>	<i>Unit</i>
Crop coefficient when CC is complete, but prior to senescence ($Kc_{Tr,x}$)	1.05	-
Decline of $Kc_{Tr,x}$ as a result of ageing, nitrogen deficiency, etc.	0.3	% day ⁻¹
Effect of CC on reducing soil evaporation in late season stage	50	%
<i>c. Biomass and yield</i>		
	<i>Value</i>	<i>Unit</i>
Normalized water productivity for ET ₀ and CO ₂ (WP^*)	33.7	Gram m ⁻²
WP^* during yield formation	100	% WP^* before yield formation
Reference harvest index (HI_0)	48-52	%
Possible increase of HI due to water stress before flowering	none	-
Excess of potential fruits	small	%
Coefficient describing positive impact of restricted vegetative growth during yield formation on HI	small	-
Coefficient describing negative impact of stomatal closure during yield formation on HI	strong	-

Allowable maximum increase of HI	15	%
<i>d. Stresses</i>		
	<i>Value</i>	<i>Unit</i>
Soil water depletion threshold for canopy expansion - upper threshold ($p_{exp,lower}$)	0.14	-
Soil water depletion threshold for canopy expansion - lower threshold ($p_{exp,upper}$)	0.72	-
Shape factor for water stress coefficient for canopy expansion	2.9	-
Soil water depletion threshold for stomatal control - upper threshold (p_{sto})	0.69	-
Shape factor for water stress coefficient for stomatal control	6.0	-
Soil water depletion threshold for canopy senescence - upper threshold (p_{sen})	0.69	-
Shape factor for water stress coefficient for canopy senescence	2.7	-
Soil water depletion threshold for failure of pollination - upper threshold (p_{pol})	0.80	-
Vol% at anaerobic point (with reference to saturation)	Moderately tolerant to water logging	-
Minimum air temperature below which pollination starts to fail (cold stress)	10.0	°C
Maximum air temperature above which pollination starts to fail (heat stress)	40.0	°C
Minimum growing degrees required for full biomass production	12.0	°C day ⁻¹
Electrical conductivity of the saturated soil-paste extract: lower threshold (at which soil salinity stress starts to occur) (EC_{en})	1.7	-
Electrical conductivity of the saturated soil-paste extract: upper threshold (at which soil salinity stress has reached its maximum effect) (EC_{ex})	10.0	-

¹ Parameter not used, because the measured/observed value in the field is available

Appendix 3 – Walkley and Black method

To begin the procedure, the soil needs to be sieved (<0.5 mm) to get a faster and more complete digestion in the chemical procedure, afterwards 0.5 g of the sieved soil is weighed and putted in a dry flask (Beaudoin, 2003). Then, 5 mL of 1.62N potassium dichromate ($K_2Cr_2O_7^{2-}$) and 7.5 mL of sulphuric acid (H_2SO_4) is added. The soil oxidizes immediately and the flask gets really hot (Schulte and Hoskins, 2009). After waiting 30 minutes to give the solution time to reach equilibrium, 100 mL of distilled water is added to give a more clearer suspension, which helps to notice the endpoint of titration (Combs and Nathan, 1998). To help eliminate the interference from ferric iron in the sample to the results of the titration, 10 mL of H_3PO_4 is added (Schumacher, 2002). Just before titration, a ferroin indicator (0.5 mL of barium di phenyl sulphonate) is added to the solution, which turns the solution black (Combs and Nathan, 1998). A mechanical stirring device is used to stir the solution while it is titrated with 0.5N iron sulphide until the solution gets a greenish color and reaches its endpoint. When the endpoint is reached, the amount of 0.5N iron sulphide that was needed is recorded (S) (Schumacher, 2002). In addition to the soil samples, a blank solution without soil also needs to follow the above procedure (B). The blank reading is used to standardize the ferrous iron (Combs and Nathan, 1998). Equation 4.1 can be used to determine the percentage of organic carbon (%OC) in the soil sample (Combs and Nathan, 1998).

$$\%OC = \frac{N(B - S) * 0.39}{S_{weight}} \quad (eq. 4.1)$$

Where B is the blank reading (mL), S is the sample reading (mL), S_{weight} is the weight of the sample (g) and N is the equivalent concentration of the potassium dichromate, which can be calculated with equation 4.2 (Estefan et al., 2013).

$$N = \frac{V_1 C_1}{B} \quad (eq. 4.2)$$

Where V_1 and C_1 are the volume and concentration of the 1.62N potassium dichromate that was used, which is 5 mL and 1.62N, respectively. Furthermore, the 0.39 in equation X consists of the equivalent weight of carbon ($3 * 10^{-3}$), a correction factor of 1.33 and 100 to get the result in percentage (Mylavarapu, 2014). The correction factor is needed because it is proven that the procedure of the Walkley and Black method leads to an incomplete oxidation of the organic carbon (Schumacher, 2002). Various studies found a recovery factor of approximately 77% to convert the easily oxidizable organic carbon to the total organic carbon (Combs and Nathan, 1998; Schumacher, 2002; Schulte and Hoskins, 2009 and Mylavarapu, 2014). So, the results need to be divided by 0.77, or multiplied by 1.33. The Walkley and Black method assumes that soil organic matter contains 58% carbon (Schulte and Hoskins, 2009). So the percentage organic carbon can be easily converted to percentage organic matter through that assumption:

$$\%OM = \frac{100}{58} \%OC = 1.724 * \%OC \quad (eq. 4.3)$$

Appendix 4 – Hydrometer method

The hydrometer method determines the percentage of sand, silt and clay using their differences in settling time. To begin, an air-dried sample is sieved (<2 mm). Then, 50 grams of the air-dried and sieved soil sample is put into a cup and 100 ml of 5% dispersing 1N sodium hexametaphosphate is added to help suspend the soil particles (Beretta et al., 2014). To break the aggregates, the cup is shaken on a horizontal shaker for 3 hours at 180 oscillations per minute (Beretta et al., 2014). Afterwards it is additionally stirred for 5 minutes and poured into a sediment cylinder of 1000 ml. The sediment cylinder needs to be filled with deionized water on room temperature and mixed for another minute by end over end shaking (Buoyoucos, 1962). The first hydrometer reading (d_1 ; g L⁻¹) needs to be conducted 40 seconds after mixing and a second hydrometer reading (d_2 ; g L⁻¹) needs to be conducted after 2 hours, when the clay particles are the only particles still in suspension (Beretta et al., 2014). The hydrometer measures the particles in suspension and, therefore, after 40 seconds, it measures the amount of clay and silt particles in suspension (Jasrotia, 2008). The equation for the percentage of sand is, therefore, 100% minus the amount of clay and silt particles in suspension (eq. 5.1). The percentage of silt in the soil is calculated by subtracting the percentage clay and sand from 100% (eq. 5.3). At both hydrometer readings, the temperature needs to be measured as well (Estefan et al., 2013). Before the soil texture can be determined, a blank reading needs to be conducted. The blank reading consists of a hydrometer reading with only solution (without soil) and follows the same procedure as the other samples. The blank reading (B) is then conducted after 40 seconds and is assumed to be constant over time (Jasrotia, 2008). The soil texture percentages are then calculated with:

$$\%sand = 100 - \left(d_1 \pm T_{1_{cf}} - B \right) \frac{V_{sol}}{M_{dry}} \quad (eq. 5.1)$$

$$\%clay = \left(d_2 \pm T_{2_{cf}} - B \right) \frac{V_{sol}}{M_{dry}} \quad (eq. 5.2)$$

$$\%silt = 100 - (\%clay + \%sand) \quad (eq. 5.3)$$

Where M_{dry} is the dried weight of the soil sample (g), V_{sol} is the volume of the 5% dispersed solution added (ml), B is the blank reading (g L⁻¹), $T_{1_{cf}}$ and $T_{2_{cf}}$ are the temperature correction factors of the first and the second reading, respectively (Jasrotia, 2008). The density of the solution is inversely proportional to the temperature, so the reading has to be corrected for the temperature of the solution. For soils in North African countries the hydrometer reading is corrected by adding or subtracting 0.4 for each degree Celsius higher or lower than 20 °C, respectively (Estefan et al., 2013). The values of the temperature correction factor for Ethiopian soils are given in table 5.1.

Table 5.1. Temperature correction factor for Ethiopian soils (Estefan et al., 2013)

Reading temperature (°C)	Temperature correction factor (T_{cf})
19	-0.4
20	0.0
21	0.4
22	0.8
23	1.2
24	1.6
25	2.0

Appendix 5 – Pedotransfer function developed by Saxton and Rawls (2006)

The PTF by Saxton and Rawls (2006) estimates the saturated hydraulic conductivity (K_s ; mm hr⁻¹) using only the organic matter content and the fraction of clay and sand (eq. 3.1 – 3.9).

$$K_s = 1930(\theta_s - \theta_{33})^{3-\lambda} \quad (\text{eq. 3.1})$$

Where θ_s is the soil moisture content at saturation (%vol), θ_{33} is the soil moisture content at a tension of 33 kPa (%vol) and λ is the slope of the logarithmic tension-moisture curve (-) and can be calculated with:

$$\lambda = \frac{\text{Ln}(\theta_{33}) - \text{Ln}(\theta_{1500})}{\text{Ln}(1500) - \text{Ln}(33)} \quad (\text{eq. 3.2})$$

Where θ_{1500} is the soil moisture content at a tension of 1500 kPa. θ_s , θ_{33} and θ_{1500} can be calculated with eq. 3.3 – 3.9.

$$\theta_s = \theta_{33} + \theta_{s-33} - 0.097S + 0.043 \quad (\text{eq. 3.3})$$

$$\theta_{33} = \theta_{33t} + (1.283(\theta_{33t})^2 - 0.374(\theta_{33t}) - 0.015) \quad (\text{eq. 3.4})$$

$$\theta_{33t} = -0.251S + 0.195C + 0.011OM + 0.006(S \times OM) - 0.027(C \times OM) + 0.452(S \times C) + 0.299 \quad (\text{eq. a5})$$

$$\theta_{s-33} = \theta_{(s-33)t} + (0.636\theta_{(s-33)t} - 0.107) \quad (\text{eq. 3.6})$$

$$\theta_{(s-33)t} = 0.278S + 0.034C + 0.022OM - 0.018(S \times OM) - 0.027(C \times OM) - 0.584(S \times C) + 0.078 \quad (\text{eq. 3.7})$$

$$\theta_{1500} = \theta_{1500t} + (0.14\theta_{1500t} - 0.02) \quad (\text{eq. 3.8})$$

$$\theta_{1500t} = -0.024S + 0.487C + 0.006OM + 0.005(S \times OM) - 0.013(C \times OM) + 0.068(S \times C) + 0.031 \quad (\text{eq. 3.9})$$

Where S is the fraction of sand, C is the fraction of clay and OM is the organic matter content (%w). Furthermore, to account for the effect of small variations of the bulk density due to, for example, structure or management, a density adjustment factor (DF) can be used. The DF has an effect on θ_s , θ_{33} and θ_{s-33} , and therefore also on K_s , but not on θ_{1500} , because the water content at such high tensions is largely determined by texture only (Saxton and Rawls, 2006). If the density needs to be adjusted, θ_s , θ_{33} and θ_{s-33} need to be corrected with eq. 3.10, 3.11 and 3.12, respectively.

$$\theta_{s,DF} = 1 - ((1 - \theta_s)DF) \quad (\text{eq. 3.10})$$

$$\theta_{33,DF} = \theta_{33} - 0.2(\theta_s - \theta_{s,DF}) \quad (\text{eq. 3.11})$$

$$\theta_{(s-33),DF} = \theta_{s,DF} - \theta_{33,DF} \quad (\text{eq. 3.12})$$

Appendix 6 – Measured soil moisture content for field 1

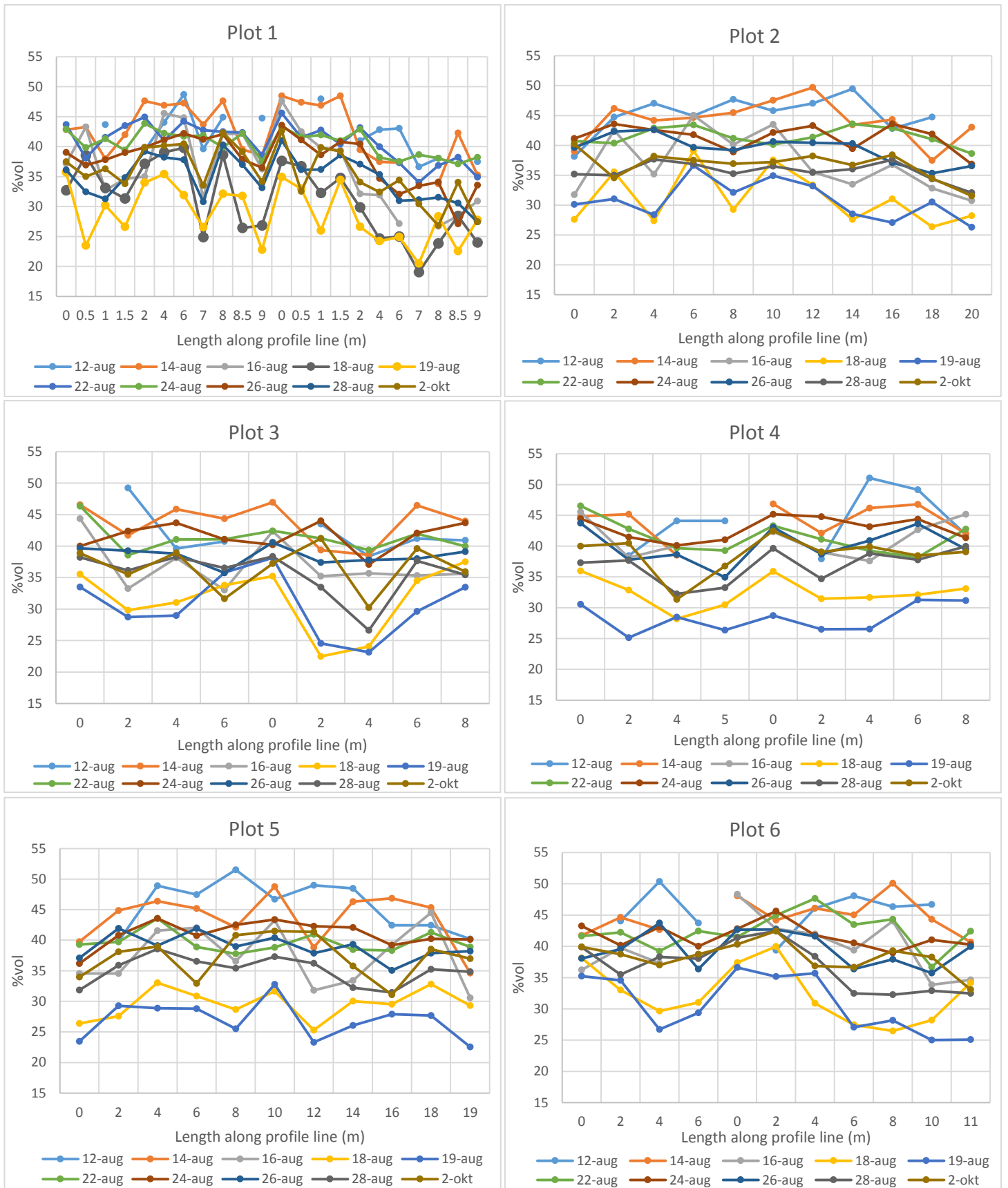


Figure 7.1. Measured soil moisture content for field 1 for each measurement day along the profile line for each plot in %vol.

Appendix 7 – Measured soil moisture content for field 2

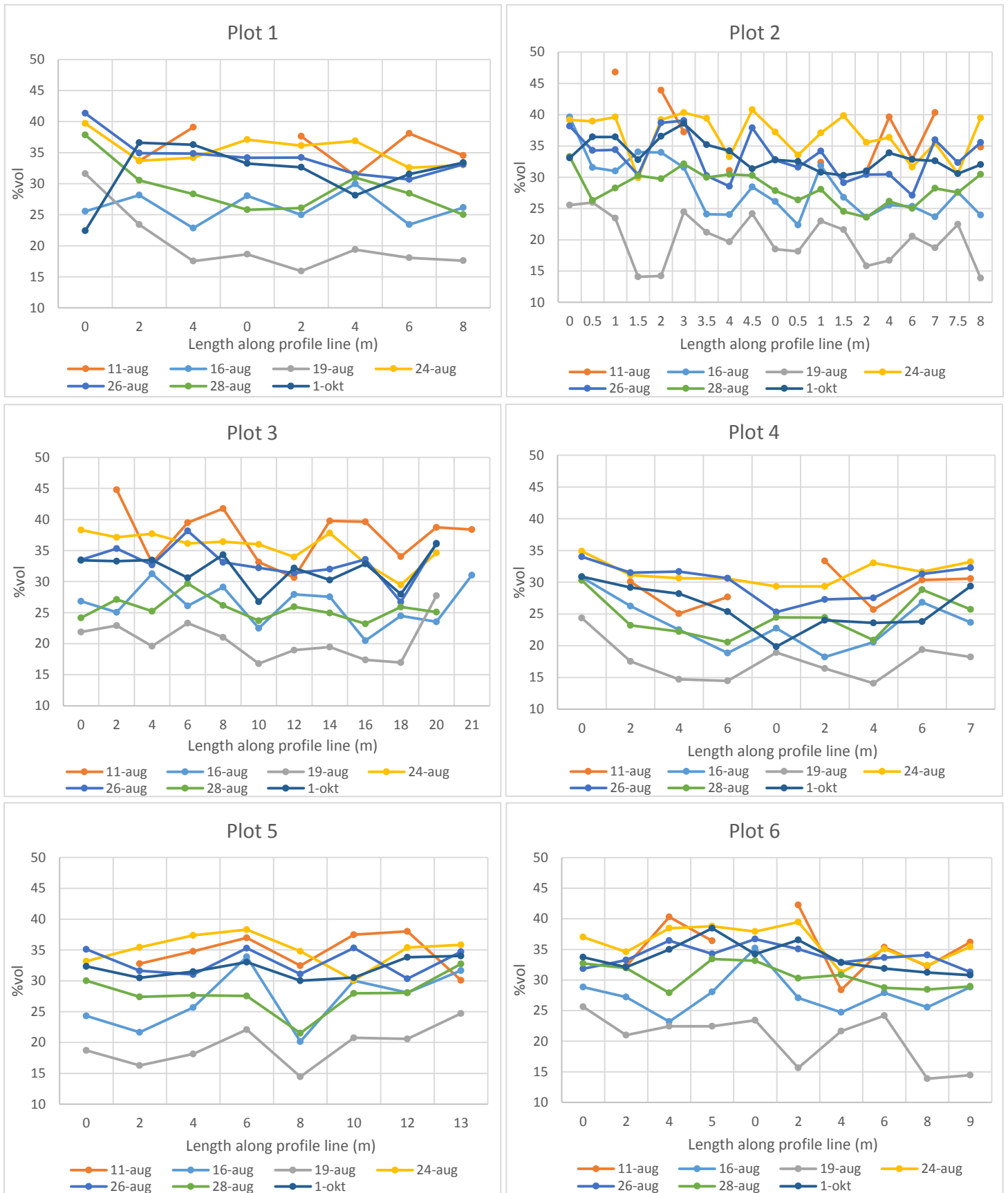


Figure 8.1. Measured soil moisture content for field 2 for each measurement day along the profile line for each plot in %vol.

Appendix 8 – Statistically significant difference in soil moisture within plots

The one-way ANOVA test is used to determine the plots with statistically significant difference in soil moisture content and the LSD post hoc test is used to determine which locations within the plot have statistically significant differences in soil moisture. The locations within the plots chosen for the within plot simulation are based on these results.

Table 8.1. Statistically significant soil moisture contents between locations within a plot of field 1. If the one-way ANOVA shows a statistically significant difference within the plot, the LSD post hoc test is used to determine which locations within the plots have a significant difference in soil moisture content. For some plots, the one-way ANOVA indicates no statistically significant difference in soil moisture within the plot, but the LSD post hoc test indicates that some locations have statistically significant soil moisture contents. These plots (plot 5 and 6b) are also used for the within plot simulations, but have less locations which are significantly different in soil moisture content. The soil moisture is significantly different when $p < 0.05$ and is indicated in bold. The numbers in the first column stand for location 1 within the plot, location 2 within the plot, etc., the second column indicates the distance from the upper boundary of the plot in meters and s.d. stands for standard deviation. The chosen locations for the within plot simulations are underlined.

Location		Average	s.d.	Significance p										
#	m	%vol	%vol	1	2	3	4	5	6	7	8	9	10	11
Plot 1a (one-way ANOVA (F(10, 99) = 2.190, p = 0.024)														
<u>1</u>	<u>0</u>	39.100	3.898	-	.475	.279	.336	.676	.330	.235	.136	.360	.737	.072
2	0.5	37.440	6.144	.475	-	.711	.803	.259	.093	.059	.434	.105	.705	.272
<u>3</u>	<u>1</u>	36.580	4.656	.279	.711	-	.904	.135	.041	.025	.680	.048	.455	.465
4	1.5	36.860	5.596	.336	.803	.904	-	.169	.054	.033	.594	.062	.530	.395
5	2	40.070	4.303	.676	.259	.135	.169	-	.576	.439	.058	.618	.452	.027
<u>6</u>	<u>4</u>	41.370	3.472	.330	.093	.041	.054	.576	-	.830	.015	.952	.191	.006
7	6	41.870	4.849	.235	.059	.025	.033	.439	.830	-	.008	.783	.129	.003
8	7	35.620	7.000	.136	.434	.680	.594	.058	.015	.008	-	.017	.247	.750
9	8	41.230	4.097	.360	.105	.048	.062	.618	.952	.783	.017	-	.212	.007
10	8.5	38.320	5.542	.737	.705	.455	.530	.452	.191	.129	.247	.212	-	.141
<u>11</u>	<u>9</u>	34.880	6.233	.072	.272	.465	.395	.027	.006	.003	.750	.007	.141	-
Plot 1b (one-way ANOVA (F(10, 99) = 5.882, p = 0.000)														
<u>1</u>	<u>0</u>	43.260	4.483	-	.202	.112	.245	.010	.000	.000	.000	.000	.000	.000
2	0.5	40.020	5.398	.202	-	.749	.909	.185	.022	.006	.000	.002	.004	.001
<u>3</u>	<u>1</u>	39.210	6.553	.112	.749	-	.664	.313	.048	.015	.001	.004	.011	.004
4	1.5	40.310	4.352	.245	.909	.664	-	.150	.017	.004	.000	.001	.003	.001
5	2	36.650	5.740	.010	.185	.313	.150	-	.328	.146	.018	.057	.117	.052
<u>6</u>	<u>4</u>	34.170	6.099	.000	.022	.048	.017	.328	-	.630	.156	.350	.551	.326
7	6	32.950	6.042	.000	.006	.015	.004	.146	.630	-	.346	.650	.909	.616
8	7	30.560	6.571	.000	.000	.001	.000	.018	.156	.346	-	.624	.407	.658
<u>9</u>	<u>8</u>	31.800	5.154	.000	.002	.004	.001	.057	.350	.650	.624	-	.734	.962
10	8.5	32.660	6.221	.000	.004	.011	.003	.117	.551	.909	.407	.734	-	.699
<u>11</u>	<u>9</u>	31.680	4.886	.000	.001	.004	.001	.052	.326	.616	.658	.962	.699	-
Plot 2 (one-way ANOVA (F(10, 99) = 1.245, p = 0.272)														
Plot 3a (one-way ANOVA (F(3, 36) = 1.198, p = 0.324)														
Plot 3b (one-way ANOVA (F(4, 45) = 2.766, p = 0.039)														
<u>1</u>	<u>0</u>	40.470	3.440	-	.086	.004	.454	.434	-	-	-	-	-	-
2	2	36.240	7.518	.086	-	.200	.322	.339	-	-	-	-	-	-
<u>3</u>	<u>4</u>	33.110	6.434	.004	.200	-	.026	.028	-	-	-	-	-	-
4	6	38.650	4.740	.454	.322	.026	-	.974	-	-	-	-	-	-
<u>5</u>	<u>8</u>	38.570	3.587	.434	.339	.028	.974	-	-	-	-	-	-	-
Plot 4a (one-way ANOVA (F(3, 36) = 1.496, p = 0.232)														

Plot 4b (one-way ANOVA (F(4, 45) = 0.459, p = 0.765)														
Plot 5 (one-way ANOVA (F(10, 99) = 1.030, p = 0.424)														
<u>1</u>	<u>0</u>	34.240	5.591	-	.284	.034	.129	.185	.029	.382	.290	.511	.125	.890
2	2	37.260	5.489	.284	-	.286	.652	.798	.256	.842	.989	.677	.639	.350
3	4	40.270	5.999	.034	.286	-	.536	.416	.946	.206	.279	.139	.548	.047
<u>4</u>	<u>6</u>	38.530	6.164	.129	.652	.536	-	.845	.493	.515	.641	.386	.986	.167
5	8	37.980	7.303	.185	.798	.416	.845	-	.379	.649	.787	.502	.831	.235
<u>6</u>	<u>10</u>	40.460	5.540	.029	.256	.946	.493	.379	-	.183	.251	.122	.504	.040
7	12	36.700	7.908	.382	.842	.206	.515	.649	.183	-	.853	.828	.504	.462
<u>8</u>	<u>14</u>	37.220	7.117	.290	.989	.279	.641	.787	.251	.853	-	.688	.629	.358
9	16	36.090	6.142	.511	.677	.139	.386	.502	.122	.828	.688	-	.377	.604
10	18	38.580	5.462	.125	.639	.548	.986	.831	.504	.504	.629	.377	-	.162
<u>11</u>	<u>19</u>	34.630	5.671	.890	.350	.047	.167	.235	.040	.462	.358	.604	.162	-
Plot 6a (one-way ANOVA (F(3, 36) = 0.251, p = 0.860)														
Plot 6b (one-way ANOVA (F(6, 63) = 1.557, p = 0.174)														
<u>1</u>	<u>0</u>	41.850	3.921	-	.964	.670	.120	.253	.040	.071	-	-	-	-
2	2	41.970	3.069	.964	-	.638	.110	.236	.036	.065	-	-	-	-
3	4	40.710	5.298	.670	.638	-	.255	.471	.101	.164	-	-	-	-
<u>4</u>	<u>6</u>	37.650	7.104	.120	.110	.255	-	.673	.606	.796	-	-	-	-
5	8	38.780	7.805	.253	.236	.471	.673	-	.350	.497	-	-	-	-
<u>6</u>	<u>10</u>	36.270	6.744	.040	.036	.101	.606	.350	-	.796	-	-	-	-
7	11	36.960	6.214	.071	.065	.164	.796	.497	.796	-	-	-	-	-

Table 8.2. Statistically significant soil moisture contents between locations within a plot of field 2. If the one-way ANOVA shows a statistically significant difference within the plot, the LSD post hoc test is used to determine which locations within the plots have a significant difference in soil moisture content. For some plots, the one-way ANOVA indicates no statistically significant difference in soil moisture within the plot, but the LSD post hoc test indicates that some locations have statistically significant soil moisture contents. These plots (plot 2a and 4a) are also used for the within plot simulations, but have less locations which are significantly different in soil moisture content. The soil moisture is significantly different when $p < 0.05$ and is indicated in bold. The numbers in the first column stand for location 1 within the plot, location 2 within the plot, etc., the second column indicates the distance from the upper boundary of the plot in meters and s.d. stands for standard deviation. The chosen locations for the within plot simulations are underlined.

Location		Average	s.d.	Significance p								
#	m	%vol	%vol	1	2	3	4	5	6	7	8	9
Plot 1a (one-way ANOVA (F(2, 18) = 0.287, p = 0.754)												
Plot 1b (one-way ANOVA (F(4, 30) = 0.077, p = 0.989)												
Plot 2a (one-way ANOVA (F(8, 54) = 0.831, p = 0.580)												
<u>1</u>	<u>0</u>	36.514	6.685	-	.568	.563	.137	.477	.643	.136	.047	.243
2	0.5	34.314	7.332	.568	-	.994	.355	.888	.914	.353	.150	.548
3	1	34.286	7.663	.563	.994	-	.359	.894	.908	.357	.152	.553
4	1.5	30.743	8.814	.137	.355	.359	-	.432	.302	.997	.601	.744
<u>5</u>	<u>2</u>	33.771	9.689	.477	.888	.894	.432	-	.803	.430	.193	.645
6	3	34.729	5.692	.643	.914	.908	.302	.803	-	.301	.123	.479
7	3.5	30.729	6.442	.136	.353	.357	.997	.430	.301	-	.603	.741
<u>8</u>	<u>4</u>	28.729	5.201	.047	.150	.152	.601	.193	.123	.603	-	.396
9	4.5	32.000	5.631	.243	.548	.553	.744	.645	.479	.741	.396	-
Plot 2b (one-way ANOVA (F(9, 60) = 0.262, p = 0.982)												
Plot 3 (one-way ANOVA (F(11, 72) = 0.690, p = 0.743)												
Plot 4a (one-way ANOVA (F(3, 24) = 2.250, p = 0.108)												
<u>1</u>	<u>0</u>	30.771	3.385	-	.189	.051	.025	-	-	-	-	-
<u>2</u>	<u>2</u>	26.971	5.113	.189	-	.490	.306	-	-	-	-	-
3	4	25.000	5.869	.051	.490	-	.733	-	-	-	-	-
<u>4</u>	<u>6</u>	24.029	6.213	.025	.306	.733	-	-	-	-	-	-
Plot 4b (one-way ANOVA (F(4, 30) = 0.756, p = 0.562)												
Plot 5 (one-way ANOVA (F(7, 48) = 0.784, p = 0.604)												
Plot 6a (one-way ANOVA (F(3,24) = 0.290, p = 0.832)												
Plot 6b (one-way ANOVA (F(5, 36) = 0.983, p = 0.442)												

Appendix 9 – Overview of measured parameters

Table 9.1: Field measurements conducted in field 1

Table 9.2: Field measurements conducted in field 2

Table 9.3: Lab measurements and calculations of field 1

Table 9.4: Lab measurements and calculations of field 2

Table 9.1. Field measurements conducted in field 1. θ_{FC} is the soil moisture content at field capacity, CC_x is the maximum green canopy cover which is equal to measured canopy cover in August.

Field measurements – Field 1												
	Plot area	Slope	Soil depth	Rooting depth	Bund height	θ_{FC}	CC_x	Plant height	#plants per m ²	#ears per plant	Biomass	Yield
Plot	m ²	°	m	m	m	%vol	%	m	-	-	ton ha ⁻¹	ton ha ⁻¹
1a	63	8.5	0.25	0.23	0.11	47.5	53.8	1.83	4.3	0.71	5.307	1.682
1b	83	15	0.62	0.40	0.05	45.9	47.3	1.63	5.5	0.59	4.395	1.912
2a	124	8.0	0.13	0.60	-	45.5	59.2	1.97	4.5	0.89	7.473	2.689
2b		14.5	0.40	0.54	-	45.3	41.0	1.77	4.0	0.81	5.712	2.411
3a	50	11.9	0.16	0.22	0.05	41.9	51.9	1.93	3.8	1.00	4.947	2.767
3b	75	16.5	0.10	0.48	0.03	41.1	46.6	1.71	4.0	1.00	4.831	2.280
4a	40	11.9	0.11	0.32	0.08	42.2	52.5	2.12	6.3	0.92	13.100	5.295
4b	74	12.3	0.34	0.34	0.03	45.3	43.8	1.93	4.8	0.74	5.331	1.579
5a	119	8.5	0.13	0.31	-	45.0	43.2	1.95	4.0	0.75	4.911	2.880
5b		10.0	0.20	0.45	-	41.7	40.6	1.61	3.0	0.92	3.780	1.162
6a	52	8.2	0.34	0.32	0.14	44.7	45.5	1.93	6.3	0.96	7.321	4.163
6b	77	10.0	0.14	0.45	0.18	40.2	40.7	1.58	5.0	0.60	4.110	1.096

Table 9.2. Field measurements conducted in field 2. θ_{FC} is the soil moisture content at field capacity, CC is the green canopy cover which is measured in August, but is not equal to CC_x .

Field measurements – Field 2												
	Plot area	Slope	Soil depth	Rooting depth	Bund height	θ_{FC}	CC	Plant height	#plants per m ²	#ears per plant	Biomass	Yield
Plot	m ²	°	m	m	m	%vol	%	m	-	-	ton ha ⁻¹	ton ha ⁻¹
1a	26	6.2	0.12	0.30	0.19	39.4	13.9	1.45	3.0	0.75	2.859	1.107
1b	48	19.0	0.13	0.35	0.02	39.9	22.5	1.60	3.3	0.85	4.663	1.673
2a	29	14.5	0.19	0.29	0.06	47.2	27.7	1.76	2.5	0.80	4.103	2.172
2b	55	16.8	0.16	0.35	0.08	38.0	15.1	1.64	2.5	1.00	3.613	1.706
3a	189	8.5	0.14	0.40	-	38.4	27.6	1.76	1.8	1.00	3.881	1.676
3b		14.5	0.10	0.29	-	38.0	15.5	1.56	3.3	0.85	5.164	2.074
4a	52	6.2	0.12	0.40	0.08	37.7	18.2	1.52	1.8	1.14	3.131	2.364
4b	111	6.2	0.10	0.35	0.14	38.4	18.8	1.55	2.7	0.72	3.070	1.209
5a	105	9.0	0.13	0.23	-	38.2	17.9	1.50	1.8	0.86	1.256	0.574
5b		18.2	0.16	0.24	-	38.4	16.9	1.90	3.8	0.80	5.522	1.413
6a	57	7.2	0.19	0.37	0.19	38.9	13.4	2.03	2.5	1.00	4.185	1.968
6b	115	16.0	0.12	0.29	0.09	39.7	17.9	1.94	3.5	0.57	3.838	1.213

Table 9.3. Lab measurements and calculations of field 1. Some measurements were only conducted for some plots. ρ^b is the bulk density, θ_{grv} is the gravimetric soil moisture content and K_{sat} is the saturated hydraulic conductivity.

Lab measurement and calculations – Field 1								
	ρ^b	Porosity	θ_{grv}	Soil texture			Organic matter	K_{sat}
Plot	$g\ cm^{-3}$	-	%vol	%Sand	%Clay	%Silt	%	$mm\ day^{-1}$
1a	1.220	0.540	36.0	45.2	23.6	31.2	0.787	440
1b	1.314	0.504	55.3	51.2	17.6	31.2	1.049	764
2a	1.396	0.473	-	-	-	-	-	563
2b	1.220	0.540	-	-	-	-	-	715
3a	1.182	0.554	43.0	51.2	19.6	29.2	1.311	685
3b	1.178	0.555	43.8	49.2	19.6	31.2	1.311	666
4a	1.130	0.574	-	-	-	-	-	767
4b	1.130	0.574	-	-	-	-	-	698
5a	1.012	0.618	35.4	50.4	16.4	33.2	1.311	848
5b	1.147	0.567	40.9	52.4	18.4	29.2	0.983	730
6a	1.166	0.560	-	-	-	-	-	848
6b	1.066	0.598	-	-	-	-	-	730

Table 9.4. Lab measurements and calculations of field 1. Some measurements were only conducted for some plots. ρ^b is the bulk density, θ_{grv} is the gravimetric soil moisture content, K_{sat} is the saturated hydraulic conductivity and CC_x is the maximum green canopy cover, which is calculated for field 2.

Lab measurement and calculations – Field 2									
	ρ^b	Porosity	θ_{grv}	Soil texture			Organic matter	K_{sat}	CC_x
Plot	$g\ cm^{-3}$	-	%vol	%Sand	%Clay	%Silt	%	$mm\ day^{-1}$	%
1a	1.120	0.577	54.4	22.4	23.2	54.4	1.377	585	35.1
1b	1.177	0.556	50.4	20.4	29.2	50.4	1.311	640	40.7
2a	1.335	0.496	-	-	-	-	-	578	51.2
2b	1.193	0.550	-	-	-	-	-	613	37.4
3a	1.111	0.581	44.5	46.4	22.4	31.2	1.901	571	41.8
3b	1.114	0.580	-	-	-	-	-	585	34.8
4a	1.135	0.572	-	-	-	-	-	503	28.8
4b	1.217	0.541	-	-	-	-	-	558	33.6
5a	1.073	0.595	29.6	44.4	26.4	29.2	2.163	435	32.3
5b	1.245	0.530	38.2	46.4	22.4	31.2	1.377	531	30.8
6a	1.077	0.593	-	-	-	-	-	435	36.7
6b	1.173	0.557	-	-	-	-	-	531	37.1

Appendix 10 – Overview of the results of the default AquaCrop simulation

Table 10.1: Simulated soil, crop and yield parameters of field 1

Table 10.2: Simulated soil, crop and yield parameters of field 2

Table 10.3: Simulated parameters of the water balance of field 1

Table 10.4: Simulated parameters of the water balance of field 2

Table 10.1. The simulated soil, crop and yield parameters of the default simulation with variable soil fertility stress for field 1. CGC is the canopy growth coefficient, CDC is the canopy decline coefficient, θ_{avg} is the average actual soil moisture content over the growing period. REW is the readily evaporable water, TAW is the total available water, temp stress is the temperature stress, exp stress is the canopy expansion stress, sto stress is the stomatal closure and HI is the harvest index.

Simulated soil, crop and yield parameters – Field 1													
	CGC	CDC	Max root extraction	θ_{avg}	REW	TAW	Temp stress	Exp stress	Sto stress	Soil fertility stress	Biomass	Yield	HI
Plot	% day ⁻¹	% day ⁻¹	m	m	mm	mm	%	%	%	%	ton ha ⁻¹	ton ha ⁻¹	%
1a	10.2	7.5	5.0	40.8	6	320	9	5	12	73	5.412	2.328	43.0
1b	10.0	6.2	3.0	39.2	6	300	9	8	8	75	4.364	1.881	43.1
2a	10.3	8.0	15.0	39.1	6	300	9	0	15	63	7.587	3.111	41.0
2b	9.8	5.4	10.0	40.0	6	303	9	1	1	68	5.755	2.417	42.0
3a	10.1	7.1	4.0	41.0	6	310	9	8	5	75	5.03	2.115	42.5
3b	10.0	6.2	14.0	35.1	6	250	9	1	2	76	4.875	2.069	42.4
4a	10.1	7.0	7.5	42.3	6	330	9	2	3	25	13.178	5.667	43.0
4b	9.9	5.8	4.0	43.6	6	340	9	6	5	70	5.434	2.339	43.0
5a	9.9	5.8	6.0	41.5	10	330	9	4	3	73	4.929	2.07	42.0
5b	9.8	5.4	4.3	39.0	6	290	9	8	3	80	3.724	1.566	42.1
6a	9.9	6.4	3.0	42.7	6	330	9	6	5	55	7.335	3.087	42.1
6b	9.8	5.4	10.0	37.5	4	262	9	1	1	78	4.14	1.739	42.0

Table 10.2. The simulated soil crop and yield parameters of the default simulation with variable soil fertility stress for field 2. CGC is the canopy growth coefficient, CDC is the canopy decline coefficient, θ_{avg} is the average actual soil moisture content over the growing period. REW is the readily evaporable water, TAW is the total available water, temp stress is the temperature stress, exp stress is the canopy expansion stress, sto stress is the stomatal closure and HI is the harvest index.

Simulated soil, crop and yield parameters – Field 2													
	CGC	CDC	Max root extraction	θ_{avg}	REW	TAW	Temp stress	Exp stress	Sto stress	Soil fertility stress	Biomass	Yield	HI
Plot	% day ⁻¹	% day ⁻¹	m	m	mm	mm	%	%	%	%	ton ha ⁻¹	ton ha ⁻¹	%
1a	9.6	4.3	4.0	35.9	9	244	9	12	6	80	3.054	1.409	46.1
1b	9.8	5.0	4.5	32.8	9	210	9	13	7	73	4.621	2.172	47.0
2a	10.0	6.2	6.0	33.7	9	240	9	9	7	80	4.125	1.952	47.3
2b	9.6	4.7	5.0	31.9	7	200	9	11	6	75	3.687	1.67	45.3
3a	9.7	5.1	4.2	35.1	9	234	9	11	6	80	3.883	1.835	47.3
3b	9.4	4.3	3.0	31.4	9	190	9	16	9	61	5.197	2.275	43.8
4a	9.3	3.5	4.0	28.9	6	165	9	14	8	74	3.317	1.473	44.4
4b	9.5	4.3	3.0	26.8	9	140	9	19	13	77	3.123	1.351	43.3
5a	9.4	4.2	4.0	31.9	8	180	9	13	7	75	3.585	1.606	44.8
5b	9.4	3.8	5.0	34	9	224	9	11	5	56	5.588	2.587	46.3
6a	9.6	4.7	6.0	33.1	9	210	9	9	4	72	4.19	1.898	45.3
6b	9.5	4.5	4.0	33.7	9	220	9	13	8	73	3.933	1.804	45.9

Table 10.3. The simulated parameters of the water balance of the default simulation with variable soil fertility stress for field 1. E_x is the Maximum soil evaporation, E is the actual soil evaporation, Tr_x is the maximum transpiration, Tr is the transpiration, ET_x is the maximum evapotranspiration and ET is the actual evapotranspiration.

Simulated water balance – Field 1								
	Drainage	Runoff	E_x	E	Tr_x	Tr	ET_x	ET
Plot	mm	mm	mm	mm	mm	mm	mm	mm
1a	648.2	0	350.6	306.9	172.4	142.3	523.8	449.5
1b	642.5	0	374.6	318.7	153.4	137.5	528.1	456.8
2a	501	158.8	325.4	284.2	192.4	154.0	519.2	438.9
2b	460.4	156.8	382.2	334.5	149.1	146.6	531.8	480.9
3a	630.4	0	358.3	311.1	165.1	155.1	524.7	466.9
3b	621.6	0	362.5	314.2	164.3	161.6	527.5	475.9
4a	624	0	343.3	302.0	180.3	172.3	524.3	474.9
4b	626.4	0	378.3	329.5	151.5	141.9	530.5	471.7
5a	471.4	137.9	380.3	344.5	150.7	143.7	530.8	488.0
5b	510	114.9	395.2	342.0	136.0	130.1	531.9	472.9
6a	636.6	0	371.9	316.6	156.0	143.9	528.7	461.6
6b	624.6	0	383.2	324.9	147.5	147.5	531.4	472.5

Table 10.4. The simulated parameters of the water balance of the default simulation with variable soil fertility stress for field 2. E_x is the Maximum soil evaporation, E is the actual soil evaporation, Tr_x is the maximum transpiration, Tr is the transpiration, ET_x is the maximum evapotranspiration and ET is the actual evapotranspiration.

Simulated water balance – Field 2								
	Drainage	Runoff	E_x	E	Tr_x	Tr	ET_x	ET
Plot	mm	mm	mm	mm	mm	mm	mm	mm
1a	685.4	0	479.3	428.5	104.3	95.1	583.2	522.9
1b	689.5	0	449.8	404.2	129.0	116.1	577.5	519.2
2a	687.6	0	408.6	375.9	158.9	145.8	567.6	521.7
2b	690.4	0	465.2	410.7	115.8	106.9	580.5	517.0
3a	551.2	128.6	432.9	393.8	144.9	133.8	577.1	526.7
3b	604.5	93.9	471.7	414.8	110.2	95.3	581.8	510.3
4a	709	0	481.8	406.2	105.8	94.0	587.7	500.4
4b	706.4	0	474.4	412.0	110.0	91.0	584.1	502.0
5a	562.5	124.6	472.7	419.0	112.1	101.0	584.6	519.8
5b	535.6	138.7	474.3	428.7	111.6	104.6	586.3	533.4
6a	675.6	0	464.6	420.9	115.8	110.4	579.9	530.4
6b	688.9	0	461.4	413.4	118.8	106.2	579.7	518.7